1-1-1968

Theoretical analysis of biaxially loaded wide flange beam columns with plastic yielding in the section.

Daniel Michael Masterson
University of Windsor

THEORETICAL ANALYSIS OF BIAXIALLY LOADED WIDE FLANGE BEAM COLUMNS WITH PLASTIC YIELDING IN THE SECTION

A Thesis
Submitted to the Faculty of Graduate Studies through the Department of Civil Engineering in Partial Fulfilment of the Requirements for the Degree of Master of Applied Science at the University of Windsor

by

Daniel Michael Masterson

B.A.Sc., University of Windsor, 1968

Windsor, Ontario
1968

ABG1105

APPROVED BY:

J. Kennedy

G. Abdel Sayed

W. McVinnie

248693

ABSTRACT

A theoretical investigation of biaxially loaded wide flange colums with plastic yielding in the section is carried out in this thesis. Computer programs are developed to perform the calculations. The effects of residual stresses and warping stresses are neglected but modifications to the procedure are suggested in order that these effects might be included in a further analysis. The theoretical results obtained are compared with experimental results and with the results of other theories.

ACKNOWLEDGEMENTS

The author wishes to express his deepest appreciation to Dr. William W. McVinnie under whose supervision this thesis was prepared. His help and encouragement made possible the success of this project.

Thanks is also expressed to the Computer Center at the University of Windsor for making its facilities available for use in this investigation. Thanks is also expressed to Mr. Harold Horneck for his assistance.

Financial assistance for this project was provided by the National Research Council of Canada.

TABLE OF CONTENTS

	Page
ABSTRACT	i
ACKNOWLEDGMENTS	ii
TABLE OF CONTENTS	iii
LIST OF FIGURES	v
LIST OF TABLES	vii
I INTRODUCTION	1
1.1 Object and Scope	1
1.2 General Comments	2
1.3 Previous Investigations	3
II THEORETICAL SOLUTION	8
2.1 Description of the Problem	8
2.2 Method of Solution	8
2.3 Assumptions	9
2.4 Column Integration	10
2.4.1 Governing Differential Equations	10
2.4.2 Numerical Integration Procedure	11
2.5 Load-Moment-Curvature Relationship	16
2.5.1 General Procedure	16
2.5.2 Developement of the Load-Moment-Curvature Equations	19
2.5.3 Introduction of Residual Stresses	22
2.5.4 Twisting Displacements	25
III COMPUTATIONS	32
3.1 Computer Programs	32
3.2 Numerical Calculations	33

		Page
IV	DISCUSSION OF RESULTS	35
	4.1 General Comments	35
	4.2 Numerical Results	36
V	CONCLUSIONS AND FUTURE RESEARCH	40
	5.1 Conclusions	40
	5.2 Future Research	40
BIBLIOGRAPHY		80
NOMENCLATURE		82
VITA		85

LIST OF FIGURES

Figure		Page
1.1	Failure at the Euler Load	48
1.2	Failure at the Collapse Load	48
2.1	Column With Moments Applied at Both Ends	49
2.2	Typical Wide Flange Cross Section	49
2.3	Ideal Stress-Strain Curve	50
2.4	Typical Column Deflection Curve	50
2.5	Projection of the Column Element	51
2.6	Correction for u_c	52
2.7	Column Deflection Curve, $\beta = 1$	53
2.8	Moment Rotation Curve	54
2.9	Moment-Curvature Curves About the x-axis	55
2.10	Moment-Curvature Curves About the y-axis	55
2.11(a)	Possible Yield Configurations of the Top and Bottom Flanges Neglecting Warping and Residual Stresses	56
2.11(b)	Possible Yield Configurations for the Wide Flange Section After Combining Top and Bottom Flanges of Fig. 2.11(a)	56
2.12	Sequence for Checking the Yield Configurations	57
2.13	Curvature Relationships for Constant Moment About Each Axis	58
2.14	Total Strain Diagram for Flange	59
2.15	Residual Stress Distribution	60
2.16(a)	Strain Distribution of a Flange(i,j) Neglecting Warping and Residual Strains	61
2.16(b)	Distribution of Warping Strains Over a	

Figure		Page
	Flange(i,j)	61
2.16(c)	Net Strain Distribution for Flange(i,j) Obtained by Superimposing Figs. 2.16(a) and 2.16(b)	61
2.17(a)	Possible Yield Configurations for a Wide Flange Section With Residual Stresses Included, Top and Bottom Separate	62
2.17(b)	Possible Yield Configurations for a Wide Flange Section With Residual Stresses Included	63
2.18	Sample Derivation Of Total Cross Section Yield Pattern	64
2.19	Column With Unequal End Moments, $\beta = 0$	65
2.20	Strain Distribution on the Flanges for the Cross Section at Mid Height of the Column	66
2.21	Rotated Principal Axis	66
4.1 through 4.13	Interaction Curves	67-79

LIST OF TABLES

Table		Page
2.1	List of Yield Patterns and Equation Constants, Residual Stresses Neglected	41a
2.2	List of Yield Patterns and Equation Constants, Residual Stresses Included	42
4.1	Tabulation of Theoretical and Experimental Results	45

Chapter 1 - Introduction

1.1 Object and Scope

A considerable amount of work has appeared in recent years concerning the behavior of columns subjected to moments applied about one principal axis of the cross section. This approximates the type of loading which would occur in planeframes. The study of such beam-column behavior presents a formidable problem because of the necessity of considering inelastic action. Buildings are of a necessity three dimensional, but are normally analyzed as a series of plane frames. However, interaction between planes often results in some members being acted upon by loads from more than one plane. For example, corner columns of such frames might well be subjected to biaxial moment, i. e., a moment about each of the principal axes of the cross section. Since little research has been done on the behavior of columns loaded in such a manner, particularly when inelastic action occurs, the object of this research is to present an analysis to study biaxially loaded wide flange beam columns. This analysis is based, to a large extent, on previous work by Scott (19).

The large amount of numerical work occurring in such an analysis necessitated the developement of computer programs to perform this numerical work. The scope of the study was limited to the consideration of columns with equal end moments, these equal end moments causing only single curvature of the column. In his study of solid, rectangular sections, Scott (19) considered double curvature and columns with moments applied only at one end.

Time did not permit this to be done for the wide flange section, which was the section used throughout the analysis.

1.2 General Comments

The expression "beam-column" refers to a member which is simultaneously subjected to an axial load and bending moments. The bending moments may result from eccentricities of the axial load or from transverse loading. As the bending moment approaches zero, the member tends to become a centrally loaded column and when the axial force approaches zero, the problem becomes that of a beam.

If the eccentrically loaded column were to remain elastic, its behavior would be represented by a load-deflection curve, which becomes asymptotic to the Euler load (Fig. 1.1), when the Euler load is given by $P_e = \frac{\pi^2 EI}{L^2}$

and	P_e	=	Euler Load
	E	=	Modulus of Elasticity for the column material
	I	=	Moment of Inertia for the column cross section
	L	=	effective column length

However, this behavior is impossible since the column becomes inelastic at a value of the load less than P_e and the result is a load-deflection curve which is similar to that shown in Fig 1.2. The collapse load represented by this curve is normally some what less than the Euler load. The reason for this reduction in load is easily explained. As the load is increased beyond initial yielding, plastification progresses along and across the column, thereby reducing the columns resistance to further loading. In Fig. 1.2 the portion of the curve from O to A represents the column behavior when the stresses are still elastic. The portion from A to B represents the range of partial yielding. Finally, when the curve reaches point B, a further increase in load becomes impossible because the internal stiffness of the column is just enough to resist the applied load and moment. It is evident that this type of failure occurs by virtue of excessive bending in the plane of the applied moment.

If the member is subjected to bending about the stronger of its two principal axes, and if no lateral support is provided, the column may twist and bend out of the plane of loading and failure occurs due to lateral-torsional buckling. This has the effect of reducing the collapse load from that shown in Fig. 1.2.

The behavior of the biaxially loaded column is similar to that of Fig. 1.2. In this case, however, the determination of the deflection plotted in this figure becomes more complex than for the uniaxially loaded column and, as a result, the determination of the collapse load also becomes more complex. This is due to the fact that three interdependent displacements of the column cross section must be considered. These are lateral displacements in the two directions and a rotation of the section about its center of twist.

1.3 Previous Investigations

The investigation of the beam column problem began with single axis bending and the early works of von Karaman, Ros and Brunner, Chwulla, Westergaard and Osgood, Jesek and others, have been reviewed quite thoroughly by Bleich (3). The works of Newmark (15), Ketter, Kaminsky and Beedle (11), Huber and Ketter (10), Ellis (6,7) and Ojalvo (16) and Bijlaard (1) have been summarized by Scott (19).

Biaxial bending is a much more complicated problem than single axis bending because three interdependent displacements are involved, i. e. two lateral displacements and a twisting displacement. Birnstiel and Michalos (2) have presented an analysis of biaxially loaded wide flange columns. In their analysis, the column is divided into a number of panel lengths. Deformations at these panel ends are assumed and values of the internal moments are computed. These internal moments are compared with the external applied moments. If the comparison is favorable, the correct deformations were assumed.. If the comparison is not favorable, the deformations must be adjusted. Internal Moments and forces are found by dividing the cross section into a number of elements by a rectangular grid, determining the strain on each element, and summing the results over all the elements of the cross section. By assuming increasing values of the second derivatives of the displacements, a curve of load versus deflection is obtained, which leads directly to the collapse load of the column. The procedure used is probably the most exact of any presented to date. Only columns symmetric about the mid height are considered in the paper. The results obtained from an analysis of a 12 WF79 column in their paper were compared with the results from an analysis of the same column using the method presented in this study and agreement was found to be very good.

Sharma (20) has presented an approximate method for determining the ultimate load of columns subjected to biaxial bending caused by an eccentrically applied load, the eccentricities at each end being equal. The procedure is based on the assumption that the lateral and twisting displacements vary sinusoidally along the column At midheight, a value of the second derivative of one of the lateral displacements is specified and equilibrium between internal and external forces and moments is established. Knowing the displacement at midheight thus determines the defected shape of the column. By incrementing the specified second derivative, a load-deflection curve is obtained. In contrast to Birnstiel and Michalos, who considered the effect of yielding of the cross section on the position of the center of twist, Sharma assumes that the location of the center of twist remainsfixed. In his study he found the warping strains to be quite small in comparison with the strains due to bending and thrust. He tried the procedure neglecting the effects of twisting and obtained loads somewhat higher than before, as was expected. The error resulting from neglecting twist was found to increase somewhat with increasing slenderness but never exceeded 8 per cent.

Considerable experimental and analytical work has been carried out in Germany and Russia on the biaxial loading of steel wide flange columns. Galambos (8) has presented a summary of the result of two papers, one by the Germans K. Klöppel and E. Winkelman (13) and the other by Chubkin (5), a Russian. The results of the tests by Kloppel and Winkelman were used by the author to check the analysis presented in this study. The report by the Germans contains the results of 74 tests on rolled steel wide-flange columns and 17 tests on rolled steel channel columns. An eccentrically placed axial load was applied to the columns and the columns were tested to failure. The eccentricities were equal at each end. The members were pinned at the ends and restrained against warping. The report also analyses the results in the light of current German buckling specifications and developes a semi-emperical design formula and an analalytical load-deformation analysis. The report by Chubkin contains the results of tests on 281 steel members tested with various types of eccentricity (axial, uniaxial, biaxial) and end conditions (warping restrained and warping free). Galambos has compared the results of the two tests with the CRC Interaction Equation

$$\frac{P}{P_o} + \frac{Pe_x}{S_x \sigma_y (1 - P/P_{ex})} + \frac{Pe_y}{S_y \sigma_y (1 - P/P_{ey})} = 1.0$$

This equation is 5.21, CRC Guide. The formula, according to the tabulation presented by Galambos, is conservative. For each set of X and Y eccentricities, the German paper (13) gave two values of ultimate load. Galambos used the lower of the two for his comparison and was always conservative.

The problem of torsional buckling of thin walled columns has been considered by several writers. Renton (18) has presented a paper which gives a general solution of the equations for the torsional flexural buckling of struts. Expressions for the end conditions are found, and their application to the buckling of frameworks described. The analysis is for elastic failure only. Chajes and Winter (4) present a simple method of calculating the elastic torsional-flexural buckling load of centrally loaded, thin walled columns with singly symmetric sections. An interaction type of equation between the torsional and flexural buckling loads is developed and used to predict the failure loads.

The effect of residual stresses on the strength of beam-columns has been considered by different researchers. Galambos (9), presents a set of moment-curvature curves which show the effect of neglecting residual stresses. Sharma (20) also considers residual stresses in his analysis. He concludes that the residual stress effect is relatively insignificant.

The procedure used in this thesis is based on an analysis given by Scott (19), who considered biaxially loaded columns of solid rectangular cross section. The procedure used and the modifications necessary for wide-flange cross sections are given in the next chapter.

Chapter 11 - Theoretical Solution

2.1 Description of the Problem

The biaxially loaded column under investigation (Fig. 2.1) is of length L and simply supported at each end, i. e., displacements are zero but rotations are permitted about the x and y axes. The bending is such that the axial load, P , is applied to the column and then end moments about the x and y axes are increased simultaneously to collapse. In this study, moments are designated as M^x or M^y where the superscript indicates the axes about which they act. Subscripts are used to designate position of the moment. For example, M^x_A is the moment about the x axis at point A in Fig. 2.1. To further define the loading, the ratio of the x-moment to y-moment at the ends of the column is designated as γ and a constant β is defined as the ratio of the x-moment at B to the x-moment at A. The ratios γ and β are considered to remain constant throughout the loading. As noted previously, only values of $\beta = 1$ are considered in this study although the method will work for any β .

A wide flange section is used throughout this investigation (Fig. 2.2). The half depth of the cross section less the thickness of the flanges is taken as D, the half width as K_1 D, the flange thickness as K_2 D and the web thickness as K_3 D . The x and y axes are orientated as shown in Fig. 2.1.

2.2 Method of Solution

The analysis presented herein involves the determination of moment-deflection curves such as the one shown in Fig. 2.8. The ordinate of the curve may be any of the end moments since all are related by β and γ . The abscissa may be any deflection, but in this study end rotations are used. For a given column, ρ, β, and γ are specified and the end moments increased until the peak moment on the moment-deflection curve is obtained. A typical point on this curve is found from the column deflection curve which is the shape a column will take if the load and deformation at a point are specified. A numerical integration procedure presented by McVinnie (16) is used to develop the column deflection curve. By consideration of many specific problems interaction curves for the biaxially loaded column can be developed.

2.3 Assumptions

In this study, the following assumptions are made:

1) Deflections and rotations are small in accordance with small deflection theory.
2) Deflections occur in the x and y direction only, no twisting of the column is allowed. In section 2.5.4 a method is suggested whereby the procedure can be modified to include the effects of twisting.
3) Plane sections remain plane after bending.
4) The material is mild structural steel which is assumed to have an elastic, perfectly plastic, stress-strain curve (Fig. 2.3). It is further assumed that the tension and compression stress-strain curves are identical. This curve is typical of mild steels, provided that strains no greater than about ten times the yield strain are considered.
5) No unloading occurs in yielded portions of the column.

6) Residual stresses are neglected. Section 2.5.3 shows how the procedure can be modified to include residual stresses.

7) Members are originally straight and prismatic.

8) Axial shortening of the column is neglected.

9) The effect of shear on the bending resistance of the column is neglected. Except for assumptions 2 and 6, the above assumptions are standard to most previous column investigations. Previous research into biaxially loaded columns (20) has shown assumptions 2 and 6 to be reasonable.

2.4 Column Integration

2.4.1 Governing Differential Equations

For the biaxially loaded beam columns, the displacements of the cross section at any point along the column are defined by the lateral displacements of the shear centre in the x and y directions, $\bar{u}$ and $\bar{v}$ respectively, and by the rotation of the section about its shear centre. Differential equations of equilibrium for this problem have been derived by Timoshenko and Gere (21). Since the effects of twisting are not initially included in this analysis, the governing differential equations reduce to,

$$B^{y}\frac{d^2\bar{u}}{dz^2} + P\bar{u} + C_1 z + C_2 = 0 \qquad (2.1)$$

$$B^{x}\frac{d^2\bar{v}}{dz^2} + P\bar{v} + C_3 z + C_4 = 0 \qquad (2.2)$$

where B^x, B^y = bending stiffness about the x and y axes

z = co-ordinate along the member

C_1, C_2, C_3, C_4 = constants of integration

For the elastic case, where the bending stiffnesses are independent and constant, Eqs. 2.1 and 2.2 are independent and define the behavior of the column in the y - z and x - z planes respectively. However, after inelastic action begins, the bending stiffnesses depend upon the extent and position of yielded material which in turn is dependent upon the axial load, applied moments, and the lateral displacements. As a result, Eqs 2.1 and 2.2 are coupled thru these stiffnesses and $\bar{u}$ and $\bar{v}$ must be determined simultaneously using a numerical integration procedure.

2.4.2 Numerical Integration Procedure

A typical element of length "a" of the column deflection curve is shown in Fig. 2.4. The x and y displacements at i are denoted by u_i and v_i respectively and those at i+1 by u_{i+1} and v_{i+1}. A projection of the element in Fig. 2.4 onto the y-z plane is shown in Fig. 2.5 (a). In this figure, Θ_i^x and Θ_{i+1}^x are the slopes of the column deflection curve at i and i+1 respectively, ψ^x is the change in slope between i and i+1 and δ_v is the deflection of $i+1$ from the tangent to the column deflection curve at i. Assuming that the projection of the element onto the y-z plane is a flat circular arc, δ_v is given by

$$\delta_v = \frac{a}{2} \tan \psi^x \tag{2.3}$$

since ψ^x is a small angle

$$\tan \psi^x = \psi^x = a\,\phi_i^x$$

and

$$\delta_v = \frac{a^2}{2}\,\phi_i^x \tag{2.4}$$

where ϕ_i^x is the x axis curvature at i

From geometry, the deflection at i+1 in the y direction is

$$v_{i+1} = v_i + a \sin \Theta_i^x - \delta_v \cos \Theta_i^x \tag{2.5}$$

and the slope of the deflection curve at $i+1$ is

$$\theta^x_{i+1} = \theta^x_i - \psi^x \qquad (2.6)$$

By considering the projection of the element onto the x-z plane, Fig. 2.5 (b), it can be shown that

$$\mu_{i+1} = \mu_i + a \sin\theta^y_i - \delta_u \cos\theta^y_i \qquad (2.7)$$

$$\theta^y_{i+1} = \theta^y_i - \psi^y \qquad (2.8)$$

Substituting for δ_v, ψ^x, δ_u and ψ^y and making the assumption that θ^x_i and θ^y_i are small angles, the equations for the displacements and rotations at $i+1$ in terms of those at i are written as

$$\nu_{i+1} = \nu_i + a\,\theta^x_i - \frac{a^2}{2}\phi^x_i \qquad (2.9)$$

$$\mu_{i+1} = \mu_i + a\,\theta^y_i - \frac{a^2}{2}\phi^y_i \qquad (2.10)$$

$$\theta^x_{i+1} = \theta^x_i - a\,\phi^x_i \qquad (2.11)$$

$$\theta^y_{i+1} = \theta^y_i - a\,\phi^y_i \qquad (2.12)$$

At this point it is convenient to introduce certain quantities which are used to put Eq. 2.9 to 2.12 into dimensionless form. These quantities are

P_y = yield load $= E\,\epsilon_y A_c$

M^x_y = yield moment $= E\,I^x \phi^x_y$

E = Young's Modulus for the Material

A_c = cross sectional area $= 2(K_3 + 2K_1K_2)D^2$

ϕ^x_y = yield curvature $= \dfrac{\epsilon_y}{(1+K_2)D}$

$$I^x = \frac{2}{3}K_3 D^4 + 4K_1K_2\left(1+\frac{K_2}{2}\right)^2 D^4$$

$$\theta^x_y = \frac{\pi}{3}\cdot\frac{\sqrt{\epsilon_y}}{1+K_2}\cdot\Lambda_x$$

Λ_x = radius of gyration $= \sqrt{\dfrac{I^x}{A_c}}$

where ϵ_y is the yield strain of the material and θ^x_y is the rotation caused by a moment of magnitude $M^x{}_y$ acting at one end of a simply supported beam of length $\pi \Lambda_x / \sqrt{\epsilon_y}$. Using these quantities, Eqs. 2.9 to 2.12 are written in dimensionless form as

$$\frac{v_{i+1}}{D} = \frac{v_i}{D} + \frac{a}{D}\cdot\frac{\pi}{3}\frac{\sqrt{\epsilon_y}}{1+K_2}\cdot\Lambda_x\frac{\theta^x{}_i}{\theta^x{}_y} - \frac{\epsilon_y}{2}\left(\frac{a}{D}\right)^2\frac{1}{(1+K_2)}\frac{\phi^x{}_i}{\phi^x{}_y} \qquad (2.13)$$

$$\frac{u_{i+1}}{D} = \frac{u_i}{D} + \frac{a}{D}\cdot\frac{\pi}{3}\frac{\sqrt{\epsilon_y}}{1+K_2}\cdot\Lambda_x\frac{\theta^y{}_i}{\theta^x{}_y} - \frac{\epsilon_y}{2}\left(\frac{a}{D}\right)^2\frac{1}{(1+K_2)}\frac{\phi^y{}_i}{\phi^x{}_y} \qquad (2.14)$$

$$\frac{\theta^x{}_{i+1}}{\theta^x{}_y} = \frac{\theta^x{}_i}{\theta^x{}_y} - \frac{3}{\pi}\left(\frac{a}{D}\right)\frac{\sqrt{\epsilon_y}}{\Lambda_x}\frac{\phi^x{}_i}{\phi^x{}_y} \qquad (2.15)$$

$$\frac{\theta^y{}_{i+1}}{\theta^x{}_y} = \frac{\theta^y{}_i}{\theta^x{}_y} - \frac{3}{\pi}\left(\frac{a}{D}\right)\frac{\sqrt{\epsilon_y}}{\Lambda_x}\frac{\phi^y{}_i}{\phi^x{}_y} \qquad (2.16)$$

It should be noted that the panel length "a" is now expressed in terms of D.

At any point on a column deflection curve (Fig. 2.4)

$$M^y = Pu$$

$$M^x = Pv$$

To construct the curve, the displacements (including rotations) are specified at a point such as B, the moments calculated, and the curvatures found by the procedure given in Section 2.5. Deflections and rotations at the next panel paint are calculated using Eqs. 2.13 to 2.16, where the subscript "i" corresponds to point B. Once the deflections at i+1 are found, this point becomes the point i and the procedure is repeated to find the deflections at the next panel point. This process is continued until the desired column length is reached. The accuracy of the deflections at i+1 is increased by first obtaining the deflections at i+1 assuming that the curvatures at i are constant from i to i+1. Using these deflections at i+1, curvatures at this point are determined and a second set of deflections at $i+1$ calculated, using the average of the curvatures at i and $i+1$.

The part of the column deflection curve (Fig. 2.4) between A and B represents the deflected shape ofthe column shown in Fig. 2.1 provided that the moments at A and B in both figures are the same. To obtain column deflection curves that are readily usable in this study requires a proper selection of initial conditions. For columns having equal moments about the x axis and equal moments about the y axis ($\beta = 1$), the point C, mid-way on the column, is selected to have zero θ_c^x and θ_c^y and a combination of displacements, u and v. Because of symmetry, only half the column length need be considered for these particular boundary conditions, For a specified v_c , u_c is found such that the combination would give a moment ratio at A equal to γ if the column were to remain elastic. The resulting column deflection curve is as shown in Fig. 2.4. If the calculated ratio, $\frac{M_A^y}{M_A^x}$, is equal to the specified γ , plus or minus an allowable amount of error, a permissible end moment has been determined and one point on the moment deflection curve obtained. If the calculated ratio is not equal to γ, plus or minus the allowable amount of error, u_c is corrected and a new column deflection curve found.

The specified v_c is incremented by trial and error so that sufficient points on the moment-deflection curve are obtained. Corrections to M_c are explained using the curve shown in Fig. 2.6. The problem is to find a value of u_c which, when combined with v_c , will give a moment ratio sufficiently close to the specified ratio,

γ. This is accomplished by approximating the curve by a series of secants. Initially the point a on the curve is calculated using the value of u_c obtained from elastic theory. A new point d is calculated from a displacement u_{c_2} which is found by extending the secant o a until it intersects the value γ at point c. If necessary, a third approximation is made using the extended secant ad which results in displacement u_{c_3} and the point f on the curve. This process is repeated until the desired accuracy is reached or until the slope of the secant becomes negative, a negative slope indicating that the curve has reached a maximum moment ratio below the value γ. In the latter case, it is evident that, for the specified v_c, no value of u_c can be found for γ; therefore, v_c must be decreased, It should be noted that in many cases the first approximation to v_c resulted in a moment ratio sufficiently close to γ.

In studying columns with moments at one end only ($\beta = 0$), the point B is selected to have zero u and v displacements and a combination of rotations θ_B^y and θ_B^x. Since there is no symmetry, the entire length of the column must be considered. The integration is started at point B and θ_B^y and θ_B^x play the same role as v_c and u_c for the case $\beta = 1$. Because of a shortage of time, no columns with $\beta = 0$ or with β of other values were studied although this would be quite simple to do by making a proper choice of initial conditions.

2.5 Load - Moment - Curvature Relationship

2.5.1 General Procedure

The procedure given in section 2.4 requires that a relationship between moments and curvatures be determined for a constant axial load and specific cross section. This relationship can be represented by the curves shown in Figs. 2.9 and 2.10. Each of the curves of Fig. 2.9 represents the variation of M^x with ϕ^x for constant values of ϕ^y while those of Fig. 2.10 represent the variation of M^y with ϕ^y for constant values of ϕ^x. The developement and use of these curves is considered in the following paragraphs and specific equations for the wide flange section are given in section 2.5.2.

Assuming that plane sections remain plane, and neglecting residual stresses, the normal strain on a cross section at any point (x, y) may be written as

$$\epsilon = \phi^x \cdot y + \phi^y \cdot x + \epsilon_o \qquad (2.17)$$

where ϵ_o is a uniform normal strain and ϕ^x and ϕ^y are the curvatures about the x and y axes respectively. With reference to the stress strain curve of Fig. 2.3, the corresponding stress distribution is

$$\sigma = E\epsilon - E[\epsilon \pm \epsilon_y] \qquad (2.18)$$

The brackets have the significance that when the absolute value of ϵ is less than ϵ_y, the term in the brackets is zero. When ϵ is negative the plus sign is used for the term inside the brackets and when ϵ is positive, the negative sign is used for the term inside the brackets.

For the equilibrium of the cross section

$$P = \int_A \sigma \, dA \qquad 2.19$$

Combining equations 2.18 and 2.19 gives

$$P = E\int_A \epsilon \, dA - E\int_A [\epsilon \pm \epsilon_Y] \, dA \qquad (2.20)$$

Similar expressions for the moments are given by Eqs. 2.21 and 2.22

$$M^x = E\int_A y\epsilon \, dA - E\int_A y[\epsilon \pm \epsilon_Y] \, dA \qquad (2.21)$$

$$M^y = E\int_A x\epsilon \, dA - E\int_A x[\epsilon \pm \epsilon_Y] \, dA \qquad (2.22)$$

In Eqs. 2.20 to 2.22, the first integral gives the value of the load or moment if the section were everywhere elastic and the second integral is considered a correction to account for yielding of the cross section, and as such its value will depend on the amount and position of yielding.

The 25 possible yield configurations for the wide flange section are shown in Fig. 2.11(b). The 25 different yield configurations can be arrived at by considering all the possible yield patterns of the top and bottom flanges as shown in Fig. 2.11(a). The different combinations of these top and bottom patterns, with elimination of impossible situations, will yield the 25 patterns used in the analysis. For each of the yield configurations, Eqs. 2.20 to 2.22 have forms in terms of the specified values of the section dimensions, P, ϕ^x, ϕ^y, and ϵ_o. Using these equations, the curves of Figs. 2.9 and 2.10 are developed in the following manner.

1) For a given value of P, the curvatures, ϕ^x and ϕ^y are specified, leaving ϵ_o the only unknown in equation 2.17.

2) Using equation 2.20, a value of ϵ_o is determined that corresponds to the specified ϕ^x, ϕ^y, P , and an assumed yield configuration. It is necessary to assume a yield configuration because of the different form of equation 2.20 for each configuration. The yield configuration that corresponds to the calculated ϵ_o is found and compared to the one assumed. If these are not the same, a new configuration must be assumed and a new value of ϵ_o calculated. The magnitudes of the bending strains at the corners of the section control the sequence of assumed yield configurations. Fig. 2.12 shows the sequence used in this study.

3) When ϵ_o is finally determined, Eqs. 2.21 and 2.22 are used to find M^x and M^y.

4) By varying ϕ^x and ϕ^y systematically over the desire range of curvatures, the required curves are determined.

The curves of Figs. 2.9 and 2.10 are developed for the load under consideration before the numerical integration is begun. Using these curves, the values of the curvatures for any combination of M^x and M^y are determined as follows:

1) For any value of M^x (for example, M^x_o), the combinations of curvatures resulting in this moment are found at the intersections of M^x_o with the constant ϕ^y curves of Fig. 2.9. A plot of these intersections is shown as curve A in Fig. 2.15.

2) For any value of M^y (for example, M^y_o) the combinations of curvatures resulting in this moment are found at the intersection of M^y_o with the constant ϕ^x curves of Fig. 2.10. A plot

of these intersections is shown as curve B in Fig. 2.13.

3) The resulting curvatures for M^x_o and M^y_o acting together are determined by the intersection of curve A (step 1) with curve B (step 2). These are designated as ϕ^x_o and ϕ^y_o in Fig. 2.13.

2.5.2 Developement of the Load - moment - Curvature Equations

The load - moment - curvature relationship for the wide flange section is developed from Eqs. 2.20, 2.21 and 2.22. Dividing these equations by the appropriate factors given in Section 2.4 results in the dimensionless equations,

$$\frac{P}{P_y} = \frac{D^2}{A}\int_A \frac{\epsilon}{\epsilon_y}\frac{dA}{D^2} - \frac{D^2}{A}\int_A \left[\frac{\epsilon}{\epsilon_y} \pm\right]\frac{dA}{D^2} \qquad (2.23)$$

$$\frac{M^x}{M^x_y} = \frac{D^4}{I^x}(1+K_2)\int_A \frac{y}{D}\frac{\epsilon}{\epsilon_y}\frac{dA}{D^2} - \frac{D^4}{I^x}(1+K_2)\int_A \frac{y}{D}\left[\frac{\epsilon}{\epsilon_y} \pm 1\right]\frac{dA}{D^2} \qquad (2.24)$$

$$\frac{M^y}{M^x_y} = \frac{D^4}{I^x}(1+K_2)\int_A \frac{x}{D}\frac{\epsilon}{\epsilon_y}\frac{dA}{D^2} - \frac{D^4}{I^x}(1+K_2)\int_A \frac{x}{D}\left[\frac{\epsilon}{\epsilon_y} \pm 1\right]\frac{dA}{D^2} \qquad (2.25)$$

where $A_c = 2(K_3 + 2K_1K_2)D^2 =$ the area of the cross section

$$I^x = \frac{2}{3}K_3D^4 + 4K_1K_2(1+K_2/2)^2D^4 =$$ the moment of inertia of the cross section about the x axis.

The first integral in each equation represents the volume (or the first moment of the volume) of the ϵ/ϵ_y distribution and may be written as,

$$\frac{D^2}{A_c}\int_A \frac{\epsilon}{\epsilon_y}\frac{dA}{D^2} = \frac{\epsilon_o}{\epsilon_y}$$

$$\frac{D^4}{I^x}(1+K_2)\int_A \frac{y}{D}\frac{\epsilon}{\epsilon_y}\frac{dA}{D^2} = \frac{\phi^x}{\phi^x_y}$$

$$\frac{D^4}{I^x}(1+K_2)\int_A \frac{x}{D}\frac{\epsilon}{\epsilon_y}\frac{dA}{D^2} = \frac{I^y}{I^x}\frac{\phi^y}{\phi^x_y}$$

where $I^y = \frac{1}{6}\left[8K_1^3K_2 + K_3^3\right] =$ the moment of inertia of the cross section about the y axis.

The second integral in each equilibrium equation is the volume (or the first moment of the volume) of the $\left[\frac{\epsilon}{\epsilon_y} \pm 1\right]$ distribution. The required volume was derived for each of the 25 yield configurations by the process described later on this page . An example of such a derivation for the top flange is shown using Fig. 2.14. These volumes, having been derived for the possible yield patterns of the top flange can be arrived at for the bottom flange and for the web by simply changing the strain numbers to suit the situation. The results are then combined, i. e., top and bottom flanges and the web, to give the equations for the 25 different yield configurations. The volumes to be subtracted for each type of yielding are found by drawing the total strain distribution diagram for the flange or web under consideration as in Fig. 2.14 . The strain at i is a compressive strain and the strain at j is a tensile one. By proportion, it is found that

$$2a_{ij}\, K_1 D = \frac{\epsilon_i + \epsilon_y}{\epsilon_i - \epsilon_j}\, K_1 D$$

$$2a_{ji}\, K_1 D = \frac{\epsilon_j - \epsilon_y}{\epsilon_j - \epsilon_i}\, K_1 D$$

The strain at any point (x, y) in terms of the yield strain is given by Eq. 2.17 divided by ϵ_y and with x and y expressed in terms of D

$$\frac{\epsilon}{\epsilon_y} = \frac{y}{D}\,\frac{\phi^x}{\phi^x_y}\,\frac{1}{1+K_2} + \frac{x}{D}\,\frac{\phi^y}{\phi^x_y}\,\frac{1}{1+K_2} + \frac{\epsilon_o}{\epsilon_y}$$

The first two terms on the right hand side represent "bending strains" and depend only on the values of the curvatures and the section dimensions. The third term depends on the magnitude of the axial load. The strain at either end is found by substituting the end coordinates into the strain equation. $\bar{\epsilon}_i$ is used to denote the "bending strains" at i and $\bar{\epsilon}_j$ to represent those at j. The shaded volumes are calculated and these are the "correction factors" for equ'n 2.20. In Fig. 2.14 , the expression for $\frac{P}{P_y}$ is

$$\frac{P}{P_y} = \epsilon_o - \frac{1}{2(K_3+2K_1K_2)D^2}\Big[2a_{ij}\,K_1D(\epsilon_i+1)\cdot\tfrac{1}{2}K_2D + 2a_{ji}\,K_1D(\epsilon_j-1)\tfrac{1}{2}K_2D\Big]$$

or $$\frac{P}{P_y} = \epsilon_o - \frac{K_1K_2}{2(K_3+2K_1K_2)}\left[\left(\frac{(\bar{\epsilon}_i+\epsilon_o+1)^2}{\bar{\epsilon}_i-\bar{\epsilon}_j}\right)+\left(\frac{(\bar{\epsilon}_j+\epsilon_o-1)^2}{\bar{\epsilon}_j-\bar{\epsilon}_i}\right)\right]$$

where all strains are understood to be divided by ϵ_y. Multiplying this equation by -1 and expanding, a quadriatic equation in ϵ_o is arrived at. The equation is of the form

$$Q\,\epsilon_o^2 + R\,\epsilon_o + S = 0$$

where

$$Q = \frac{A}{\bar{\epsilon}_i-\bar{\epsilon}_j} + \frac{A}{\bar{\epsilon}_j-\bar{\epsilon}_i} = 0$$

$$R = 2A\left[\frac{\bar{\epsilon}_i+1}{\bar{\epsilon}_i-\bar{\epsilon}_j} + \frac{\bar{\epsilon}_j-1}{\bar{\epsilon}_j-\bar{\epsilon}_i}\right] - 1$$

$$S = A\left[\frac{(\bar{\epsilon}_i+1)^2}{\epsilon_i-\epsilon_j} + \frac{(\bar{\epsilon}_j-1)^2}{\bar{\epsilon}_j-\bar{\epsilon}_i}\right] + \frac{P}{P_y}$$

$$A = \frac{K_1K_2}{2(K_3+2K_1K_2)}$$

In this case, $Q=0$ and the equation in ϵ_o takes the form

$$R\,\epsilon_o + S = 0$$

or $$\epsilon_o = -S/R$$

If Q is non zero, then ϵ_o is described by

$$\epsilon_o = \frac{-R-\sqrt{R^2-4QS}}{2Q}$$

For this analysis, the equations are all linear or quadratic. In this example, of course, the strain in only one flange was considered. To arrive at the net equation in ϵ_o, the expressions for Q, R and S for the two flanges and the web are derived and the results superimposed. Expressions for Q, R, and S for all possible flange and web yield patterns are given in table 2.1.

Once $\frac{\epsilon_o}{\epsilon_y}$ has been found for the given ϕ^x/ϕ^x_y, ϕ^y/ϕ^x_y, and P/P_y, a check load and the bending moments are found using a summationprocedure. Essentially, this procedure divides the section into small elements (20 elements per flange, web). The stress corresponding to strain at the centre of each element is found and the contribution of each element to the load or to the moment is determined. Total loads and moments are calculated by summing the contributions from each element. The load determined in this manner is checked against the specified load and thus a number of programming and derivation errors were eliminated. If the calculated load agrees with the original load, the calculated moments are regarded as legitimate output and are used in the column integration procedure.

2.5.3 Introduction of Residual Stresses

Residual stresses are stresses set up in the member due to cooling. Their distribution is generally assumed to be that of Fig. 2.15. These stresses are compressive at the flange tips and tensile at the centre. Sharma (20) uses a σ_{rc} (compressive residual stress) of 12 Ksi and assumes σ_{rt} (tensile residual stress) to be constant along the web. The magnitude of σ_{rt} is such to maintain equilibrium of the cross section. Adding the strain distribution due to residual stresses of 2.16 (b) to the strain distribution of Fig. 2.16 (a) will result in the distribution of Fig. 2.16 (c). The equation describing the magnitude of the resudual strain at any point (x,y) in the cross section is

$$\epsilon_R = \frac{\epsilon_c - \epsilon_t}{b} |x| + \epsilon_t$$

where ϵ_c = compressive residual strain at the tips of the flanges

ϵ_t = tensile residual strain at the centre of the flanges

b = width of half section

ϵ_R = residual strain at any point (x, y)

Therefore, the total strain equation now becomes

$$\epsilon = \phi^x \cdot y + \phi^y \cdot x + \epsilon_o + z|x| + \epsilon_t$$

where $z = \frac{\epsilon_c - \epsilon_t}{b}$

or, non dimensionalizing

$$\frac{\epsilon}{\epsilon_Y} = \frac{\phi^x}{\phi^x_Y} \cdot \frac{y}{D} \cdot \frac{1}{1+K_2} + \frac{\phi^y}{\phi^x_Y} \cdot \frac{x}{D} \cdot \frac{1}{1+K_2} + z\left|\frac{x}{D}\right| + \frac{\epsilon_t}{\epsilon_Y}$$

where
$$z = \frac{\epsilon_c/\epsilon_Y - \epsilon_t/\epsilon_Y}{b/d}$$
$$= \frac{\epsilon_c/\epsilon_Y - \epsilon_t/\epsilon_Y}{K_1}$$

Because of the introduction of residual stresses to the analysis, the number of possible yield configurations increases considerably. The possible configurations are again arrived at by considering the types of yielding that could occur in the top and bottom flanges and superimposing the results.

The possible yield configurations are as shown in Fig. 2.17 (a).

The constants Q, R and S for the yield patterns have been derived and are listed in Table 2.2. The strain distribution and subsequent equations for Q, R and S for the web will be the same as for the case with no residual stress with the exception that the constant ϵ_{rt} will be added to all of the strains. When the different equations are combined to form a yield pattern for the cross section, P/P_y must be added to the expression for S to make it complete. This necessity arises from the fact that in deriving the expressions, the load in only that branch of the total cross section under consideration is taken into account. The expression $P = f(\epsilon)$ results in P occurring in the last coefficient S of the quadratic expression. Summing the three S's, i. e. for the two flanges and for the web will yield the total P for the cross section. It is therefore simpler to add P to the total expression for S than to add a part of it to each particular branch of the cross section.

To illustrate the procedure outlined, consider the example of Fig. 2.18. Configuration 1 and configuration 12 are united to give the resulting total yield configuration for the cross section, the yield configuration for the web automatically determined by the two flanges. Therefore, the expressions for Q, R and S will be found by combining 1 , 12 , and 19 from table 2.2 and adding P/P_y to the resulting expression for S. The equations are then

$$Q = \frac{A^*}{2(\bar{\epsilon}_5 - \bar{\epsilon}_1)} + 0 + 0 = \frac{A}{2(\bar{\epsilon}_5 - \bar{\epsilon}_1)}$$

$$R = A\left(\frac{\bar{\epsilon}_5 - 1}{\bar{\epsilon}_5 - \bar{\epsilon}_1} - 1\right) + 0 + 2B^*\left[\frac{\bar{\epsilon}_5 - \bar{\epsilon}_6 - 2}{\bar{\epsilon}_5 - \bar{\epsilon}_6} - 1\right]$$

$$S = A\left[\frac{(\bar{\epsilon}_5 - 1)^2}{2(\bar{\epsilon}_5 - \bar{\epsilon}_1)} - \frac{\bar{\epsilon}_5 + \bar{\epsilon}_1}{2} - 1\right] + 0 + B\left[\frac{(\bar{\epsilon}_5 + \bar{\epsilon}_6)(\bar{\epsilon}_5 - \bar{\epsilon}_6 + 2)}{\bar{\epsilon}_5 - \bar{\epsilon}_6}\right] + \frac{P}{P_y}$$

*Symbols A and B are defined in the Nomenclature.

2.5.4 Twisting Displacements

As mentioned previously, the effect of twisting on the strength of the column has been shown to be small in many cases (20) and has been neglected in this study. However, an approximate procedure whereby these displacements could easily be in corporated in the analysis is given in this section. This procedure is based on the following assumptions:

1) The shear center and centroid of the cross section coincide, i. e. the effect of partial yielding of the cross section on the position of the shear center is neglected.
2) Twisting displacements of the column vary according to the equation

$$\alpha = \alpha_0 \sin \frac{\pi z}{L} \tag{2.26}$$

where α = twisting displacement at z

α_0 = twisting displacement at mid height of of the column.

3) The yield pattern in the flanges at any inelastic cross section is the same as that at mid height of the column.

Assumptions 1 and 2 have been used by previous investigatiors (20). Assumption 3 is used to determine the effect of warping strains on the principal axis curvatures and since these strains are small, it should be a reasonable assumption.

According to Timoshenko and Gere (21) the warping strain of a thin-walled, open cross section subjected to twisting is given

248693

by $$\epsilon_z = \frac{\partial \omega}{\partial z} = (\bar{\omega}_s - \omega_s)\frac{d^2\alpha}{dz^2}$$

where $$\omega_s = \int_0^S r\,ds$$

$$\bar{\omega}_s = \frac{1}{m}\int_0^S r\,ds$$

ω = warping displacement

m = the length of centre line of the cross section.

α = the angle of rotation of any corss section.

r = the radial distance from the axis of rotation to a point on the centre line of the cross section.

ϵ_z = the warping strain set up in the cross section caused by the warping displacements

and S is measured along the centreline of the cross section.

In this study it is necessary to apply this equation to a wide flange section subjected to biaxial loading, the section having some plastic yielding.

In order to evaluate ω, the extent of yielding in the cross section must be known, as only the unyielded portion of the cross section can contribute to the strength of the section. Since the warping strains are small compared to the bending strains, it should suffice to determine the yielded portion of the cross section neglecting twist. The extent of the yielding can easily be calculated if ϕ^x, ϕ^y and ϵ_o are known by using Eq. 2.17. The procedure for determining the constant - curvature - moment - curvature curves requires that ϵ_o be determined for predetermined combinations of ϕ^x and ϕ^y. These calculated values of ϵ_o can easily be used to determine ϵ_o for any combination of curvatures not specified. $\bar{\omega}_s$ and ω_s can then be calculated using only that portion of the cross section which remains elastic.

The problem remaining is to find a value for α_o (Eq. 2.26). The torsional moment is given by the equation

$$M^z = M_A^x \frac{du}{dz} + M_A^y \frac{dv}{dz} + \frac{d\alpha}{dz} \int_A \sigma_c r^2 dA \qquad (2.28)$$

The resisting torsional moment can be divided into two parts; the part called M_1^z, due to pure torsion and the part M_2^z, due to warping of the cross section. The first part is

$$M_1^z = C \frac{d\alpha}{dz} \qquad (2.29)$$

where C is the St. Venant torsional stiffness for the section, which for small angles of twist is normally assumed to be unaffected by partial yielding of the cross section due to normal stresses. The second part is

$$M_2^z = -C_\omega \frac{d^3\alpha}{dz^3} \qquad (2.30)$$

where C_ω is the warping constant. According to Sharma (20)

$$M_2^z = -Eh^2(I_{f_1} + I_{f_2}) \frac{d^3\alpha}{dz^3} \qquad (2.31)$$

where $I_{f_1} + I_{f_2}$ = moment of intertia of the elastic portion of the cross section about the y-axis

and h = depth of the section

For equilibrium of the cross section

$$M^z = M_1^z + M_2^z$$

Substituting from Eqs. 2.28, 2.29, and 2.31 into Eq. 2.32 gives

$$M_A^x \frac{dv}{dz} - M_A^y \frac{du}{dz} + \frac{d\alpha}{dz} \int_A \sigma_c r^2 dA$$

$$= C \frac{d\alpha}{dz} - Eh^2(I_{f_1} + I_{f_2}) \frac{d^3\alpha}{dz^3} \qquad (2.33)$$

Differentiating with respect to z , Eq. 2.33 becomes

$$M_A^x \phi^y - M_A^y \phi^x + \frac{d^2\alpha}{dz^2} \int_A \sigma_c r^2 dA =$$

$$C \frac{d^2\alpha}{dz^2} - E h^2 (I_{f_1} + I_{f_2}) \frac{d^4\alpha}{dz^4} \tag{2.34}$$

$\int_A \sigma_c r^2 dA$ can be evaluated once the yield configuration is known. The quantity $E(I_{f_1} + I_{f_2})$ can be evaluated by the expression

$$E(I_{f_1} + I_{f_2}) = \frac{M^y}{\phi^y} \tag{2.35}$$

Using the assumed variation of α (Eq. 2.36) and $z = \frac{L}{2}$ in Eq. 2.34 yields

$$\alpha_o = \frac{M_A^x \phi^y - M_A^y \phi^x}{(\frac{\pi}{L})^2 [\int_A \sigma_c r^2 dA - C - (\frac{h\pi}{L})^2 \frac{M^y}{\phi^y}]} \tag{2.36}$$

where all quantities are evaluated at the mid height of the column ($z = \frac{L}{2}$).

Having established α_o and the yield configuration, the warping strains can be calculated from Eq. 2.27 and their effect on the strength of the cross section at mid height, or any location for that matter, can be readily determined. Referring to Fig. 2.20, the change in the extent of yielding due to warping strains is shown cross hatched and may result in either an increase or decrease in the amount of yielding. The amount of the change can be readily determined by geometry. This change in yielding will change the effective moments of inertia (moments of inertia of the elastic portion of the cross section), the amount of which is readily calculated. Let

$\Delta I_o^x, \Delta I_o^y$ = change in the effective moments of inertia at the mid heights of the column about the x and y axes respectively. Positive values correspond to a decrease in moment of inertia.

By using assumption 3 (page 25), the change in the moments of inertia at any point z on the cross section are approximated by

$$\Delta I^{x} = \Delta I_{o}^{x} \sin \frac{\pi z}{L} \tag{2.37}$$

$$\Delta I^{y} = \Delta I_{o}^{y} \sin \frac{\pi z}{L} \tag{2.38}$$

Knowing ΔI^{x} and ΔI^{y}, the change in curvatures at any point can be found as

$\Delta \phi^{x}$ = change in x-axis curvature due to warping strains

$$= -\left[\frac{M^{x}}{E(I^{x})} - \frac{M^{x}}{E(I^{x}-\Delta I^{x})}\right] \tag{2.39}$$

$\Delta \phi^{y}$ = change in y-axis curvature due to warping strains

$$= -\left[\frac{M^{y}}{E(I^{y})} - \frac{M^{y}}{E(I^{y}-\Delta I^{y})}\right] \tag{2.40}$$

It should be noted that if ΔI_{o}^{x} or ΔI_{o}^{y} are negative (the moments of inertia increase), the curvature decreases.

A further consequence of twisting is that moments about the principal axes are no longer simply M^{x} and M^{y}. Refering to Fig. 2.21, it is apparent that moments on the rotated cross section must be referred to the ξ and η axes. It can be shown that

$$M^{\xi} = M^{x} + \alpha M^{y} \tag{2.41}$$

$$M^{\eta} = M^{y} - \alpha M^{x} \tag{2.42}$$

$$\phi^{x} = \phi^{\xi} - \alpha \phi^{\eta} \tag{2.43}$$

$$\phi^{y} = \phi^{\eta} - \alpha \phi^{\xi} \tag{2.44}$$

where the superscripts refer to the axis in Fig. 2.21. Eqs. 2.41 to 2.44 are used to transform from one axis system to the other.

Making use of the equations developed in the proceeding paragraphs, the following procedure is suggested for the inclusion of twist in the analysis:

1) Assume (as usual) a pair of mid height displacements u and v.
2) Neglecting twist, determine a column deflection curve for the displacements of step 1.
3) Using the column deflection curve of step 2, determine (from Eq. 2.36), the yield configuration at mid height, and ΔI_o^x and ΔI_o^y.
4) Construct a new column deflection curve for the u and v displacements of step 1 and the assumed twisting (Eq. 2.26) using the following procedure:
5) At a panel point i calculate

$$M_i^x = P v_i$$
$$M_i^y = P \mu_i$$

Using these moments find the moments about the rotated principal axes using Eqs. 2.41 and 2.42.

6) Determine the curvatures ϕ_i^ξ and ϕ_i^η using the procedure given in Sec 2.5.1 and apply the corrections given by Eqs. 2.39 and 2.40.
7) Determine ϕ_i^x and ϕ_i^y using Eqs. 2.43 and 2.44. Find the displacements at i + 1 using Eqs. 2.13 to 2.16.
8) Go to the next panel point (which now becomes i and repeat

steps 5 to 7. Repeat until the desired length of column is reached.

9) Check the ratio $\frac{M_A^A}{M_A^x}$ with γ as usual and modify the assumed mid height displacements accordingly.

The procedure given on preceding pages is good for equal end moments. However, if different boundary conditions are considered, the assumption that α varies sinusoidally is no longer reasonable. Consider the case where the bending moments at one end are zero ($\beta = 0$). Since the transcendental functions are symmetric, we will simply modify the former function to fit the new situation. Fig. 2.19 depicts the manner in which this might be done. The column is divided at the point of maximum deflection as before. The difference now is that the point of maximum deflection is not at the centre due to the unsymmetrical boundary conditions. One function will not describe the twisting behavior of both parts of the column and thus we will use the two functions $\alpha = \alpha_o \sin \frac{\pi z}{L_1}$ and $\alpha = \alpha_o \sin \frac{\pi z}{L_2}$, where L_1 and L_2 are the lengths of column above and below the point of maximum deflection respectively. The first equation applies for z from 0 to L_1 and the second for z from L_1 to L_2. For a known δ_{max}, L_1 and L_2 can be determined neglecting twist and α_o can be calculated in much the same manner as for the equal end moment case. Once the variation of α is known, the twisting displacements can be included in the manner just described.

Chapter III - Computations

3.1 Computer Programs

The procedure used in this project necessitated the extensive use of a computer. During the study an IBM 1620, and IBM 7040 and an IBM 360/40 computer were used. In this respect the analysis contains ample variety.

Two sets of programs were used to complete the analysis. The first set of programs established the constant - curvature, moment - curvature curves for the given section, loads and specified values of the curvatures. The equations used in this program and the flow of the program had to be developed from scratch, so to speak, and the "debugging" process was quite tedious because of the relatively large number of yield configurations. To further complicate matters, the IBM 1620 computer was the only machine available during the initial writing and "debugging" of the program. Because of the limited capacity of this machine, the program controlling the sequence of assumed yield configurations, i. e. the moment curvature program, was divided into four parts, according to the O, A, B and C divisions of Fig. 2.12. The data from these four parts was then combined to form a complete set of data. This procedure greatly augmented the amount of time spent in setting up the procedure and "debugging" it. The 1620 was also very slow in execution. Thus, when the opportunity came, the four parts of the program were combined and run on a larger machine. More time was spent correcting the programs after they were combined but after this initial period of detective work, the time saved was great. One set of moment curvature curves for one axial load required about one half hour of running on the 1620 machine. On the 360/40, moment curvature curves for five loads could be run in about five minutes. Also, with the program all in one piece it was much easier to correct any errors in the equations or in the flow. The column integration program was also run on the 360/40 machine after it was available and execution time was drastically cut. Results which required six to eight hours of running on the 1620 could be run in approximately fifteen minutes on the 360/40.

The column integration program determined moment - deflection curves for the case $\beta = 1$. In this program, a curvature subprogram was used to determine specific values of curvature for the moments calculated at each panel point on the column - deflection curve. A program treating the case $\beta = 0$ was available from Scott (19) but the program was never set up and run for wide flange sections as time did not permit. It should be emphasized that although the only boundary conditions studied were $\beta = 1$ that $\beta = 0$ or $\beta = -1$ or any inbetween set of boundary conditions are also possible with only minor alterations to the programs.

3.2 Numerical Calculations

The numerical calculations involved curve interpolation and finding the coordinates of the intersection of two curves.

The curvature subprogram, used to determine specific values of curvature for the moments calculate at each panel point on the column deflection curve, requires a method of interpolating between specific points on the constant - curvature moment curvature curves. For example, the constant moment curves of Fig. 2.15 showing the relationship between ϕ^x and ϕ^y are found by interpolating from points on the curves of Figs. 2.11 and 2.12. Second-degree polynomials derived from three data points bounding the value of the independent variable were used for all interpolations. These curves have the general shape of most of the curves found in this study, at least over the limited range of three data points.

The curvature determination (Section 2.5) requires that the coordinates of the intersection of two curves be found. Two parts on each curve are selected and a linear equation is written thru each pair. The coordinates of the intersection of these two straight lines are found and compared with the coordinates of the points determining the lines. If the coordinates of the intersection are bounded by the points, an approximation to the intersection has been obtained. If the coordinates of the intersection are not bounded, then a new point on one or both curves is selected and the process repeated. Once the intersection is bounded, a second degree equation is written thru the two bounding points plus a third point on each curve. The curves are thus approximated by the equations.

$$\phi_1^y = a(\phi_1^x)^2 + b(\phi_1^x) + c$$

$$\phi_2^y = d(\phi_2^x)^2 + e(\phi_2^x) + f$$

At any intersection, the following must hold

$$\phi_1^y = \phi_2^y$$

$$\phi_1^x = \phi_2^x$$

Equating the two ϕ^y values gives a quadratic equation in ϕ^x. This is solved using Newton's second order method where the first approximation to the root is given by the linear equations written thru each pair of bounding points.

Chapter IV - Discussion of Results

4.1 General Comments

A number of factors affect the behavior of biaxially loaded columns. Among these are the relative dimensions of the cross section (K_1, K_2, K_3), the slenderness ratio L/r_y , the ratio of end moments (β), the ratio of moments at each end (γ), and the axial load (P). Consideration of all of these factors would require the solution of an extremely large number of problems. The lack of a suitable computer and available computer time limited the number of problems that could be considered. With the conversion of the program to the 360/40 system a run of 3 3/4 hours on the IBM 1620 was reduced to less than 10 minutes on the 360/40 machine. This 10 minutes of running yielded three interaction curves of five points each of the type shown in Fig. 4.1.

A number of elastic points on the moment deflection curves were obtained and served to check the computer programming. In addition, a series of hand calculations were made by Scott (19) for the square cross section with $P/P_y = 0.6$, $L/r_y = 100$, $\beta = 1$, and $\gamma = 1$, in order to check the column integration computer program. The maximum error found by these hand computations was 0.3%. In the present analysis of wide flange columns, the same column integration program was used, the only changes being in certain constants which depend on section properties.

In the develonement of the column deflection curves, the panel length, "a", was taken as no more than four times the smallest radius of gyration of the cross section; exact values were selected to give the required slenderness ratio.

4.2 Numerical Results

Interaction curves for the wide flange sections considered in this study are shown in Fig.'s 4.1 to 4.13. These curves are all for columns with $\beta = 1$. Four different sections were studied with width to depth ratios (b/d) varying from 0.6 to 1. L/r_y was varied from 60 to 90 to 120 and γ was taken as .4, .8, 1.2, 1.4 and 2.0. For the section with b/d ratio of 1, the axial load P/P_y was varied from .1 through .9 to give the interaction curves of Fig. 4.1. The interaction curves were obtained by considering a number of axial loads and calculating the ultimate or maximum moment for that particular load and section. The ultimate moment was obtained from the moment-rotation curve (Fig. 2.8) by taking the maximum moment attained by the curve. The value assumed for P/P_y was then plotted against this value of M/M_y to give one point on the interaction curve. The rest of the interaction curves have a maximum P/P_y of .3 or .5. This was due to the fact that time and space on the 1620 did not permit a larger range of loads. After installation of the 360/40, more moment-curvature curves were developed and more extensive interaction curves drawn.

From the curves it can be seen that as the load is increased, the moment carrying capacity at all slenderness ratios is substantially decreased. The effect of an increase in slenderness ratio is to decrease the load carrying capacity of the column. Decreasing the b/d ratio from 1 to .6 decreases the moment carrying capacity by about 26% for an axial load of $P/P_y = 0.1$ and by about 28% for $P/P_y = 0.3$. At all values of γ , the interaction curves shift to the right as b/d increases. In other words, for constant load, the moment capacity increases with b/d. Comparing the interaction curves at constant load shows that as γ is increased, the moment carrying capacity of the column is substantially reduced for all b/d and slenderness ratios.

No laboratory tests were performed in this study to substantiate the theory. However, a number of tests on biaxial bending of wide flange columns has been carried out in Germany and Russia. Test results obtained by Kloppel and Winkelman (13) and presented by Galambos are used to check the theoretical solution. These results are for columns loaded with equal eccentricities at each end with the load being increased to failure. The specimens were rolled steel wide-flange columns and their cross sections had width to depth ratios varying from .5 to 1. The end conditions were such that the members were essentially pinned against rotation, and warping was restrained by heavy end plates. For the most part, the interaction curves presented in Figs. 4.1 to 4.13 are for the values of γ, L/r_y and cross sections used by Kloppel and Winkelman.

Prediction of the ultimate load that an eccentrically loaded column will carry is based on the interaction curves and the fact that the relationship between load and moment for the test is given by the equation

$$M^x = Pe^x \qquad (4.1)$$

or in dimensionless form as

$$\frac{M^x}{M^x_y} = \frac{P}{P_y}\,\frac{(1+K_2)}{(\mu^x/D)^2}\left(\frac{e^x}{D}\right) \qquad (4.2)$$

This is the equation of a straight line passing through the origin where P/P_y and M^x/M^x_y are the variables and $\frac{1+K_2}{(r_x/D)^2} \cdot \frac{e^x}{D}$ is the reciprocal of the slope. Equation 4.1 is plotted on the interaction curve and its intersection with the interaction curve gives the theoretical ultimate load that the column can carry.

The results of the comparison between the theoretical and experimental loads are tabulated in table 4.1. As can be seen the theory is unconservative in all cases but three. There are possible explanations for part of the differences. It was noted in the tabulated data of the German tests that two failure loads were given for the same section in many cases. It would seem that more that one specimen of the same cross section was tested and that a maximum and a minimum value were recorded. The algebraic average of the two values was used, were available, to compare with the theoretical results. However, it is quite possible that this average is not the true mean value and that the lower axial loads are closer to the truth. Also, the effect of warping strains and residual strains was not included in the analysis. Also, it was assumed that the material used by the Germans was perfectly elastic-perfectly plastic. The yield strains needed in the column integration program were taken from the table of results presented in the paper (13) and may have only been approximations or values taken from a handbook. Sharma (20) also used these results to test his theory and he shows no better, if as good, agreement.

To further check the theory, the procedure described above was used to obtain the ultimate load on a 12 Wideflange 79 section which had been previously analysed by Birnstiel and Michalos (2). The predicted ultimate load was identical to that presented, indicating that the two theories are compatible.

Chapter V - Conclusions and Future Research

5.1 Conclusions

An analysis of a biaxially loaded column has been presented which is specifically applicable to the wide flange cross section. Since the wide flange is a commonly used section, the analysis can be used widely.

Although a relatively small amount of data was collected, the following conclusions can be made:

1) End moments at collapse are substantilly decreased with an increase in slenderness ration and/or axial load on the column.
2) An increase in minor principal axis bending moment (M^y) can substantially reduce the column's ability to carry major principal axis bending (M^x) for a given slenderness ratio and axial load.
3) Interaction curves for the biaxially loaded column can be developed for use in the design of such members.
4) Comparison of theoretical results with available experimental results shows fairly good agreement. A comparison with an "exact" analysis also showed very good agreement. It is likely that some of the error noted in the results came from the lack of the consideration of residual strain and twisting displacements in the analysis. It is unlikely that these factors could contribute more than 8 per cent to the error however (20).

5.2 Future Research

Laboratory tests on biaxially loaded wide flange columns should be made in which a high degree of control could be obtained. Specifically, material properties of each specimen tested should be exactly determined. A larger number of end conditions (end moment ratios (β) and loading conditions (P)) should be checked in order to broaden the horizons of the results of this study. The effects of warping and residual strains should be included in the analysis and these results compared with results obtained without the inclusion of these effects and with the experimental results.

Table 2.1 List of yield patterns and quadratic equation constants for the top and bottom flanges and the web for the analysis excluding residual stresses. All strains are divided by ϵ_y

YIELD PATTERN	Q	R	S
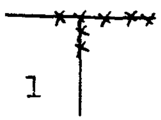 1	$\dfrac{A^*}{\bar{\epsilon}_2 - \bar{\epsilon}_1^*}$	$2A\,\dfrac{(\bar{\epsilon}_2 - 1)}{\bar{\epsilon}_2 - \bar{\epsilon}_1}$	$A\,\dfrac{(\bar{\epsilon}_2 - 1)^2}{\bar{\epsilon}_2 - \bar{\epsilon}_1}$
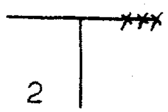 2	$\dfrac{A}{\bar{\epsilon}_2 - \bar{\epsilon}_1}$	$2A\,\dfrac{(\bar{\epsilon}_2 - 1)}{\bar{\epsilon}_2 - \bar{\epsilon}_1}$	$A\,\dfrac{(\bar{\epsilon}_2 - 1)^2}{\bar{\epsilon}_2 - \bar{\epsilon}_1}$
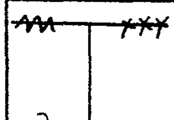 3	0	$2A\left(\dfrac{\bar{\epsilon}_2 - 1}{\bar{\epsilon}_2 - \bar{\epsilon}_1} + \dfrac{\bar{\epsilon}_1 + 1}{\bar{\epsilon}_1 - \bar{\epsilon}_2}\right)$	$A\left[\dfrac{(\bar{\epsilon}_1 + 1)^2}{\bar{\epsilon}_1 - \bar{\epsilon}_2} + \dfrac{(\bar{\epsilon}_2 - 1)^2}{\bar{\epsilon}_2 - \bar{\epsilon}_1}\right]$
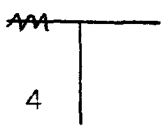 4	$\dfrac{A}{\bar{\epsilon}_1 - \bar{\epsilon}_2}$	$2A\,\dfrac{(\bar{\epsilon}_1 + 1)}{\bar{\epsilon}_1 - \bar{\epsilon}_2}$	$A\left[\dfrac{(\bar{\epsilon}_1 + 1)^2}{\bar{\epsilon}_1 - \bar{\epsilon}_2}\right]$
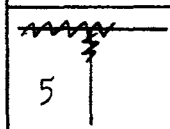 5	$\dfrac{A}{\bar{\epsilon}_1 - \bar{\epsilon}_2}$	$2A\,\dfrac{(\bar{\epsilon}_1 + 1)}{\bar{\epsilon}_1 - \bar{\epsilon}_2}$	$A\,\dfrac{(\bar{\epsilon}_1 + 1)^2}{\bar{\epsilon}_1 - \bar{\epsilon}_2}$
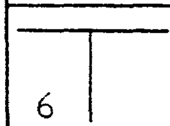 6	0	0	0
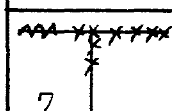 7	0	$2A\left[\dfrac{\bar{\epsilon}_2 - 1}{\bar{\epsilon}_2 - \bar{\epsilon}_1} + \dfrac{\bar{\epsilon}_1 + 1}{\bar{\epsilon}_1 - \bar{\epsilon}_2}\right]$	$A\left[\dfrac{(\bar{\epsilon}_1 + 1)^2}{\bar{\epsilon}_1 - \bar{\epsilon}_2} + \dfrac{(\bar{\epsilon}_2 - 1)^2}{\bar{\epsilon}_2 - \bar{\epsilon}_1}\right]$

Table 2.1 (cont'd)

YIELD PATTERN	Q	R	S
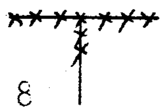 8	0	$2A$	$A(\bar{\epsilon}_1 + \bar{\epsilon}_2 + 2)$
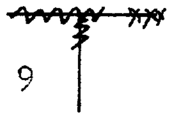 9	0	$2A\left(\frac{\bar{\epsilon}_2 - 1}{\bar{\epsilon}_2 - \bar{\epsilon}_1} + \frac{\bar{\epsilon}_1 + 1}{\bar{\epsilon}_1 - \bar{\epsilon}_2}\right)$	$A\left[\frac{(\bar{\epsilon}_1 + 1)^2}{\bar{\epsilon}_1 - \bar{\epsilon}_2} + \frac{(\bar{\epsilon}_2 - 1)^2}{\bar{\epsilon}_2 - \bar{\epsilon}_1}\right]$
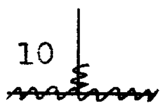 10	0	$2A$	$A(\bar{\epsilon}_3 + \bar{\epsilon}_4 - 2)$
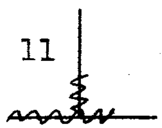 11	$\frac{A}{\bar{\epsilon}_3 - \bar{\epsilon}_4}$	$2A\,\frac{(\bar{\epsilon}_3 + 1)}{\bar{\epsilon}_3 - \bar{\epsilon}_4}$	$A\,\frac{(\bar{\epsilon}_3 + 1)^2}{\bar{\epsilon}_3 - \bar{\epsilon}_4}$
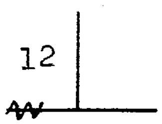 12	$\frac{A}{\bar{\epsilon}_3 - \bar{\epsilon}_4}$	$2A\,\frac{(\bar{\epsilon}_3 + 1)}{\bar{\epsilon}_3 - \bar{\epsilon}_4}$	$A\,\frac{(\bar{\epsilon}_3 + 1)^2}{\bar{\epsilon}_3 - \bar{\epsilon}_4}$
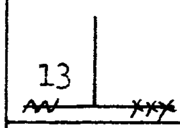 13	0	$2A\left(\frac{\bar{\epsilon}_3 + 1}{\bar{\epsilon}_3 - \bar{\epsilon}_4} + \frac{\bar{\epsilon}_4 - 1}{\bar{\epsilon}_3 - \bar{\epsilon}_4}\right)$	$A\left[\frac{(\bar{\epsilon}_3 + 1)^2}{\bar{\epsilon}_3 - \bar{\epsilon}_4} + \frac{(\bar{\epsilon}_4 - 1)^2}{\bar{\epsilon}_3 - \bar{\epsilon}_4}\right]$
 14	$\frac{B}{\bar{\epsilon}_5 - \bar{\epsilon}_6}$	$2B^*\,\frac{(\bar{\epsilon}_5 - 1)}{\bar{\epsilon}_5 - \bar{\epsilon}_6}$	$B\,\frac{(\bar{\epsilon}_5 - 1)^2}{\bar{\epsilon}_5 - \bar{\epsilon}_6}$
 15	0	$2B\left(\frac{\bar{\epsilon}_5 - 1}{\bar{\epsilon}_5 - \bar{\epsilon}_6} + \frac{\bar{\epsilon}_6 + 1}{\bar{\epsilon}_6 - \bar{\epsilon}_5}\right)$	$B\left[\frac{(\bar{\epsilon}_5 - 1)^2}{\bar{\epsilon}_5 - \bar{\epsilon}_6} + \frac{(\bar{\epsilon}_6 + 1)^2}{\bar{\epsilon}_6 - \bar{\epsilon}_5}\right]$

Table 2.1 (cont'd)

YIELD PATTERN	Q	R	S
16 	$\dfrac{B}{\bar{\epsilon}_6 - \bar{\epsilon}_5}$	$2B\dfrac{(\bar{\epsilon}_6+1)}{\bar{\epsilon}_6 - \bar{\epsilon}_5}$	$B\dfrac{(\epsilon_6+1)^2}{\bar{\epsilon}_6 - \bar{\epsilon}_5}$
17 	0	$2B - 1$	$B(\bar{\epsilon}_5 + \bar{\epsilon}_6 - 2)$

$$* \; A = \frac{K_1 K_2}{2(K_3 + 2K_1K_2)}$$

$$B = \frac{K_3}{2(K_3 + 2K_1K_2)}$$

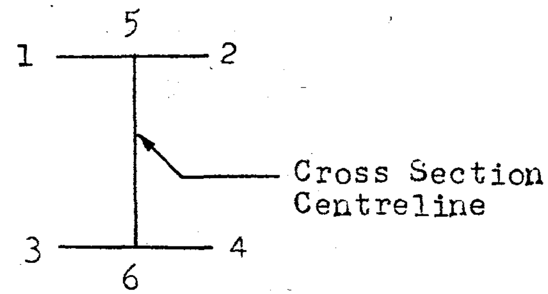

$\bar{\epsilon}_1 = \epsilon_1 - \epsilon_0$

= bending strain at point 1

Table 2.2 List of yield patterns and quadratic equation constants for the top and bottom flanges for the analysis with residual stresses. All strains are divided by ϵ_y

YIELD PATTERN	Q	R	S
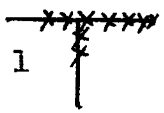	$\frac{A^*}{2(\bar\epsilon_5^* - \bar\epsilon_1)}$	$A\left(\frac{\bar\epsilon_5 - 1}{\bar\epsilon_5 - \bar\epsilon_1} - 1\right)$	$A\left[\frac{(\bar\epsilon_5 - 1)^2}{2(\bar\epsilon_5 - \bar\epsilon_1)} - \frac{\bar\epsilon_5 + \bar\epsilon_1}{2} - 1\right]$
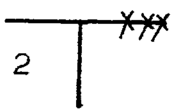	$\frac{A}{2(\bar\epsilon_2 - \bar\epsilon_5)}$	$A\left(\frac{\bar\epsilon_2 - 1}{\bar\epsilon_2 - \bar\epsilon_5} - 2\right)$	$A\left[\frac{(\bar\epsilon_2 - 1)^2}{2(\bar\epsilon_2 - \bar\epsilon_5)} - \frac{\bar\epsilon_1 + \bar\epsilon_2}{2} - \bar\epsilon_5\right]$
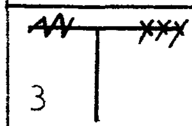	$\frac{A}{2(\bar\epsilon_1 - \bar\epsilon_5)} + \frac{A}{2(\bar\epsilon_2 - \bar\epsilon_5)}$	$A\left(\frac{\bar\epsilon_1 + 2}{\bar\epsilon_1 - \bar\epsilon_5} + \frac{\bar\epsilon_2 - 2}{\bar\epsilon_2 - \bar\epsilon_5} - 1\right)$	$A\left[\frac{(\bar\epsilon_1 + 1)^2}{2(\bar\epsilon_1 - \bar\epsilon_5)} + \frac{(\bar\epsilon_2 - 1)^2}{2(\bar\epsilon_2 - \bar\epsilon_5)} - \frac{\bar\epsilon_1 + \bar\epsilon_2}{2} - \bar\epsilon_5\right]$
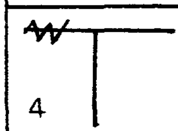	$\frac{A}{2(\bar\epsilon_1 - \bar\epsilon_5)}$	$A\left(\frac{\bar\epsilon_1 + 1}{\bar\epsilon_1 - \bar\epsilon_5} - 2\right)$	$A\left[\frac{(\bar\epsilon_1 + 1)^2}{2(\bar\epsilon_1 - \bar\epsilon_5)} - \frac{\bar\epsilon_1 + \bar\epsilon_2}{2} - \bar\epsilon_5\right]$
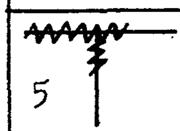	$\frac{A}{2(\bar\epsilon_5 - \bar\epsilon_2)}$	$A\left(\frac{\bar\epsilon_5 + 1}{\bar\epsilon_5 - \bar\epsilon_2} - 1\right)$	$A\left[\frac{(\bar\epsilon_5 + 1)^2}{2(\bar\epsilon_5 - \bar\epsilon_2)} - \frac{\bar\epsilon_5 - \bar\epsilon_2}{2} + 1\right]$
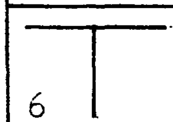	0	$-2A$	$-A\left[\frac{\bar\epsilon_1 + \bar\epsilon_2}{2} + \bar\epsilon_5\right]$
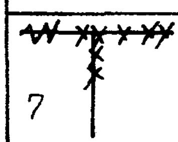	0	$\frac{2A}{\bar\epsilon_5 - \bar\epsilon_1}$	$A\left[\frac{\bar\epsilon_5 + \bar\epsilon_1}{\bar\epsilon_5 - \bar\epsilon_1} + 1\right]$

Table 2.2 (cont'd)

YIELD PATTERN	Q	R	S
8	0	0	0
9	0	$-2A$	$A\left(1-\frac{\bar{\epsilon}_2+\bar{\epsilon}_5}{\bar{\epsilon}_2-\bar{\epsilon}_5}\right)$
10	$\frac{A}{2(\bar{\epsilon}_5-\bar{\epsilon}_1)}+\frac{A}{2(\bar{\epsilon}_5-\bar{\epsilon}_2)}$	$A\left[\frac{\bar{\epsilon}_5-1}{\bar{\epsilon}_5-\bar{\epsilon}_1}+\frac{\bar{\epsilon}_5-1}{\bar{\epsilon}_5-\bar{\epsilon}_2}-2\right]$	$A\left[\frac{(\bar{\epsilon}_5-1)^2}{2(\bar{\epsilon}_5-\bar{\epsilon}_1)}+\frac{(\bar{\epsilon}_5-1)^2}{2(\bar{\epsilon}_5-\bar{\epsilon}_2)}-\frac{\bar{\epsilon}_1+\bar{\epsilon}_2}{2}-\bar{\epsilon}_5\right]$
11	$\frac{A}{2(\bar{\epsilon}_5-\bar{\epsilon}_2)}$	$A\left[\frac{\bar{\epsilon}_5-1}{\bar{\epsilon}_5-\bar{\epsilon}_1}+\frac{\bar{\epsilon}_5-1}{\bar{\epsilon}_5-\bar{\epsilon}_2}+\frac{\bar{\epsilon}_1+2}{\bar{\epsilon}_1-\bar{\epsilon}_5}-2\right]$	$A\left[\frac{(\bar{\epsilon}_5-1)^2-(\bar{\epsilon}_1+1)^2}{2(\bar{\epsilon}_5-\bar{\epsilon}_1)}+\frac{(\bar{\epsilon}_5-1)^2}{2(\bar{\epsilon}_5-\bar{\epsilon}_2)}-\frac{\bar{\epsilon}_1+\bar{\epsilon}_2}{2}-\bar{\epsilon}_5\right]$
12	0	0	0
13	$\frac{A}{2(\bar{\epsilon}_6-\bar{\epsilon}_4)}$	$A\left[\frac{\bar{\epsilon}_6+1}{\bar{\epsilon}_6-\bar{\epsilon}_4}-1\right]$	$A\left[\frac{(\bar{\epsilon}_6+1)^2}{2(\bar{\epsilon}_6-\bar{\epsilon}_4)}-\frac{\bar{\epsilon}_6-\bar{\epsilon}_4}{2}+1\right]$
14	$\frac{A}{2(\bar{\epsilon}_3-\bar{\epsilon}_6)}$	$A\left[\frac{\bar{\epsilon}_3+1}{\bar{\epsilon}_3-\bar{\epsilon}_6}-2\right]$	$A\left[\frac{(\bar{\epsilon}_3+1)^2}{2(\bar{\epsilon}_3-\bar{\epsilon}_6)}-\bar{\epsilon}_6-\frac{\bar{\epsilon}_3+\bar{\epsilon}_4}{2}\right]$
15	$\frac{A}{2(\bar{\epsilon}_3-\bar{\epsilon}_6)}+\frac{A}{2(\bar{\epsilon}_4-\bar{\epsilon}_6)}$	$A\left[\frac{\bar{\epsilon}_3+2}{\bar{\epsilon}_3-\bar{\epsilon}_6}+\frac{\bar{\epsilon}_4-2}{\bar{\epsilon}_4-\bar{\epsilon}_6}-1\right]$	$A\left[\frac{(\bar{\epsilon}_3+1)^2}{2(\bar{\epsilon}_3-\bar{\epsilon}_6)}+\frac{(\bar{\epsilon}_4-1)^2}{2(\bar{\epsilon}_3-\bar{\epsilon}_6)}+\frac{-\bar{\epsilon}_3-\bar{\epsilon}_4}{2}-\bar{\epsilon}_6\right]$

Table 2.2 (cont'd)

YIELD PATTERN	Q	R	S
16	0	$-2A$	$A\left[1-\dfrac{\bar{\epsilon}_4+\bar{\epsilon}_6}{\bar{\epsilon}_4-\bar{\epsilon}_6}\right]$
17	$\dfrac{A}{2(\bar{\epsilon}_3-\bar{\epsilon}_6)}+\dfrac{A}{2(\bar{\epsilon}_4-\bar{\epsilon}_6)}$	$A\left[\dfrac{\bar{\epsilon}_3+2}{\bar{\epsilon}_3-\bar{\epsilon}_6}+\dfrac{\bar{\epsilon}_4+2}{\bar{\epsilon}_4-\bar{\epsilon}_6}-1\right]$	$A\left[\dfrac{(\bar{\epsilon}_3+1)^2}{2(\bar{\epsilon}_3-\bar{\epsilon}_6)}+\dfrac{(\bar{\epsilon}_4+1)^2}{2(\bar{\epsilon}_4-\bar{\epsilon}_6)}-\dfrac{\bar{\epsilon}_3+\bar{\epsilon}_4}{2}-\bar{\epsilon}_6\right]$
18	0	$-2B^*$	0
19	0	$2B\left[\dfrac{\bar{\epsilon}_5-\bar{\epsilon}_6-2}{\bar{\epsilon}_5-\bar{\epsilon}_6}-1\right]$	$B\left[\dfrac{(\bar{\epsilon}_5+\bar{\epsilon}_6)(\bar{\epsilon}_5-\bar{\epsilon}_6+2)}{\bar{\epsilon}_5-\bar{\epsilon}_6}\right]$
20	$\dfrac{B}{\bar{\epsilon}_5-\bar{\epsilon}_6}$	$2B\left[\dfrac{\bar{\epsilon}_5-1}{\bar{\epsilon}_5-\bar{\epsilon}_6}-1\right]$	$B\,\dfrac{(\bar{\epsilon}_5-1)^2}{\bar{\epsilon}_5-\bar{\epsilon}_6}$
21	$\dfrac{B}{\bar{\epsilon}_6-\bar{\epsilon}_5}$	$2B\left(\dfrac{\bar{\epsilon}_6+1}{\bar{\epsilon}_6-\bar{\epsilon}_5}-1\right)$	$B\,\dfrac{(\bar{\epsilon}_6+1)^2}{\bar{\epsilon}_6-\bar{\epsilon}_5}$

$* \quad A=\dfrac{K_1K_2}{2(K_3+2K_1K_2)}$, $\bar{\epsilon}_i=\epsilon_i-\epsilon_o$ = "bending" strain at any point i along the cross section centreline

$B=\dfrac{K_3}{2(K_3+2K_1K_2)}$

Table 4.1 TABULATION OF THEORETICAL AND EXPERIMENTAL RESULTS

1 SECTION PROPERTIES OF COLUMN	2 $\gamma = \frac{M^y_A}{M^x_A}$	3 $\frac{P_{THEOR}}{P_y}$	4 $\frac{P_{TEST}}{P_y}$ (13)*	5 % DIFF $\frac{4-3}{4} \times 100$	6 $\frac{P_{THEOR}}{P_y}$ (20)*
$K_1=1.17$ $K_2=0.168$ $K_3=0.117$ $\frac{L}{r_y} = 57$	.365	.250 .409 .168 .530	.239 .396 .176 .550	4.6 3.3 4.8 -3.6	.268 .423 .219 .600
	.182	.295	.263	12.0	.256
	1.093	.256	.242	6.0	.252
	.244	.195	.173	12.5	.189
	.729	.315	.281	12.0	.328
$K_1=1.0$ $K_2=0.2308$ $K_3=0.1231$ $\frac{L}{r_y} = 71$	.293	.156 .215 .357	.136 .163 .353	14.7 32.0 1.1	- - -
	.494	.189	.149	27.0	-
	.879	.224	.186	20.0	-
	.195	.165	.144	14.5	-
	.098	.199	.169	18.0	-
$K_1=0.8385$ $K_2=0.2301$ $K_3=0.1231$ $\frac{L}{r_y} = 85$	.2377	.147 .200	.114 .170	29.0 17.0	- -
	.358	.175	.129	35.6	-
	.716	.204	.165	24.0	-
	.159	.165 .249	.141 .219	17.0 14.0	- -

* The numbers in brackets refer to corresponding references

Table 4.1 (cont'd)

1	2	3	4	5
SECTION PROPERTIES OF COLUMN	$\gamma = \frac{M^y{}_A}{M^x{}_A}$	$\frac{P_{THEOR}}{P_y}$	$\frac{P_{TEST}}{P_y}$ (13)*	% DIFF $\frac{4-3}{4} \times 100$
K_1=0.7615	.1343	.165	.141	14.0
K_2=0.2307	.2015	.200	.170	18.0
		.147	.114	29.0
K_3=0.123	.605	.202	.174	16.0
$\frac{L}{r_y}$ = 91	.302	.174	.156	11.5
	.0671	.186	.142	31.0
K_1=0.6307	.548	.165	.144	14.6
K_2=0.2307	.182	.172	.164	5.0
		.126	.112	11.0
K_3=0.5476	.122	.144	.144	0
$\frac{L}{r_y}$ = 114				
K_1=1.2578	.75	.215	.246	-12.5
		.406	.381	6.5
K_2=0.2578		.277	.256	8.5
K_3=0.1886	2.25	.242	.213	13.5
$\frac{L}{r_y}$ = 83	1.50	.300	.279	7.5
	4.25	.360	.314	14.5
	.563	.195	.162	20.0
	.188	.270	.250	8.0

* The bracketed 13 refers to reference 13

* The bracketed 13 refers to reference 13

Table 4.1 (cont'd)

1 SECTION PROPERTIES OF COLUMN	2 $\gamma = \frac{M^y_A}{M^x_A}$	3 $\frac{P_{THEOR}}{P_y}$	4 $\frac{P_{TEST}}{P_y}$ *(13)	5 % DIFF $\frac{4-3}{4} \times 100$
$K_1=1.0264$	1.0	.190	.171	11.0
$K_2=0.2578$		.268	.246	9.0
$K_3=0.1886$				
$\frac{L}{r_y} = 102$				
$K_1=0.8805$	.50	.267	.240	11.0
$K_2=0.2578$		.210	.183	14.5
$K_3=0.1886$	.25	.273	.237	15.0
$\frac{L}{r_y} = 121$				

* The bracketed 13 refers to reference 13

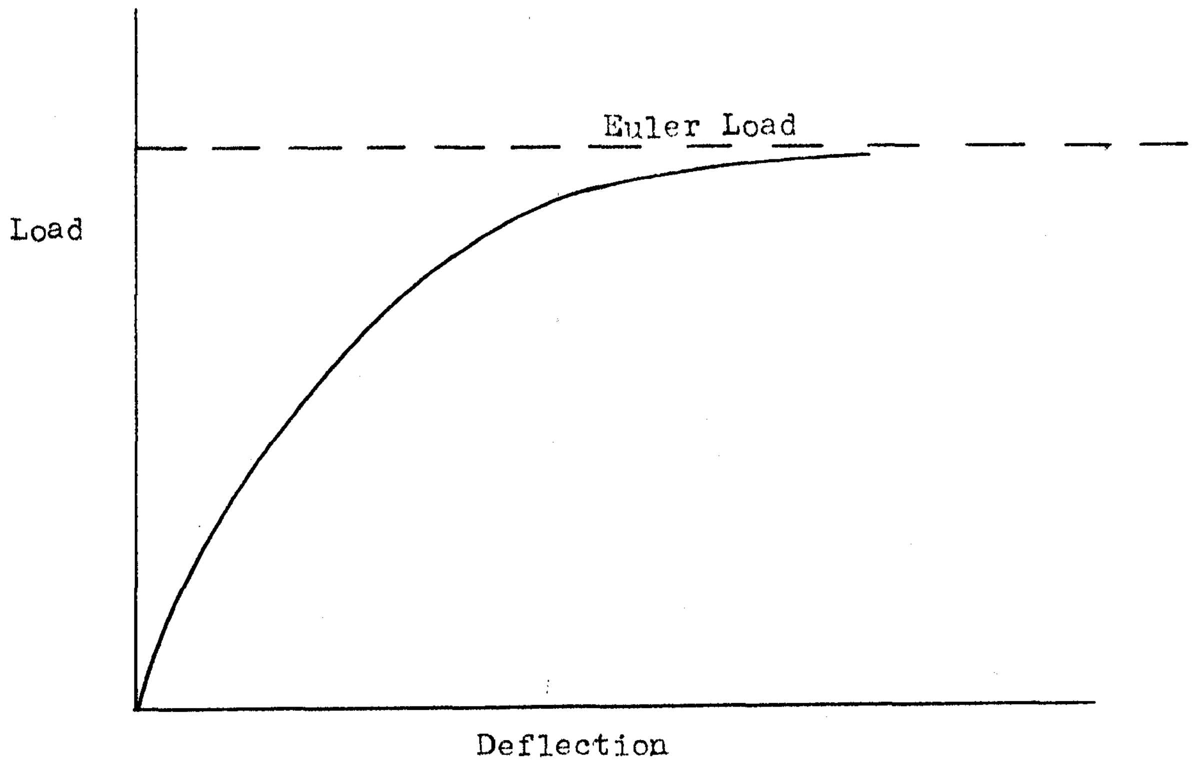

Fig. 1.1 Failure at the Euler Load

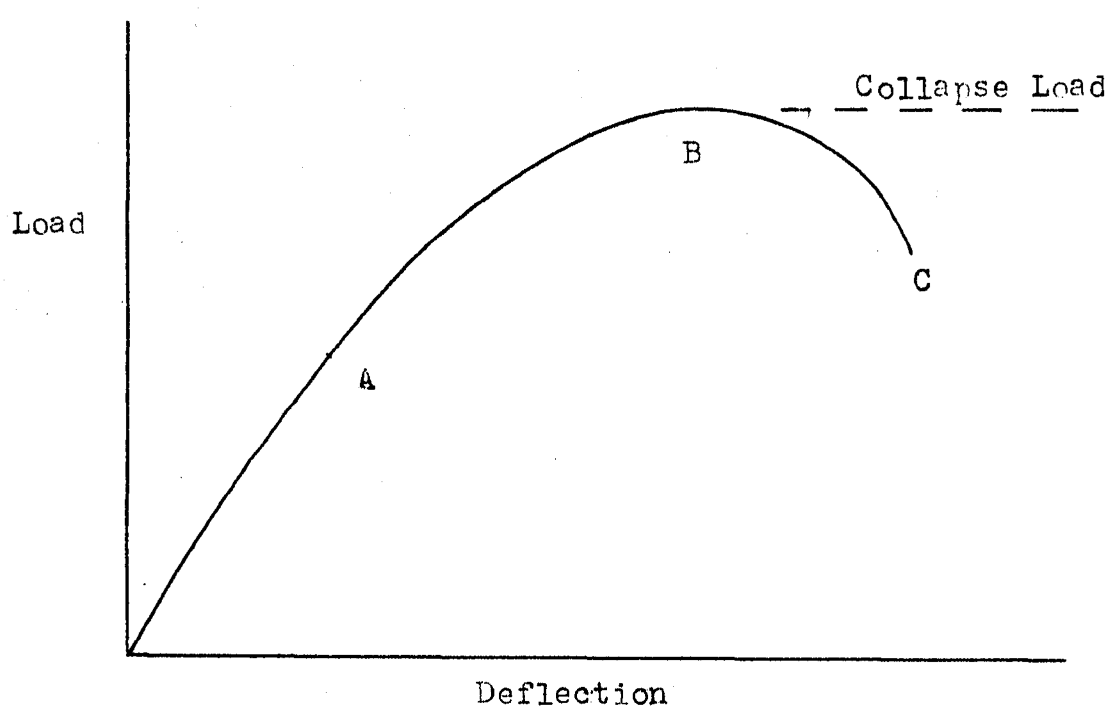

Fig. 1.2 Failure at the Collapse Load

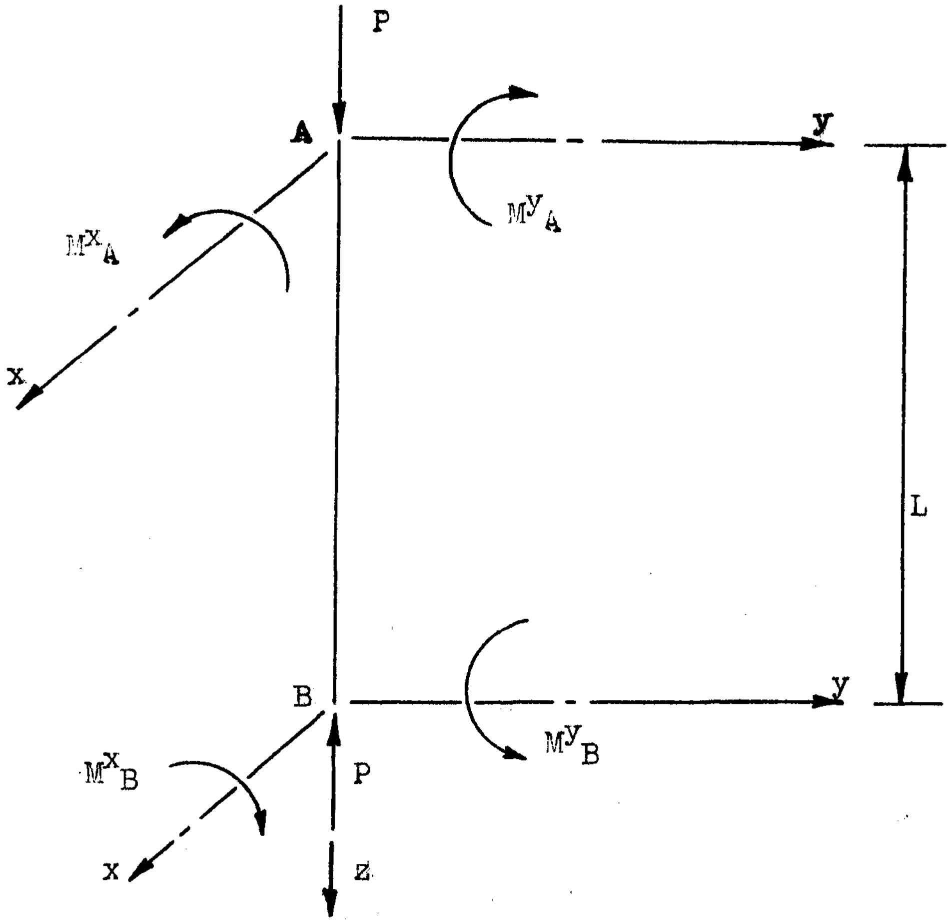

Fig. 2.1 Column With Moments Applied at Both Ends

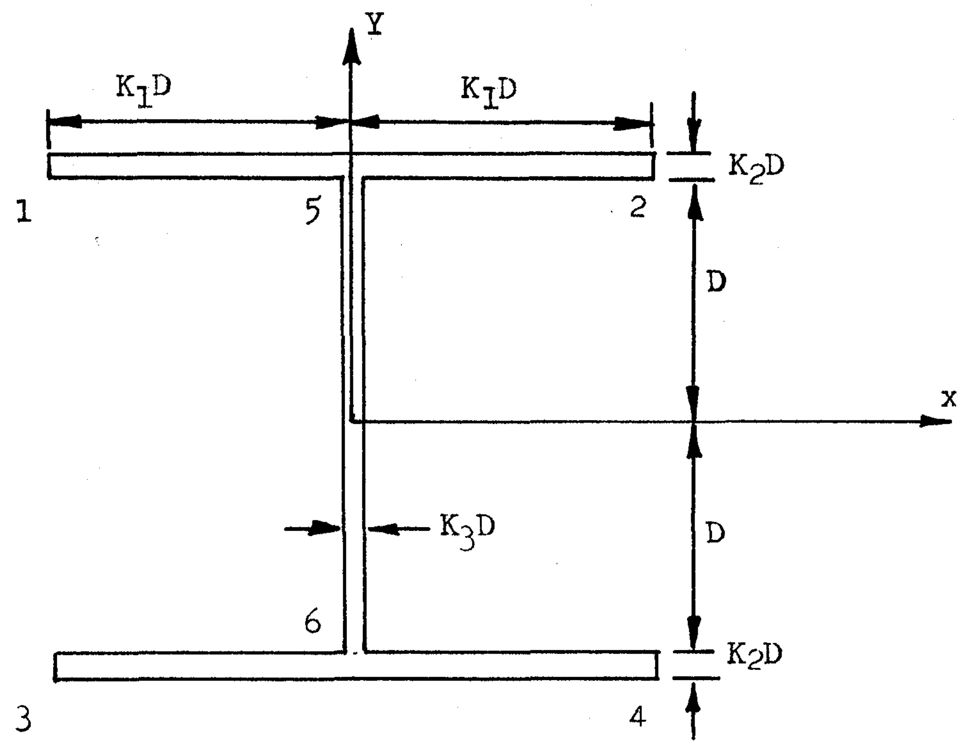

Fig. 2.2 Typical Wide Flange Cross Section

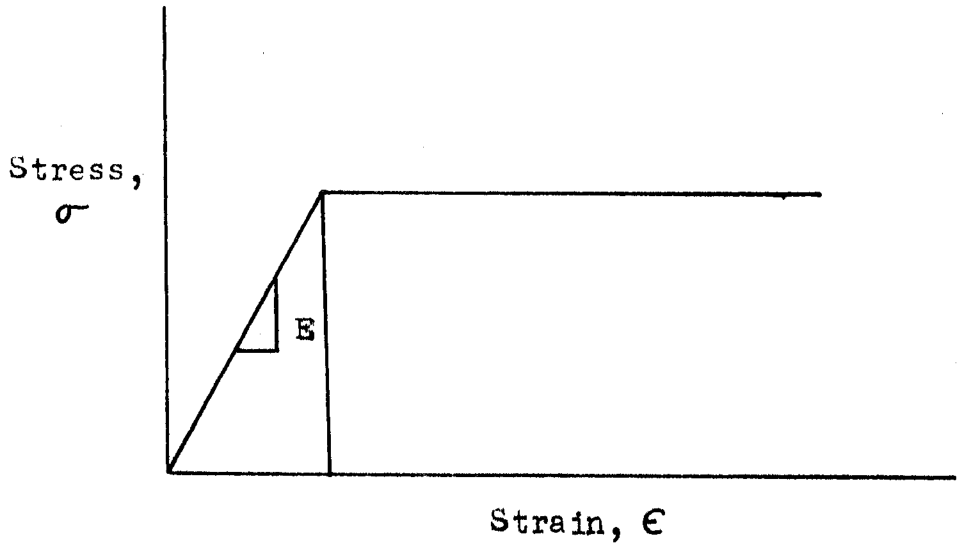

Fig. 2.3 Ideal Stress-Strain Curve

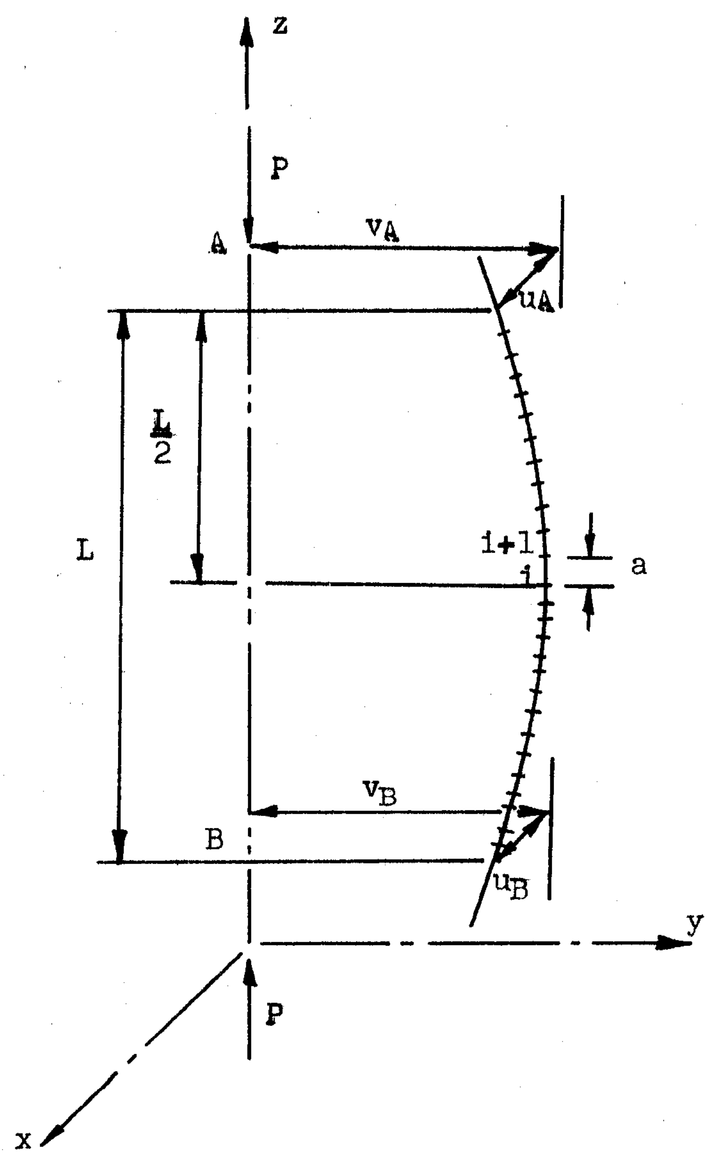

Fig. 2.4 Typical Column Deflection Curve

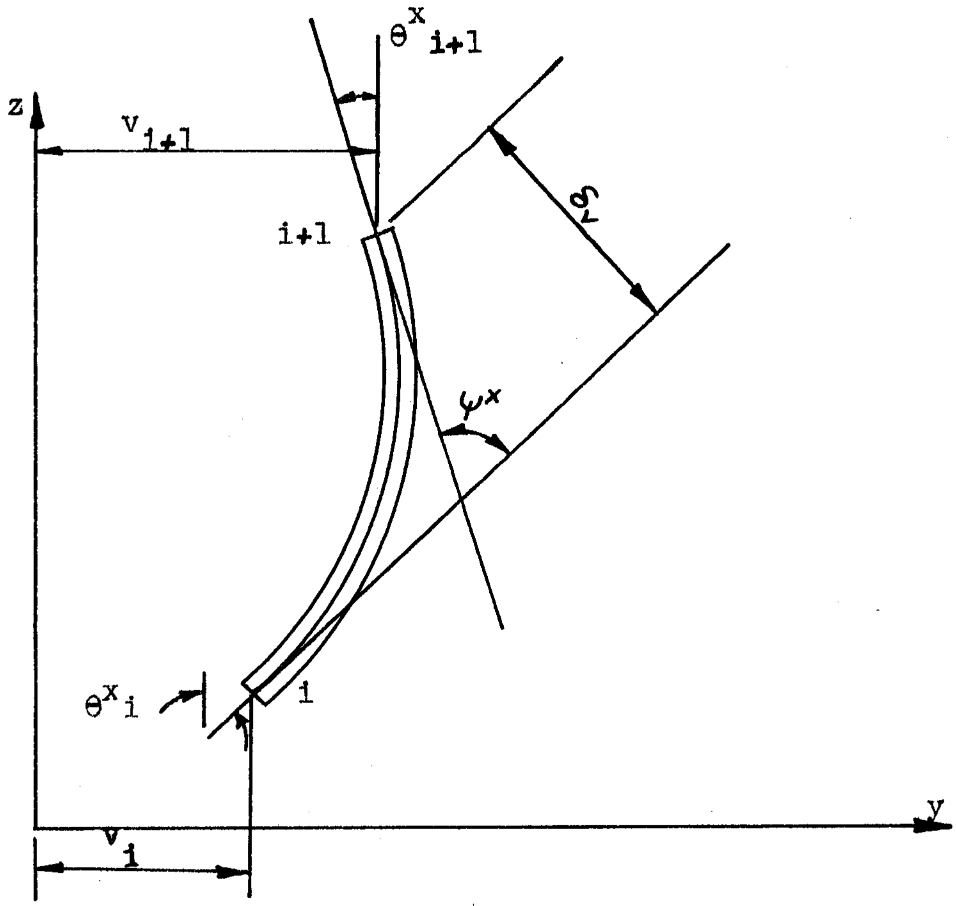

(a) Projection onto the y-z Plane

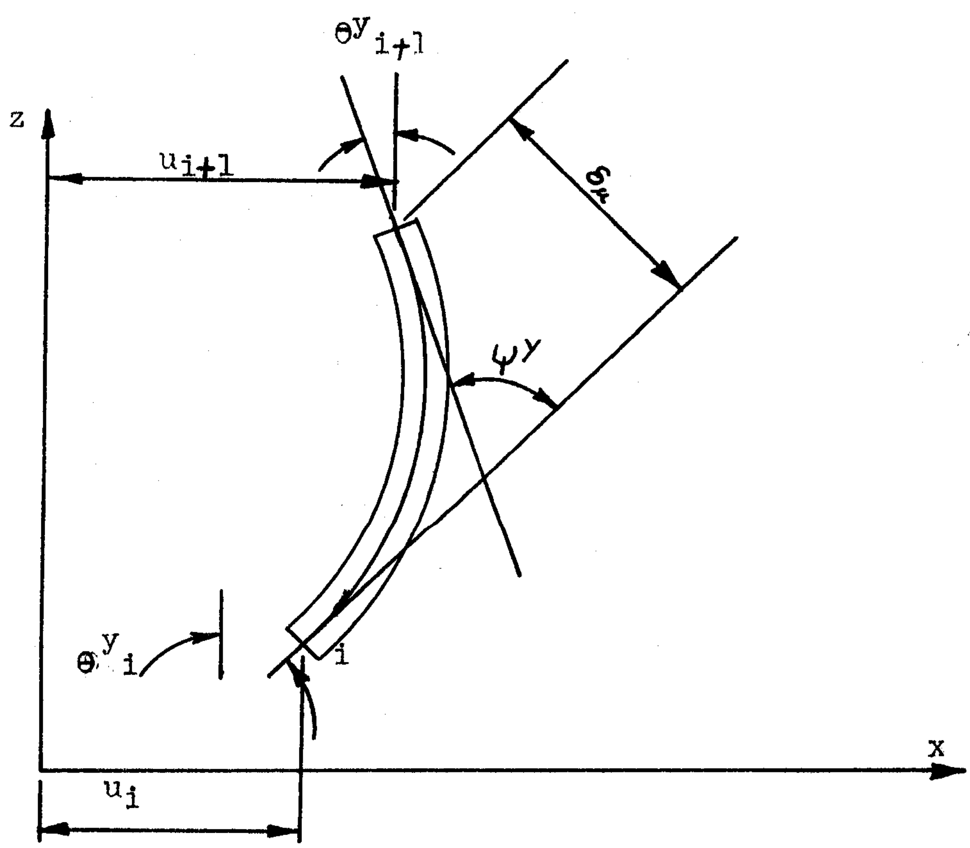

(b) Projection onto the x-z Plane

Fig. 2.5 Projections of the Column Element

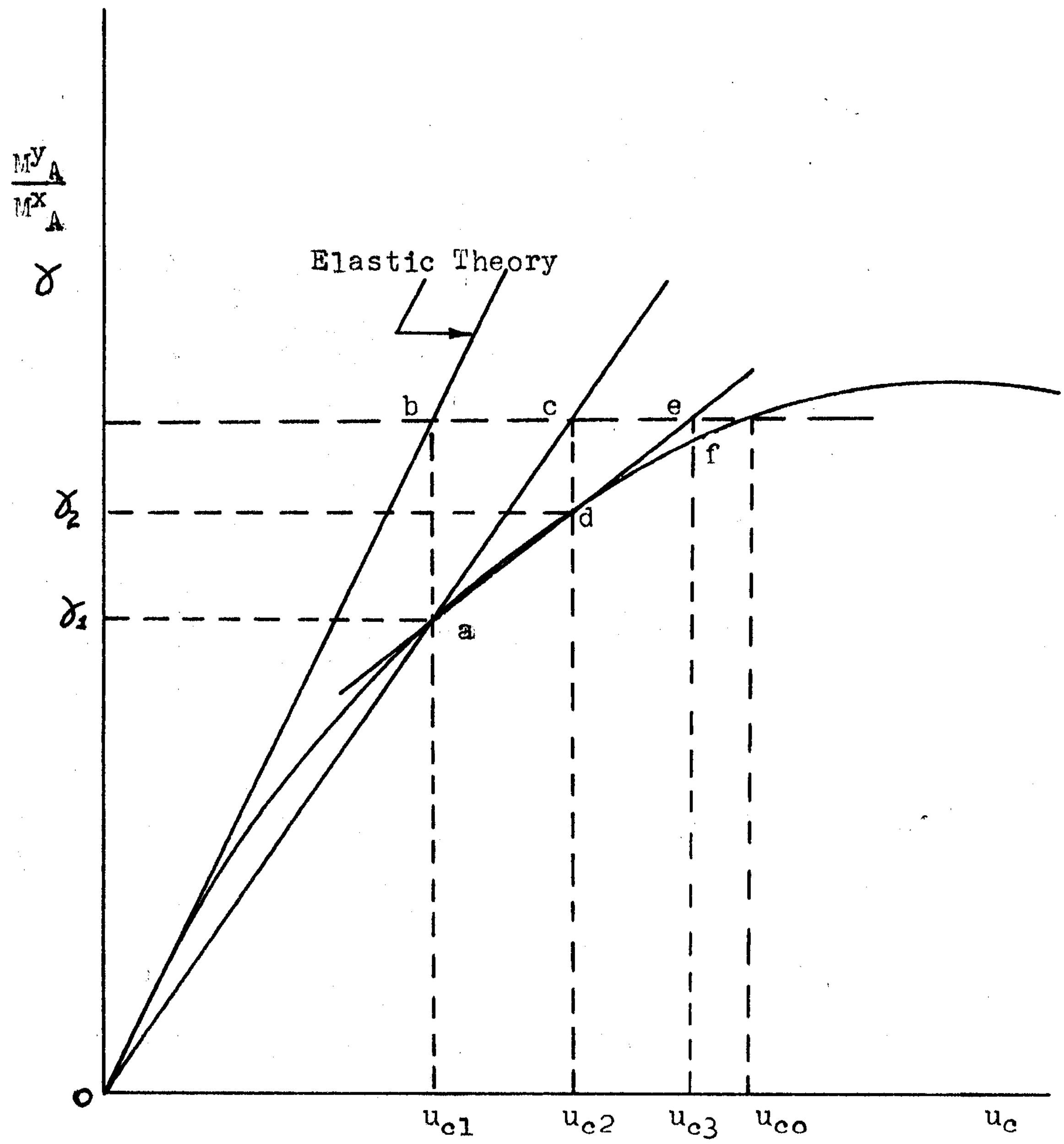

Fig. 2.6 Correction For u_c

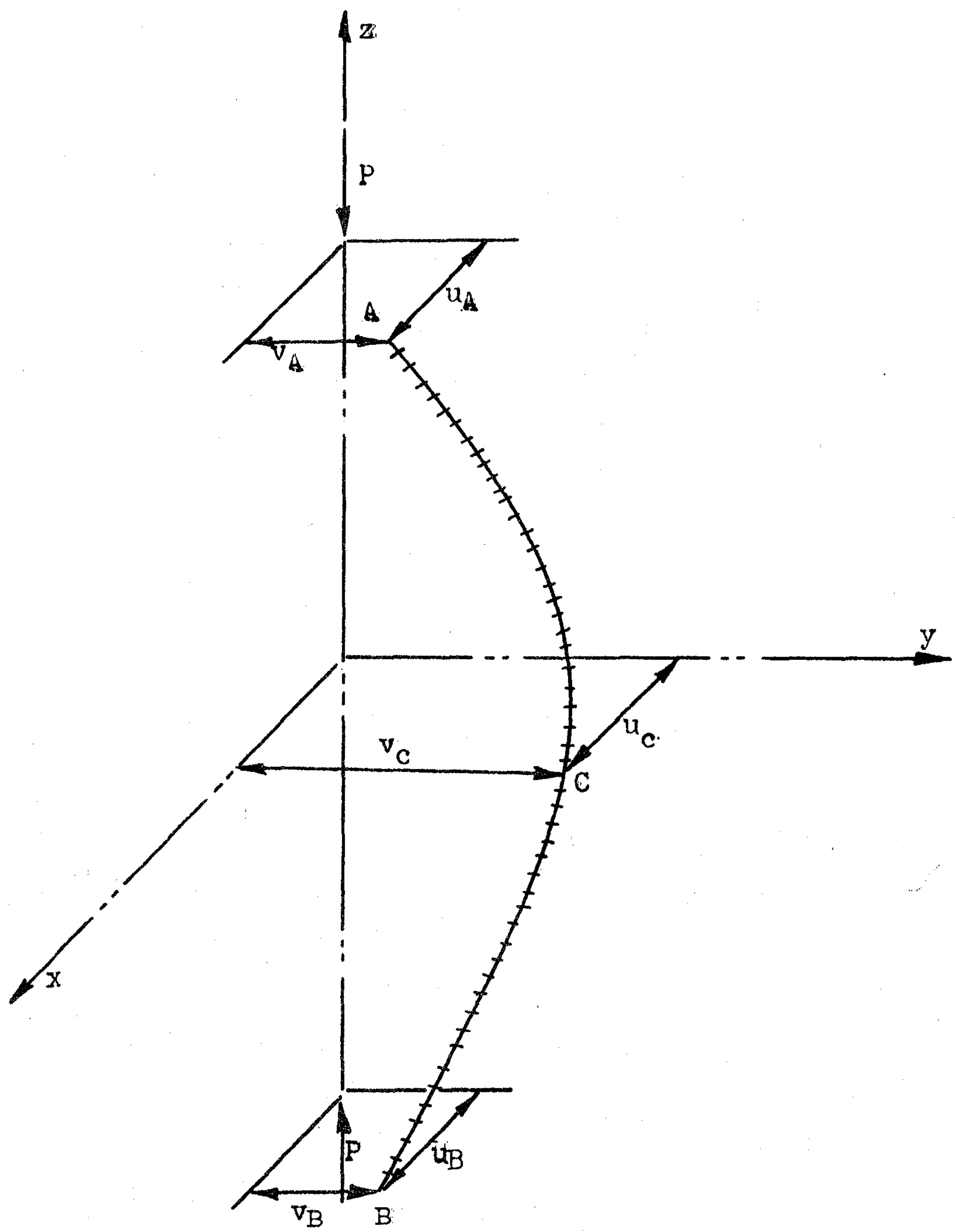

Fig. 2.7 Column Deflection Curve, $\beta = 1$

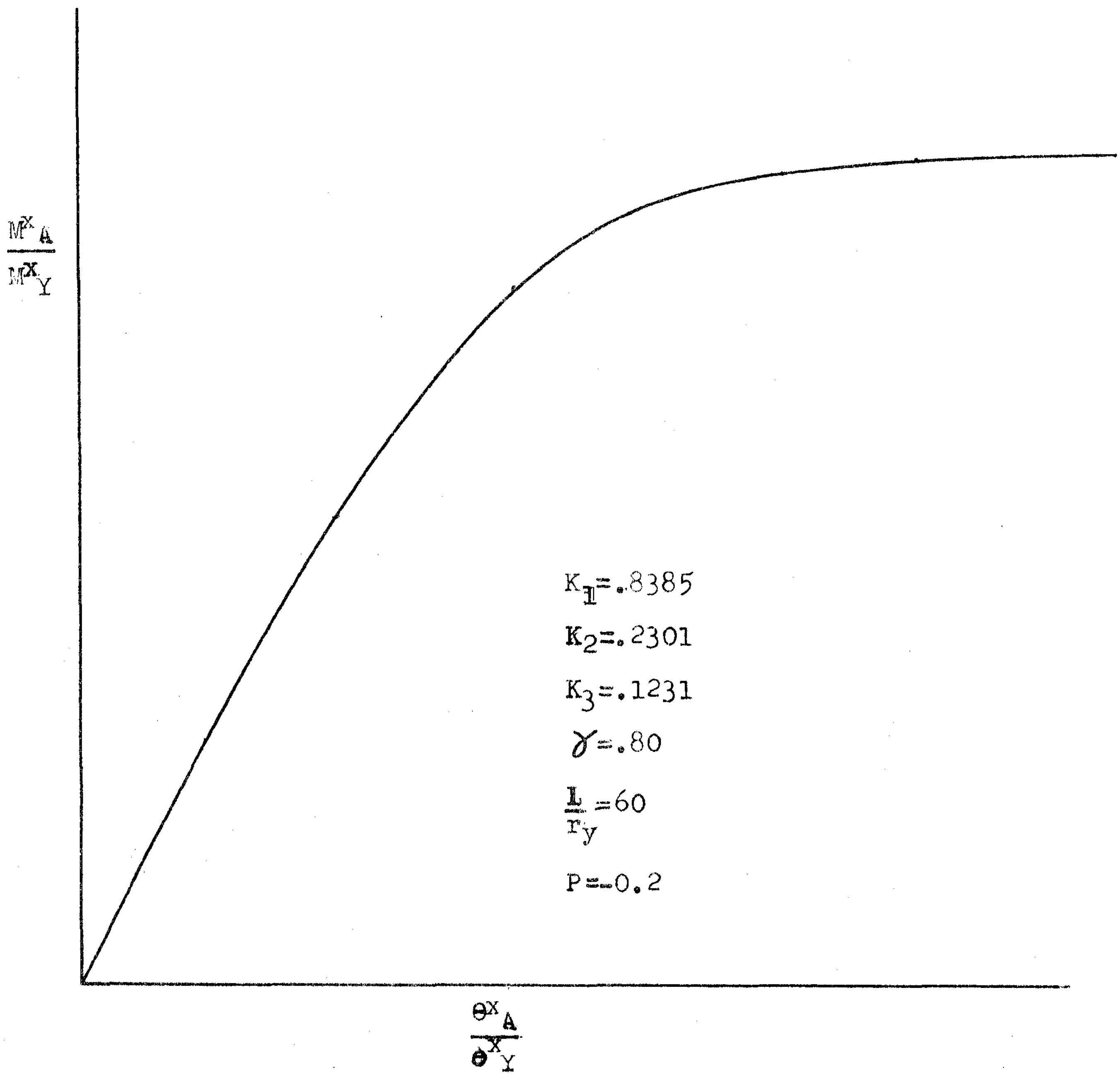

Fig. 2.8 Moment-Rotation Curve

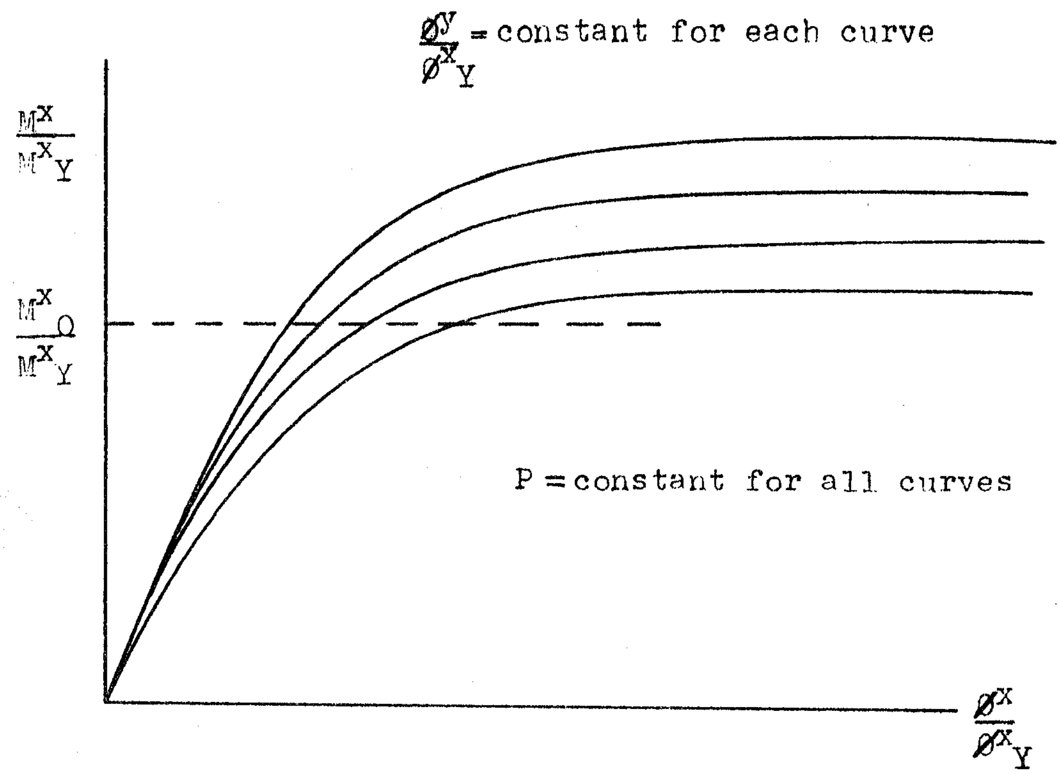

Fig. 2.9 Moment-Curvature Curves About the x-Axis

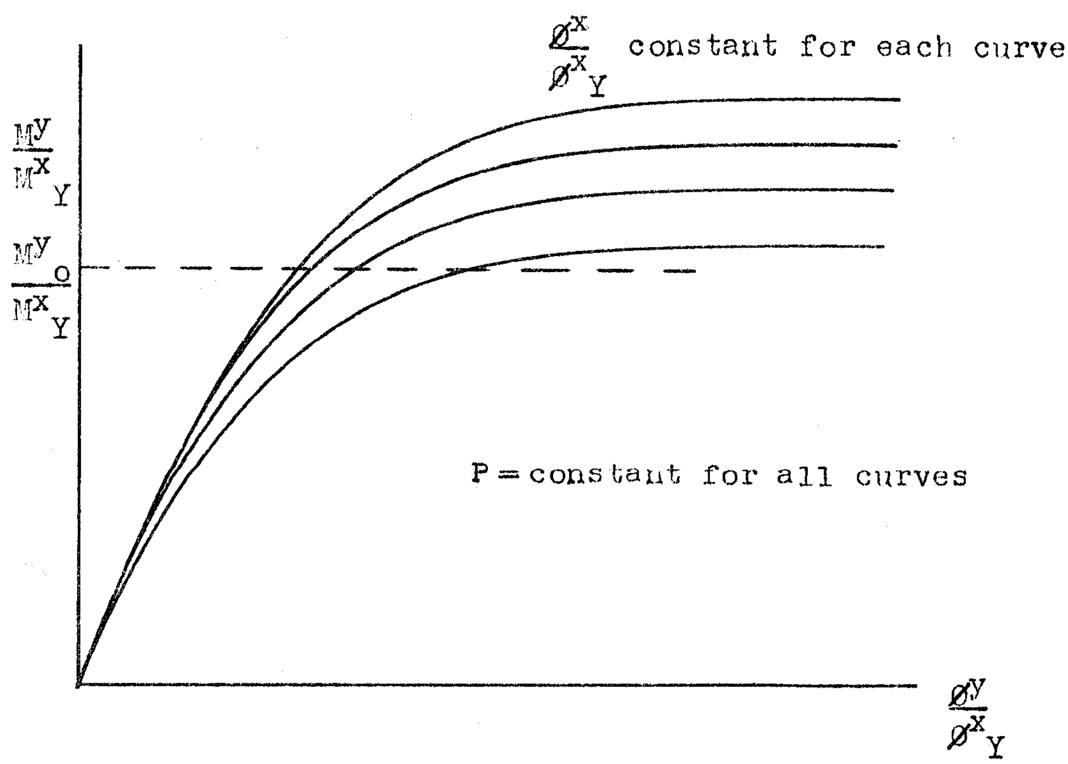

Fig. 2.10 Moment-Curvature Curves About the y-Axis

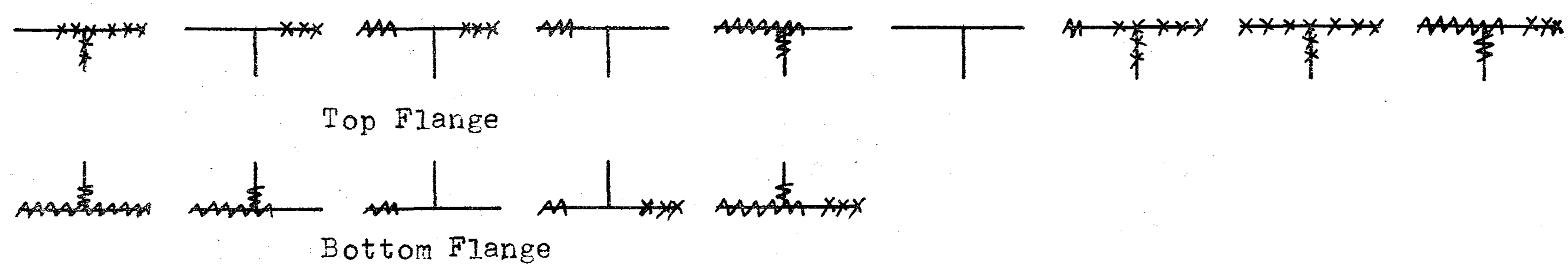

Fig. 2.11(a) Possible Yield Configurations of the Top And Bottom Flanges Neglecting Warping and residual Stress

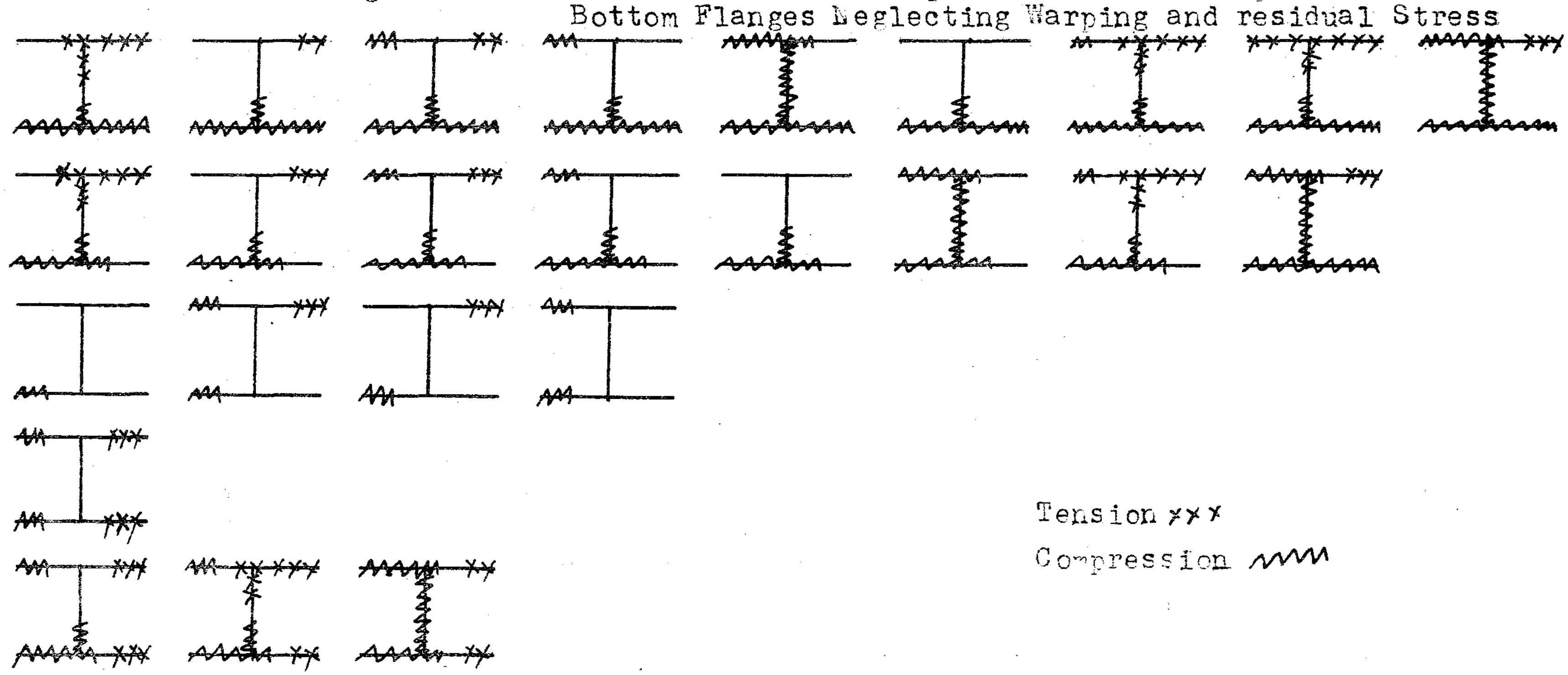

Fig. 2.11(b) Possible Yield Configurations for the Wide Flange Section After Combining Top and Bottom Flanges of Fig. 2.11(a)

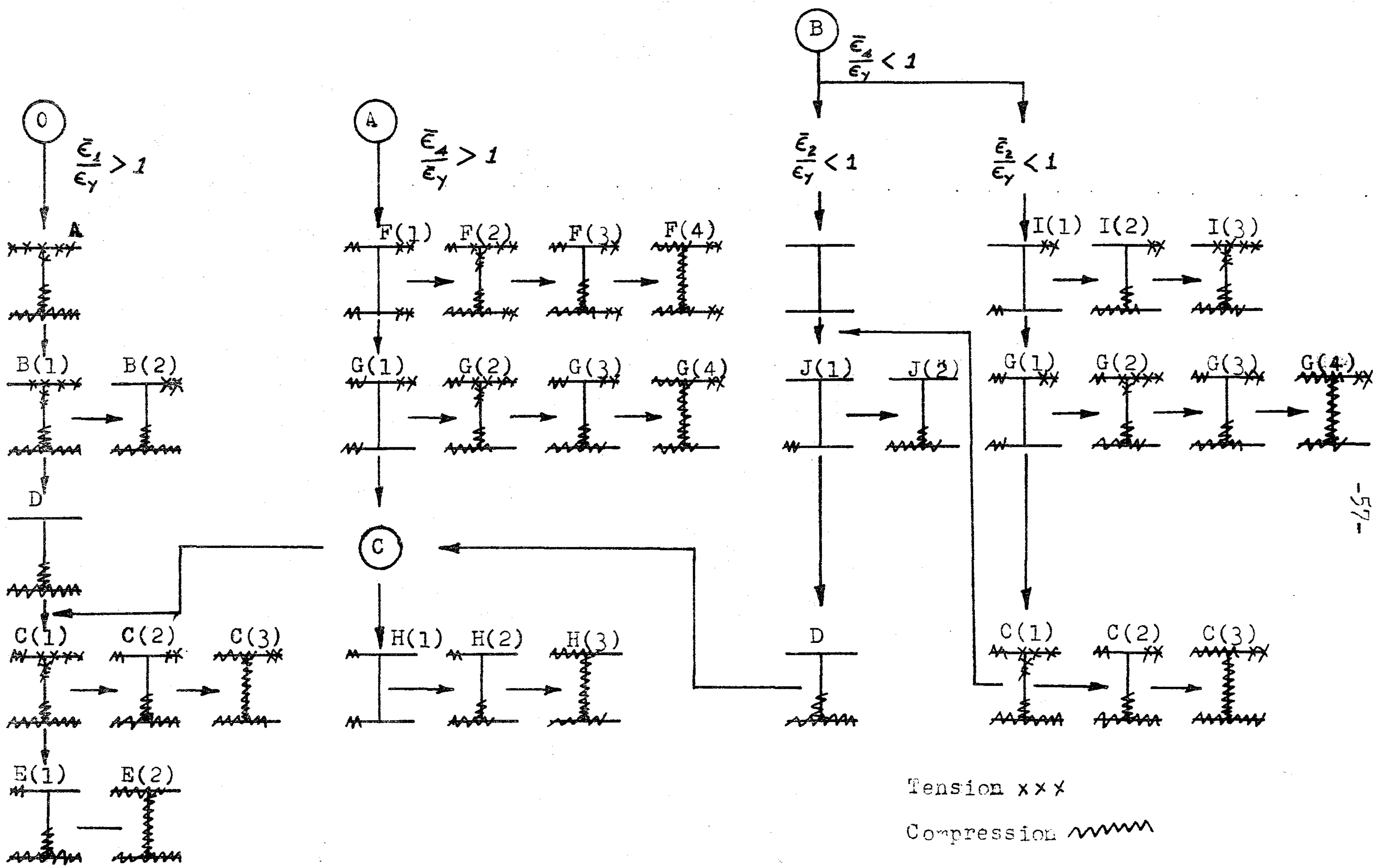

Fig. 2.12 Sequence for Checking the Yield Configurations

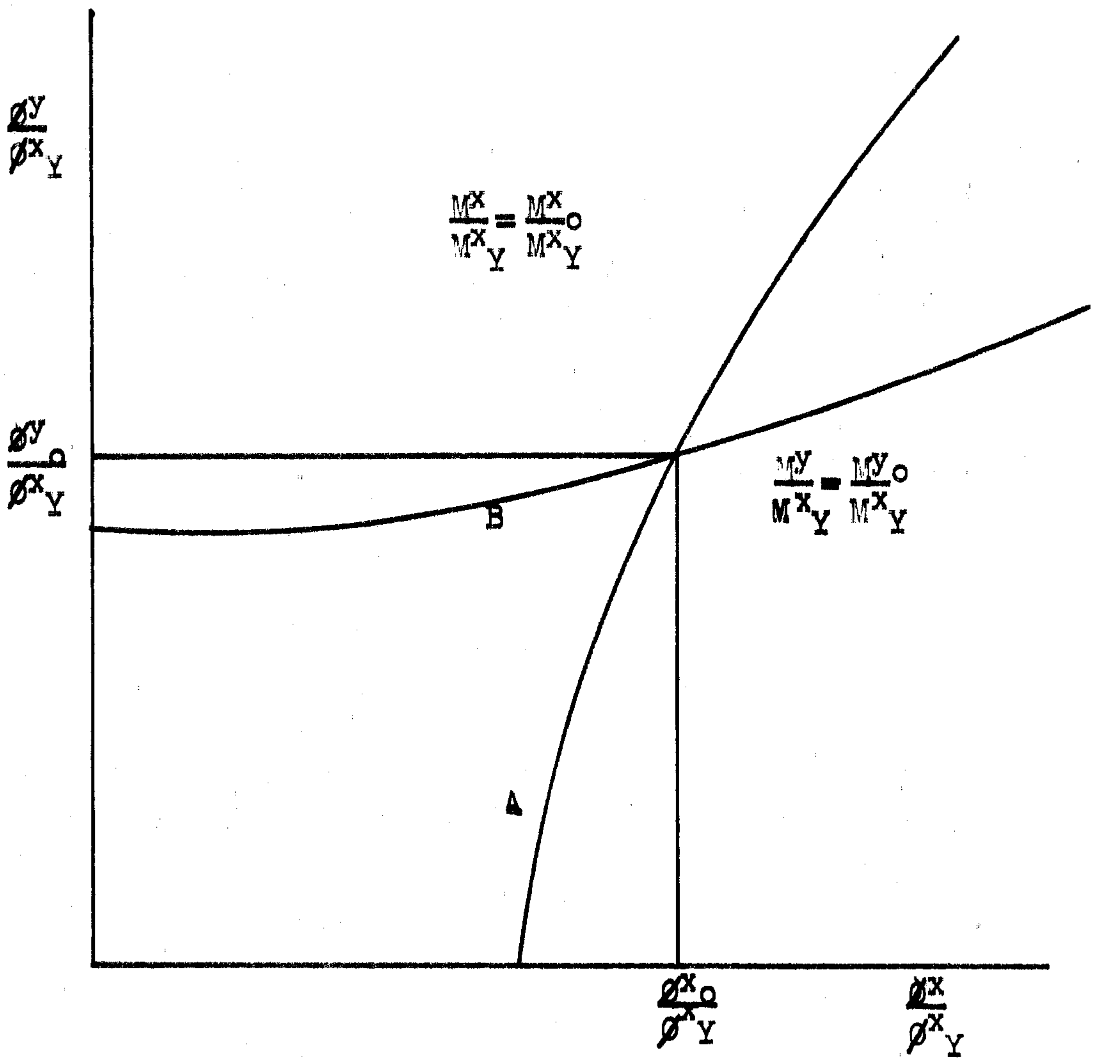

Fig. 2.13 Curvature Relationship for Constant Moment About Each Axis

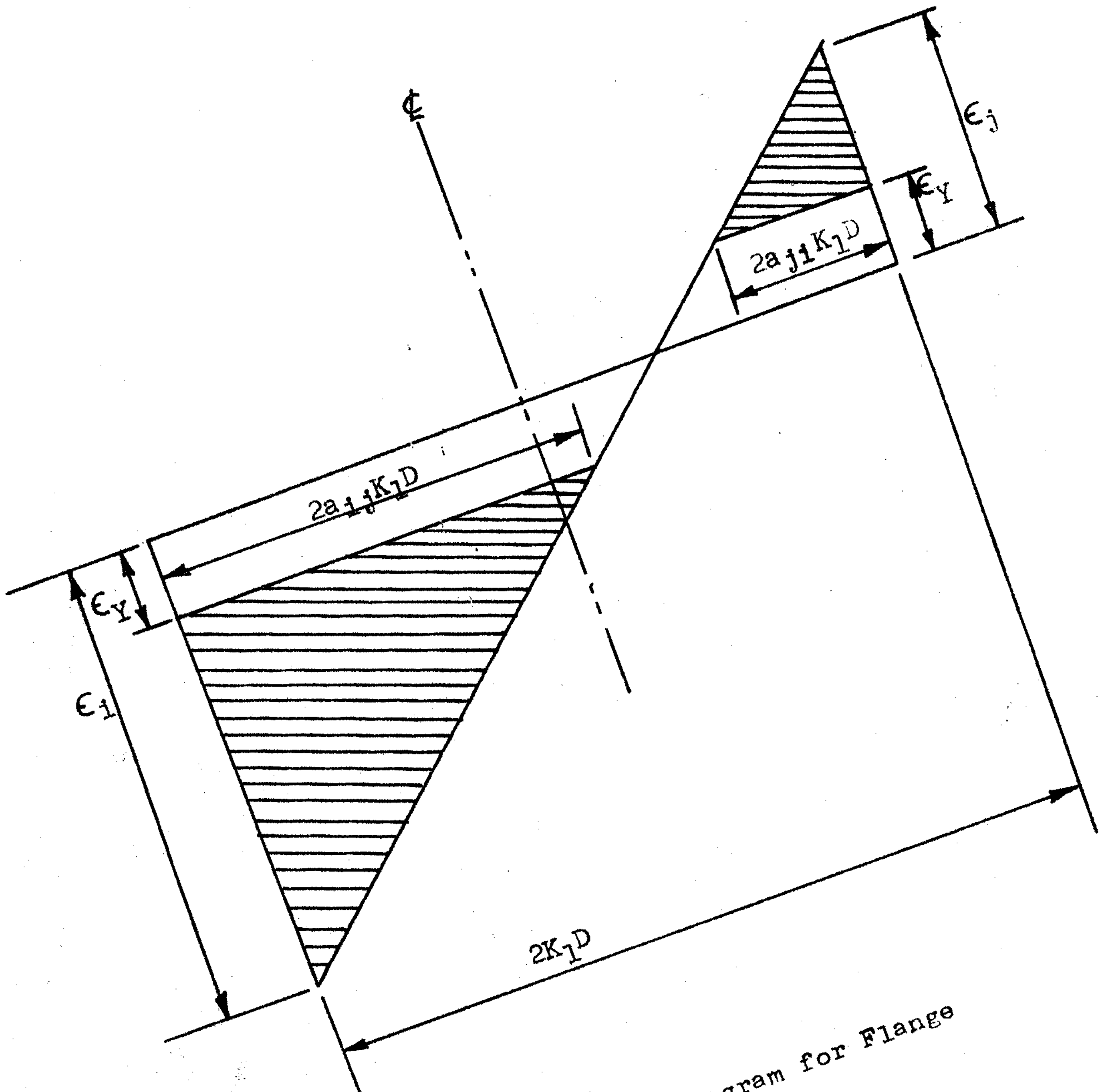

Fig. 2.14 Total Strain Diagram for Flange

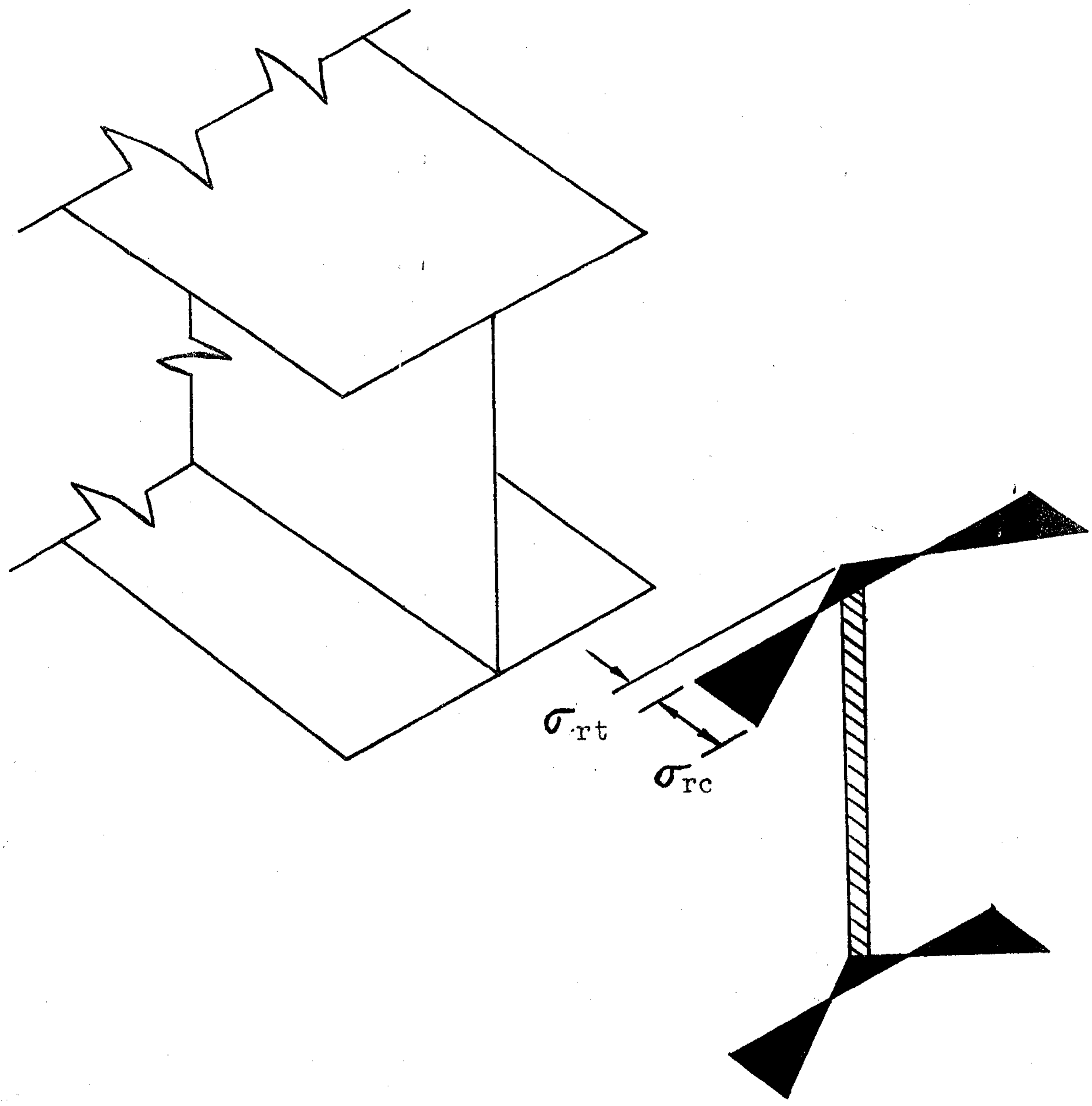

Fig. 2.15 Residual Stress Distribution

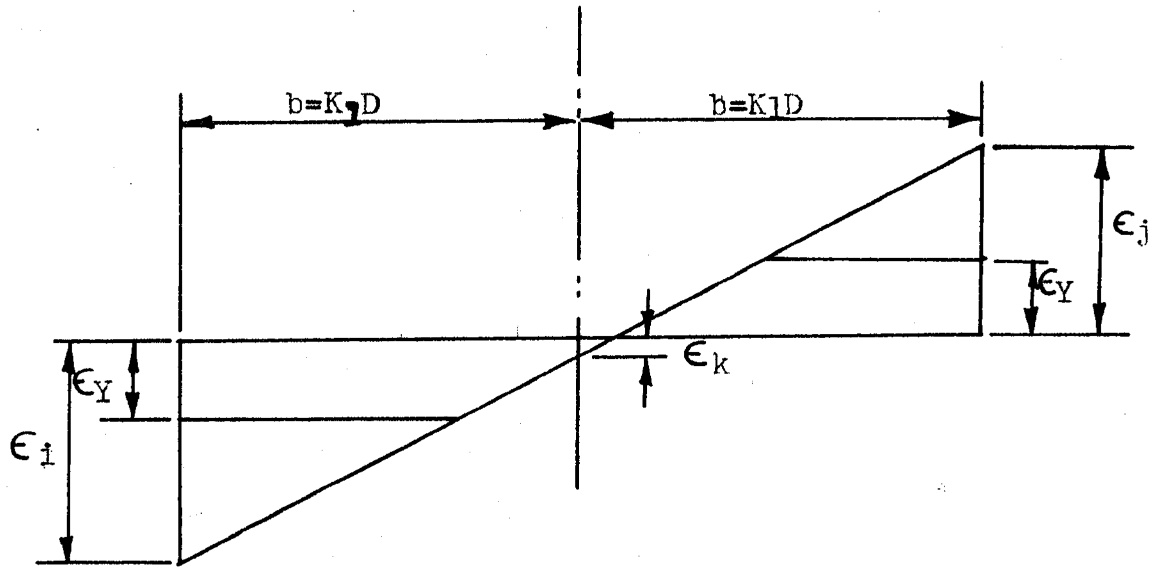

Fig. 2.16(a) Strain Distribution of a Flange (i,j) Neglecting Warping and Residual Strains

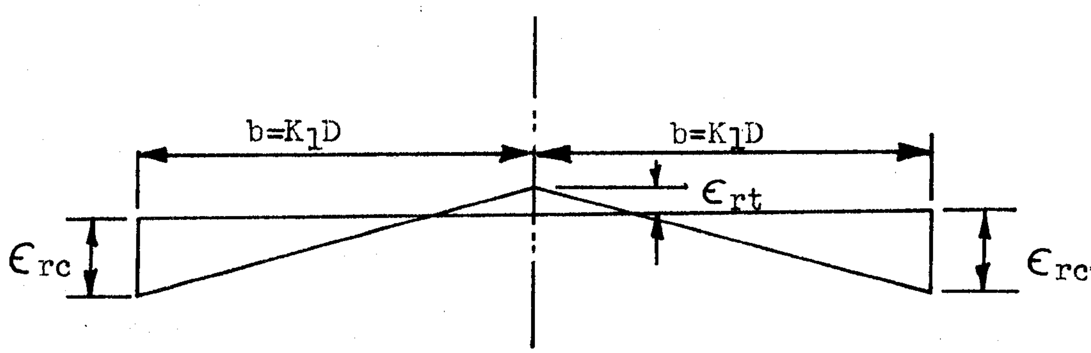

Fig. 2.16(b) Distribution of Residual Strains over a Flange (i,j)

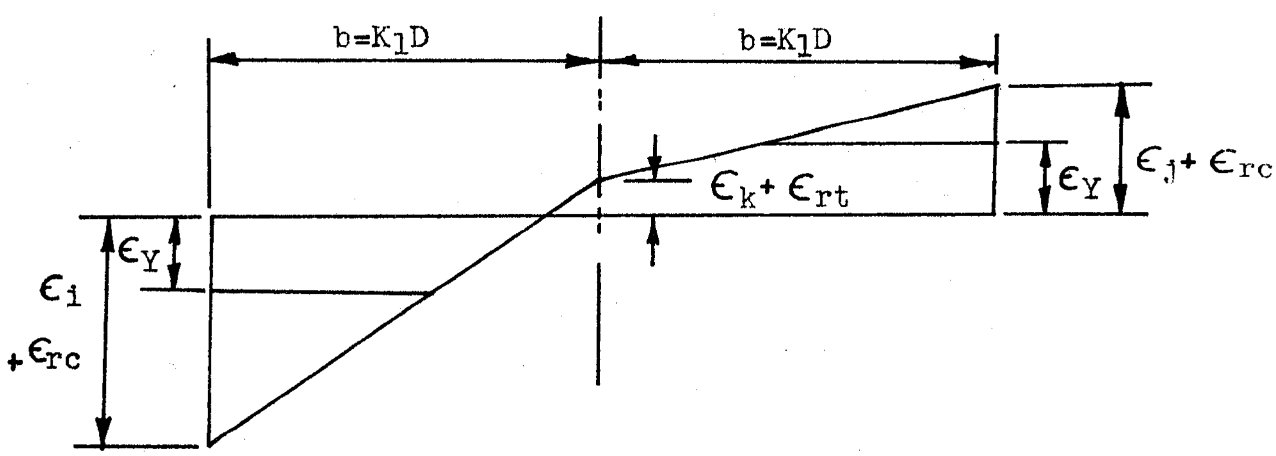

Fig. 2.16(c) Net Strain Distribution for Flange (i,j) Obtained by Superimposing 2.16 (a) & 2.16 (b)

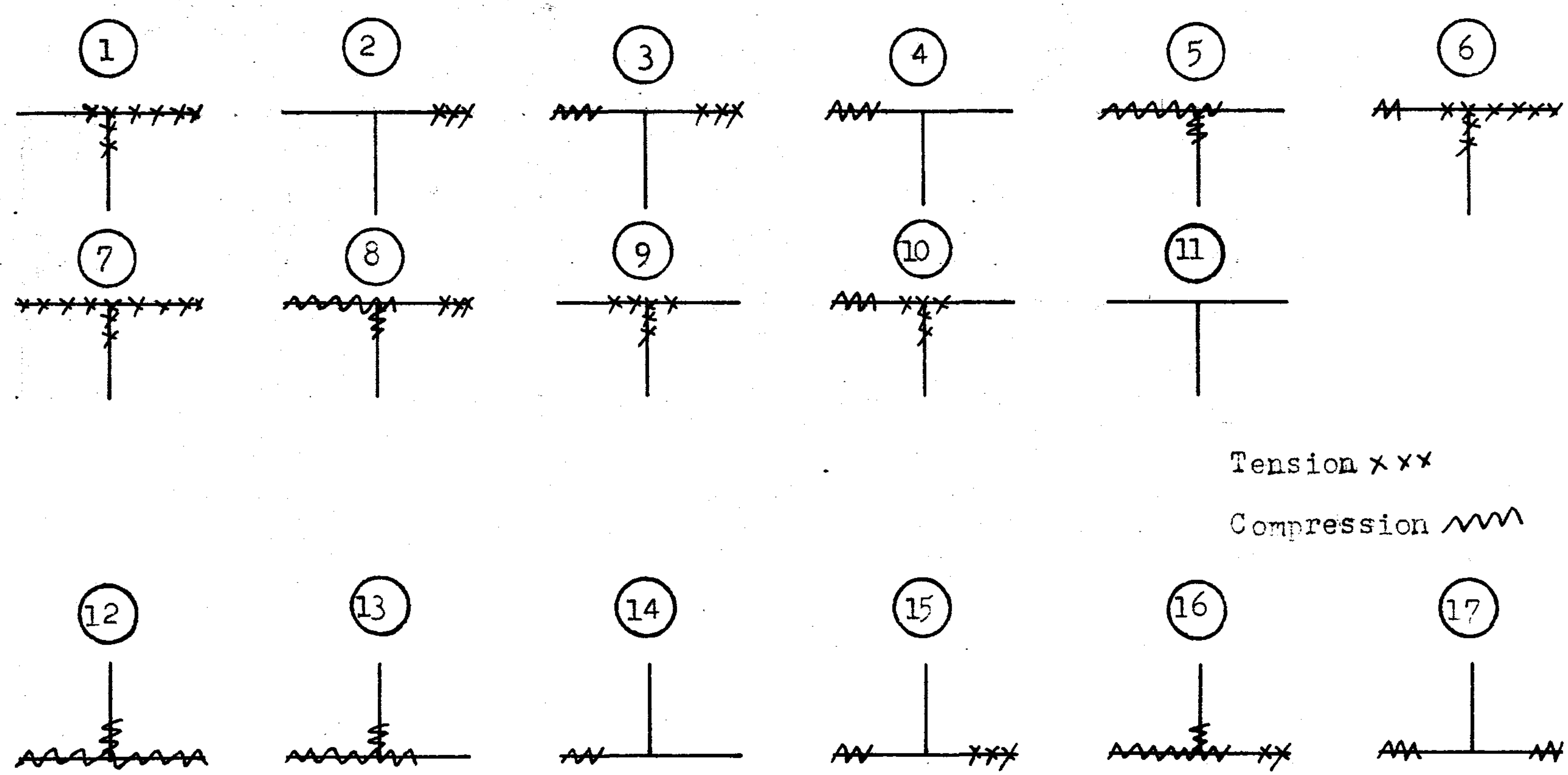

Fig. 2.17(a) Possible Yield Configurations for a Wide Flange Section With Residual Stresses Included, Top and Bottom Flange Separate

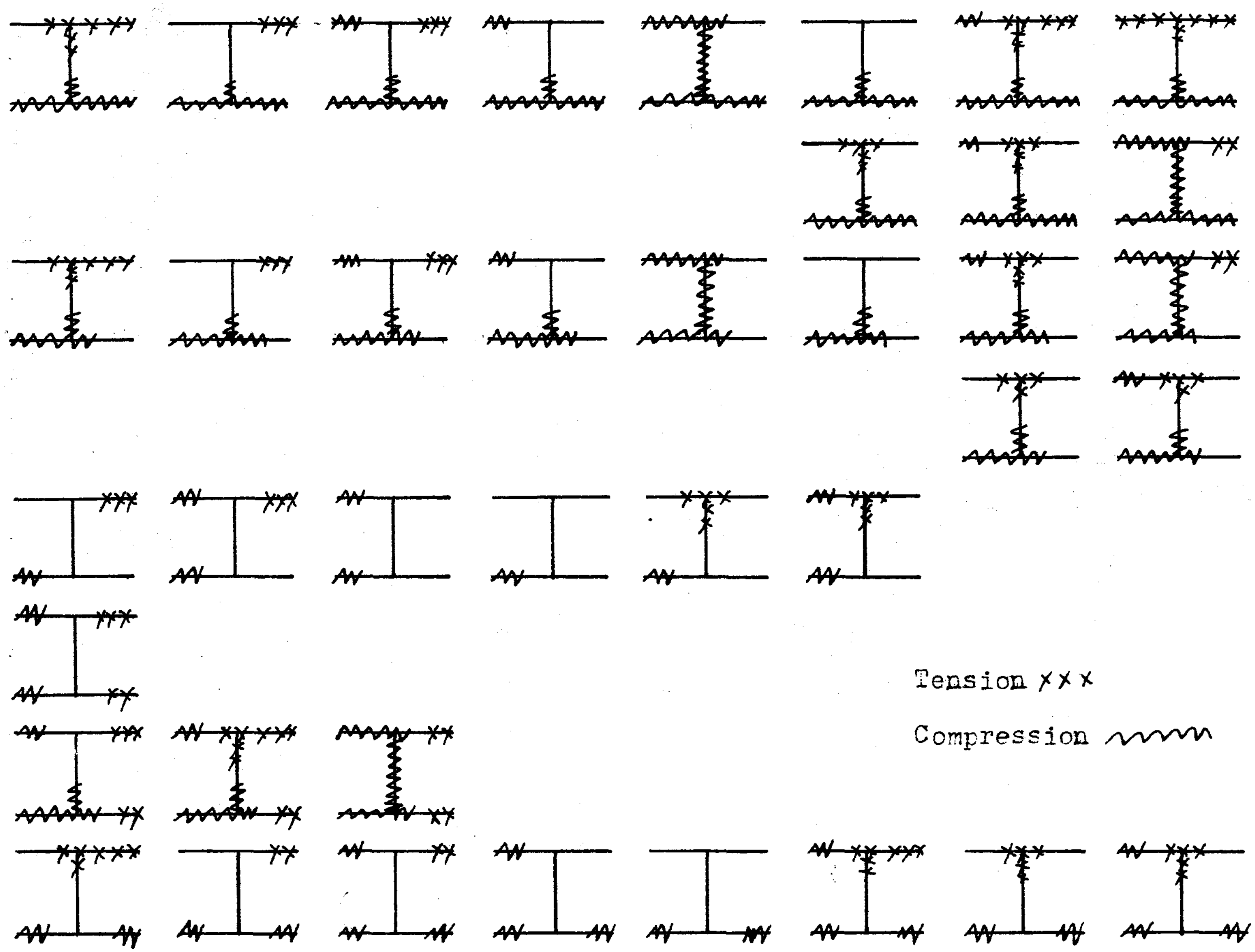

Fig. 2.17(b) Possible Yield Configurations for a Wide Flange Section With Residual Stresses Included

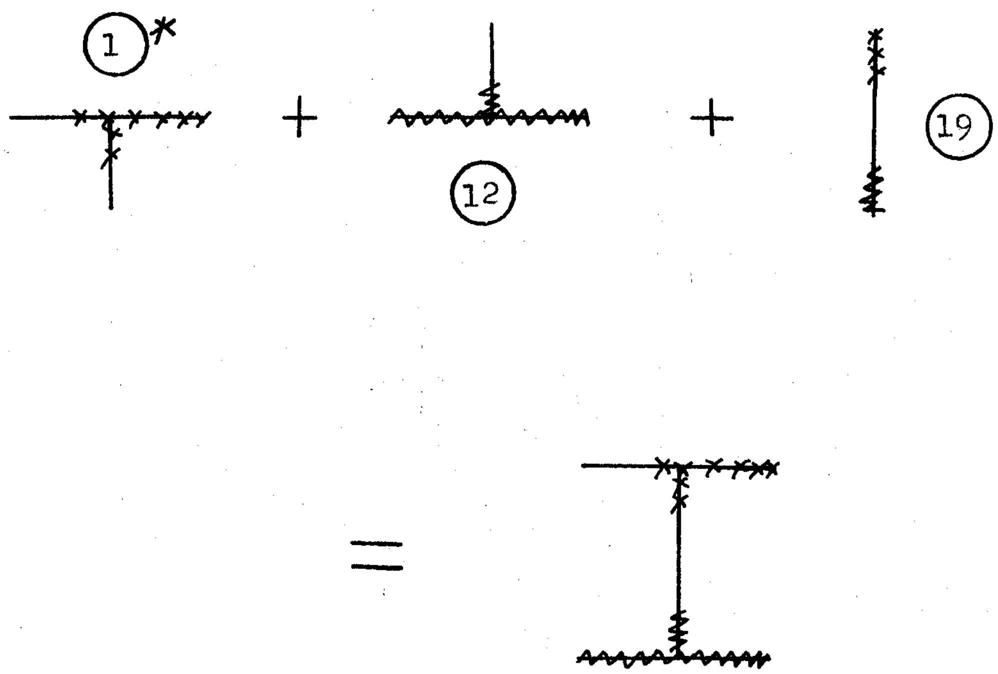

* Number refers to Table 2.2

Fig. 2.18 Sample Derivation of Total Cross Section Yield Pattern

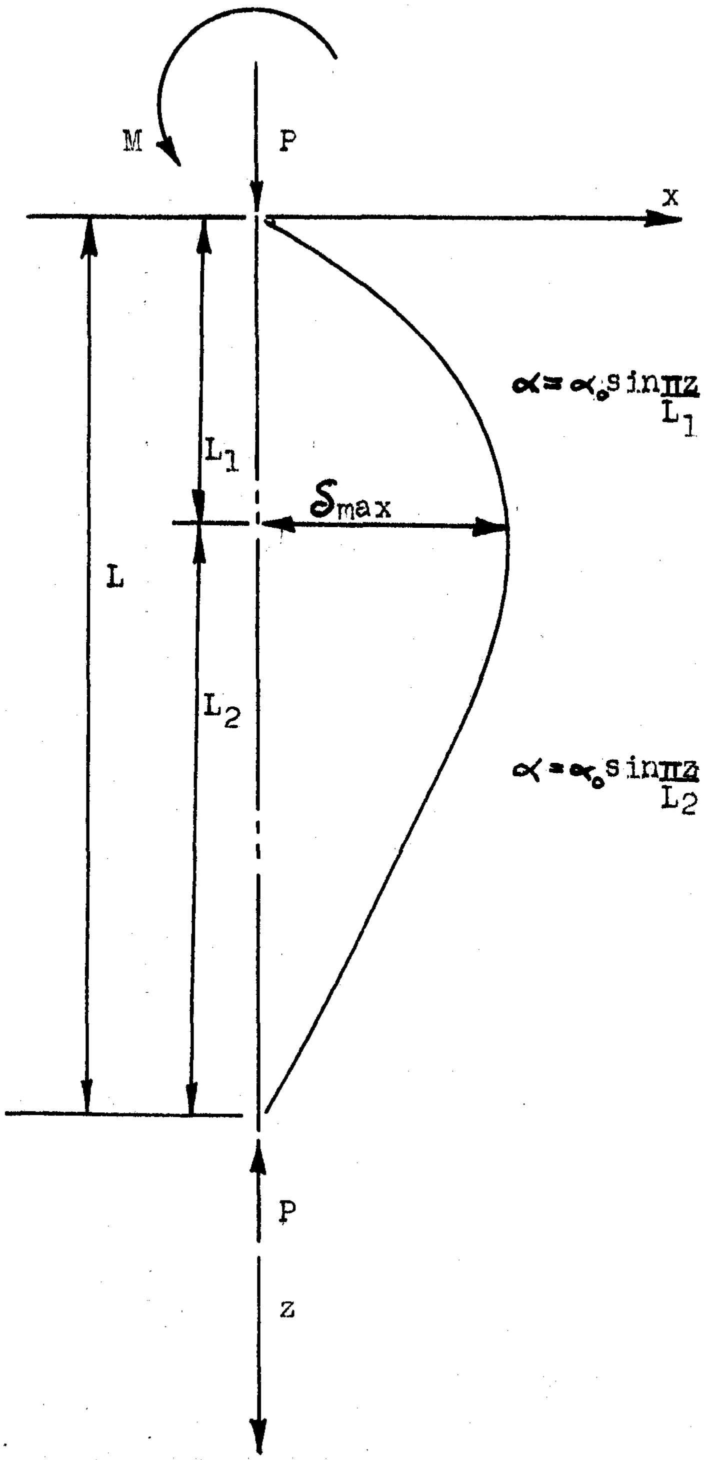

Fig. 2.19 Column With Unequal End Moments (β=0)

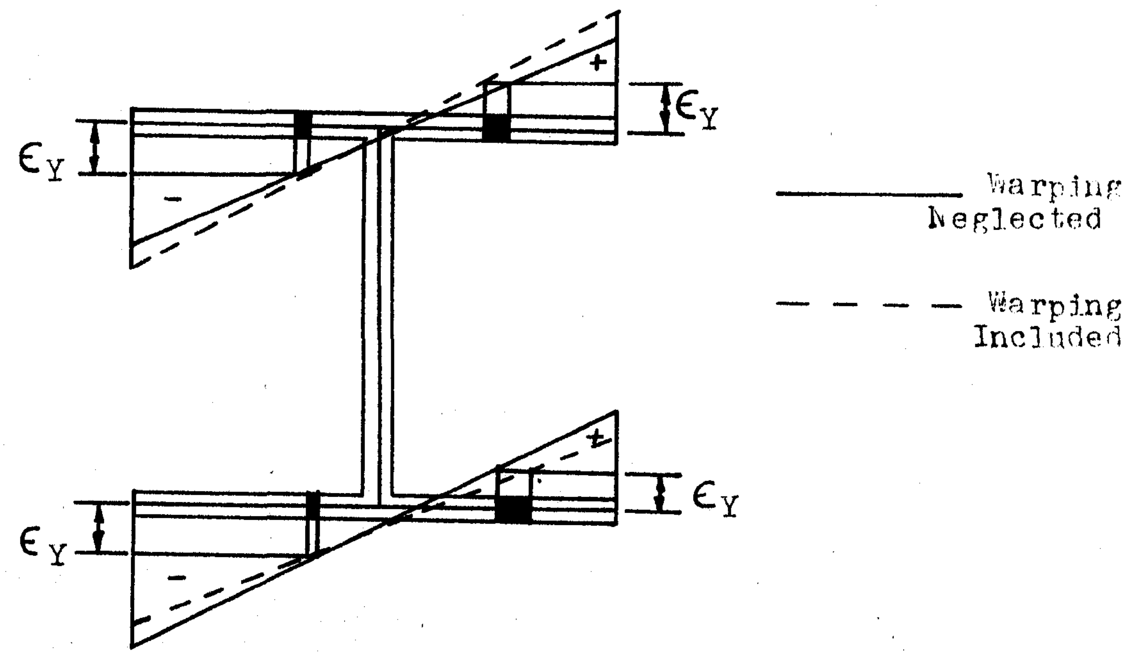

Fig 2.20 Strain Distribution on the Flanges for the Cross Section at Mid Height of the Column

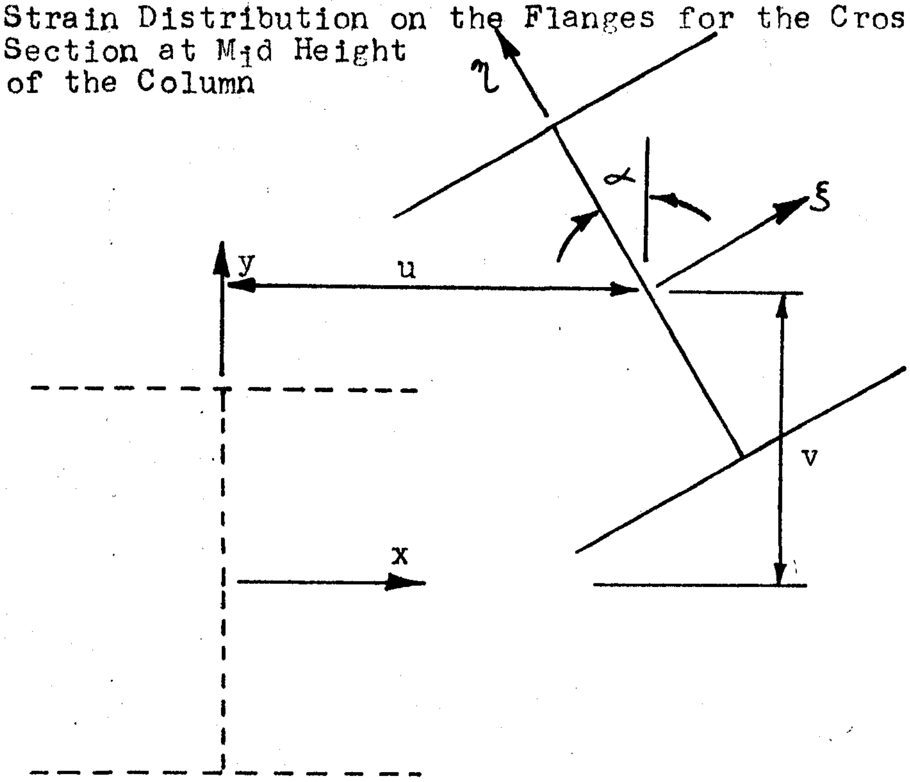

Fig. 2.21 Rotated Principal Axis

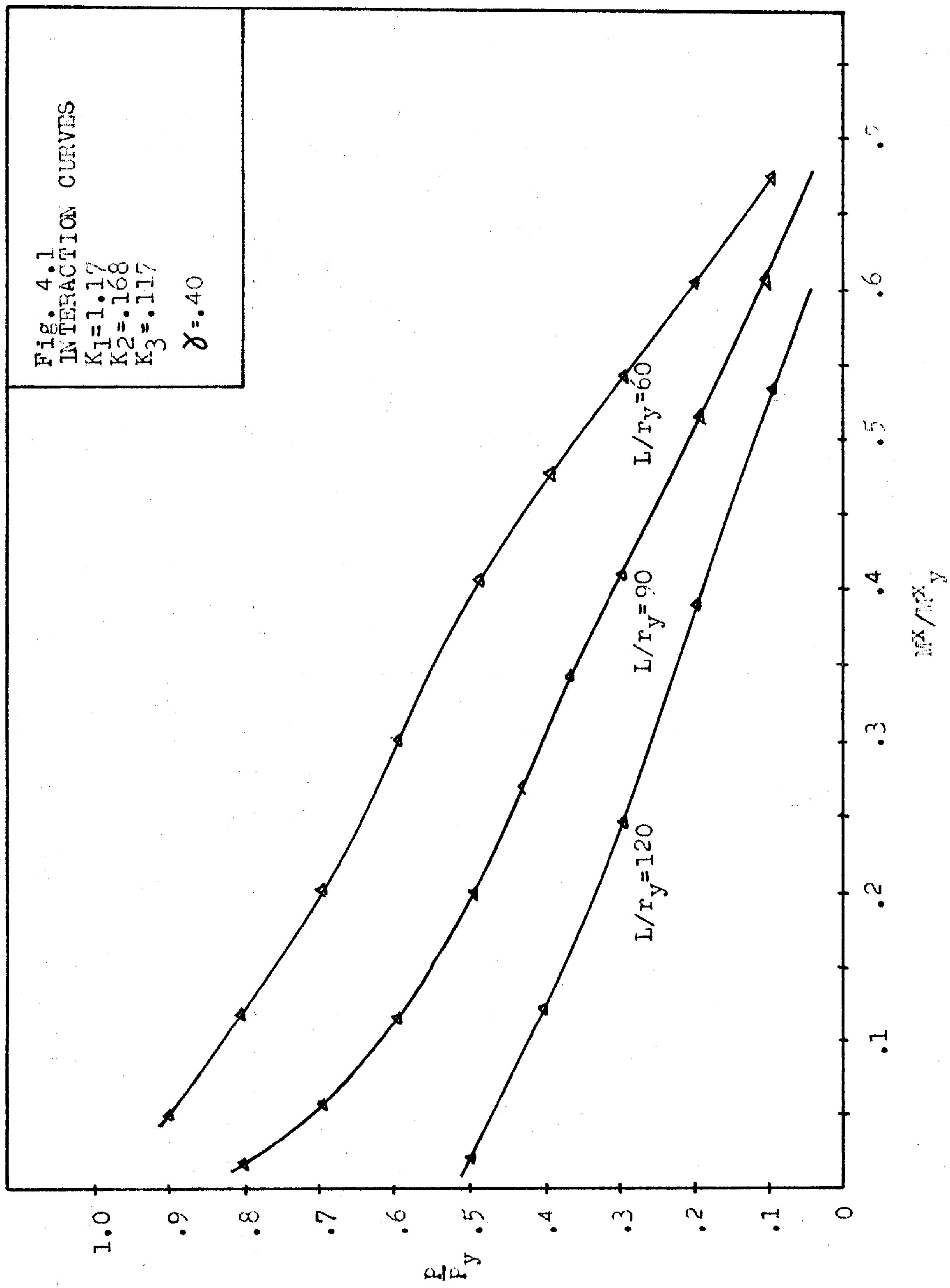
Fig. 4.1
INTERACTION CURVES
$K_1 = 1.17$
$K_2 = .168$
$K_3 = .117$
$\gamma = .40$
$L/r_y = 60$
$L/r_y = 90$
$L/r_y = 120$
P/P_y
M^x/M^x_y
1.0
.9
.8
.7
.6
.5
.4
.3
.2
.1
0
.1
.2
.3
.4
.5
.6
.7

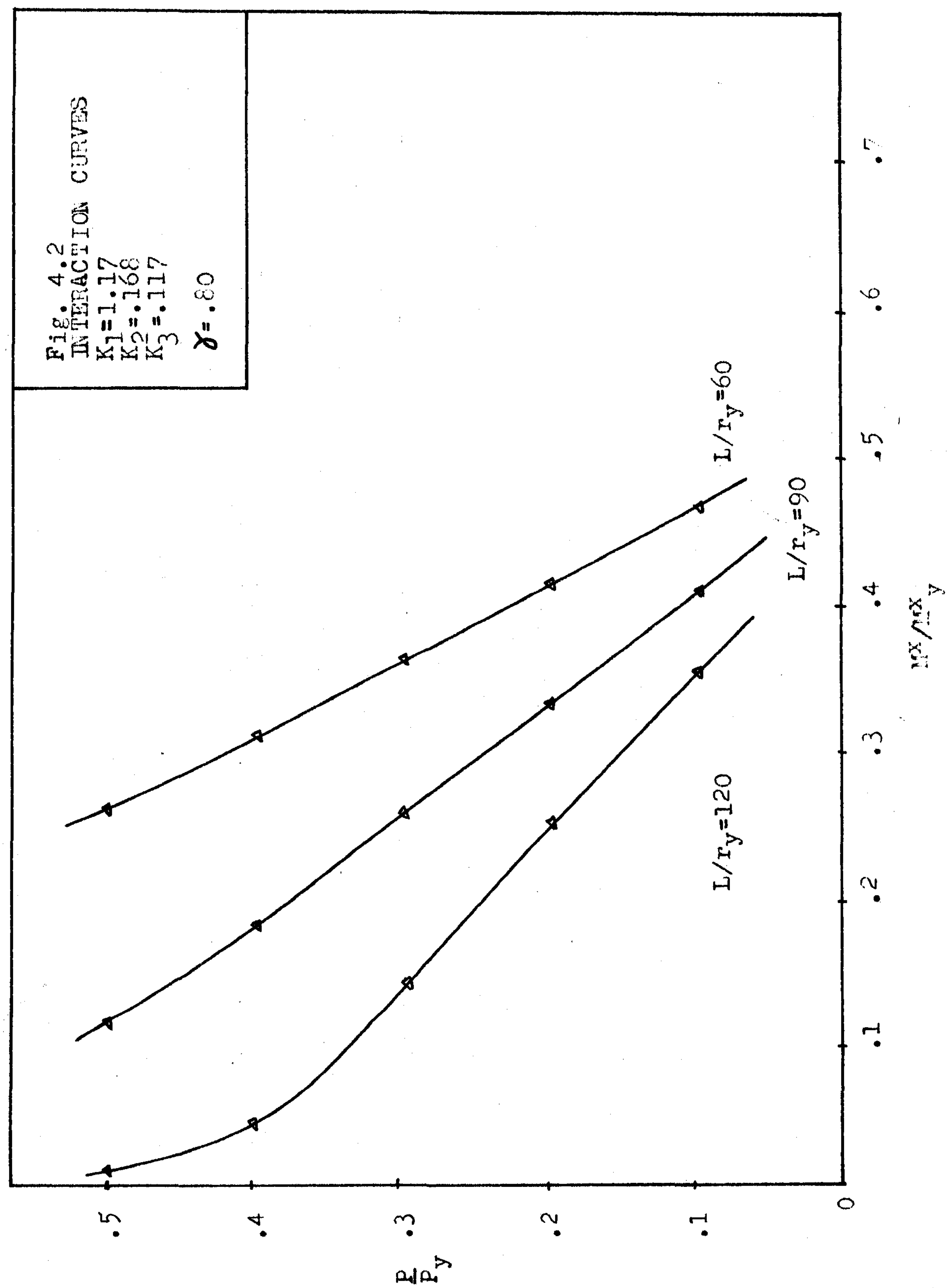

Fig. 4.2
INTERACTION CURVES
K_1=1.17
K_2=.168
K_3=.117
γ=.80
L/r_y=60
L/r_y=90
L/r_y=120
M_x/M_{x_y}
$\frac{P}{P_y}$
0
.1
.2
.3
.4
.5
.6
.7

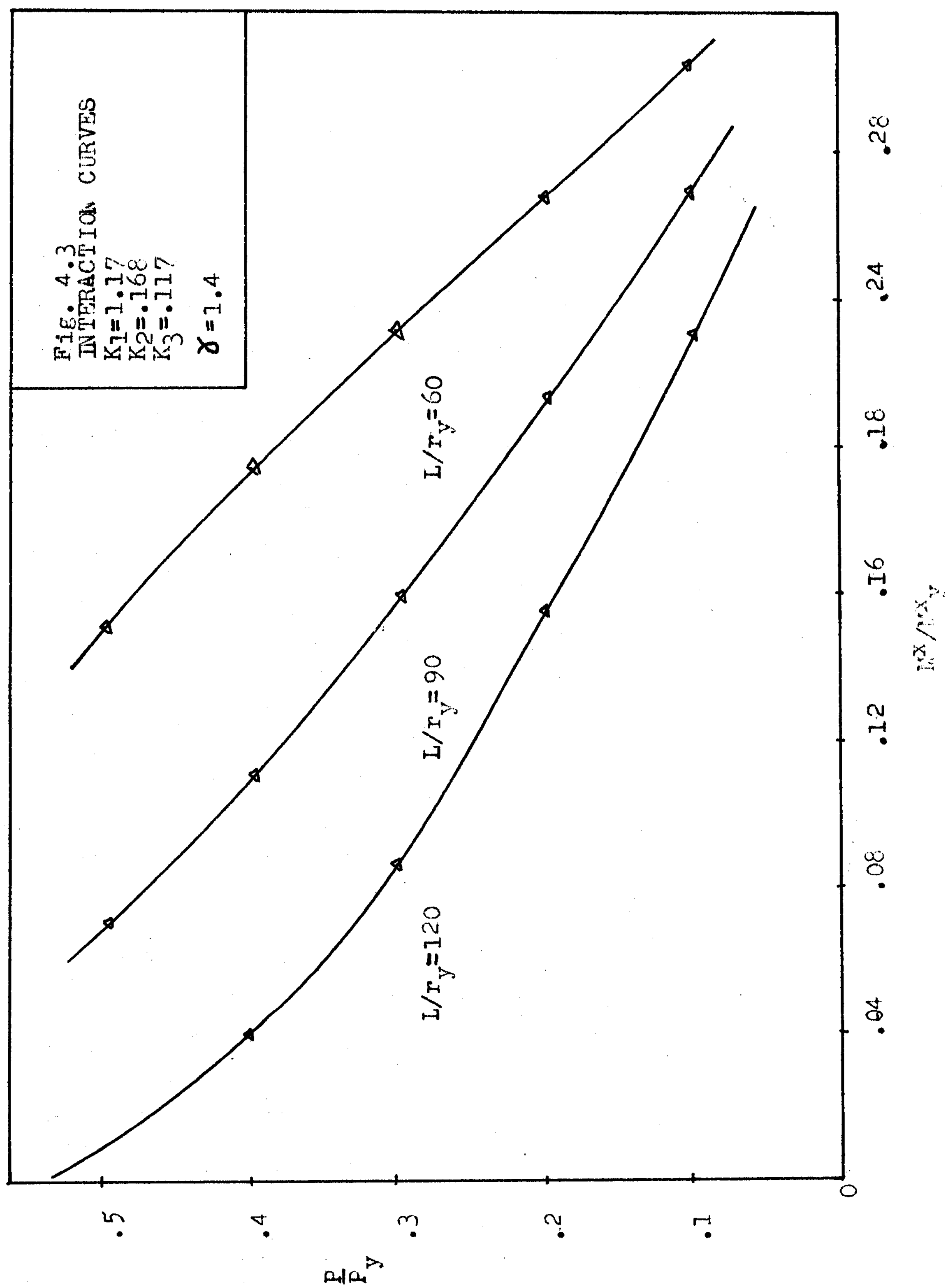
Fig. 4.3
INTERACTION CURVES
K1=1.17
K2=.168
K3=.117
γ=1.4
L/ry=60
L/ry=90
L/ry=120
P/Py
.5
.4
.3
.2
.1
0
.04
.08
.12
.16
.18
.24
.28

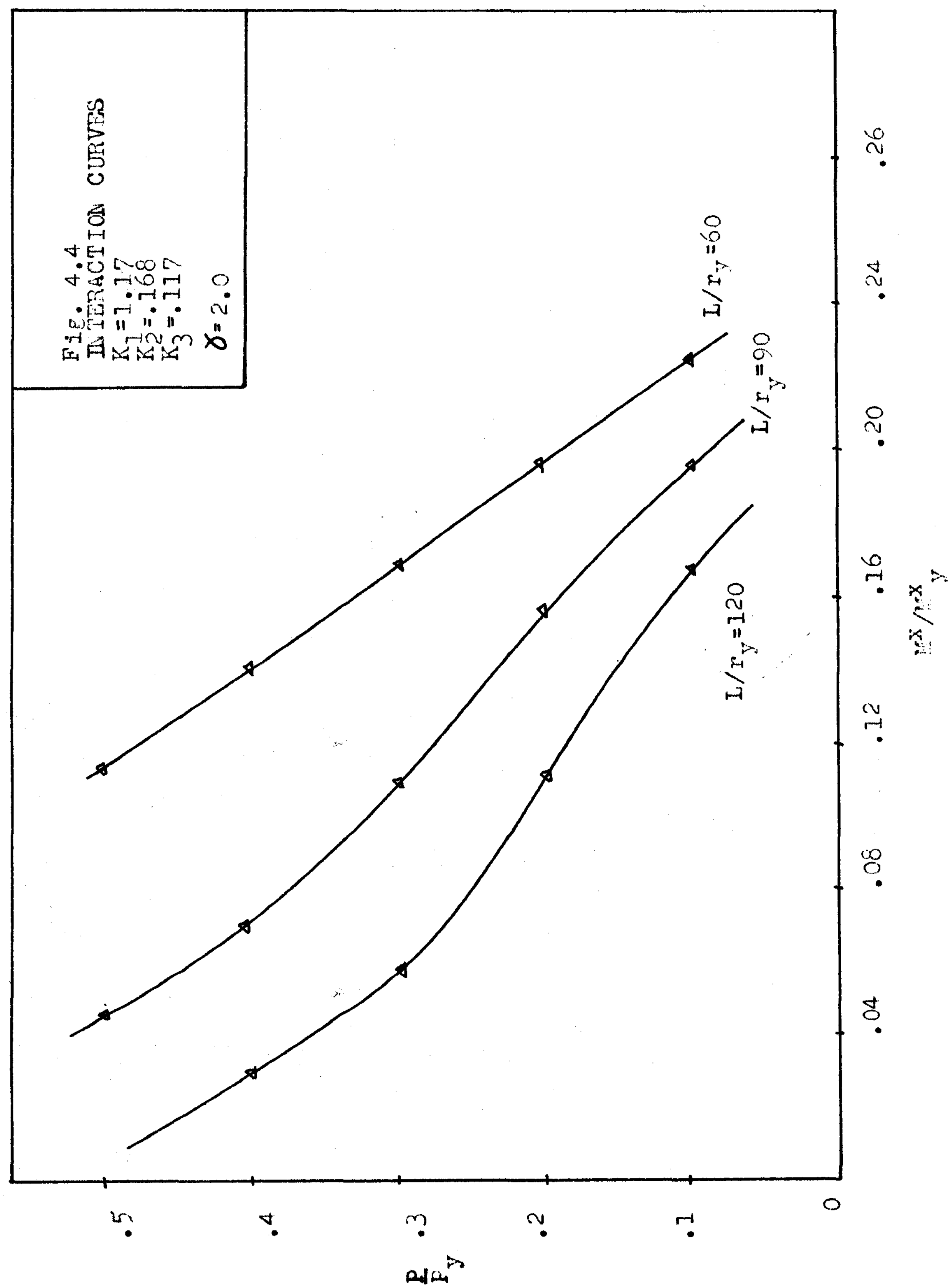
Fig. 4.4
INTERACTION CURVES
K_1=1.17
K_2=.168
K_3=.117
δ=2.0
L/r_y=60
L/r_y=90
L/r_y=120
P/P_y
.5
.4
.3
.2
.1
0
.04
.08
.12
.16
.20
.24
.26
M^x/M^x_y

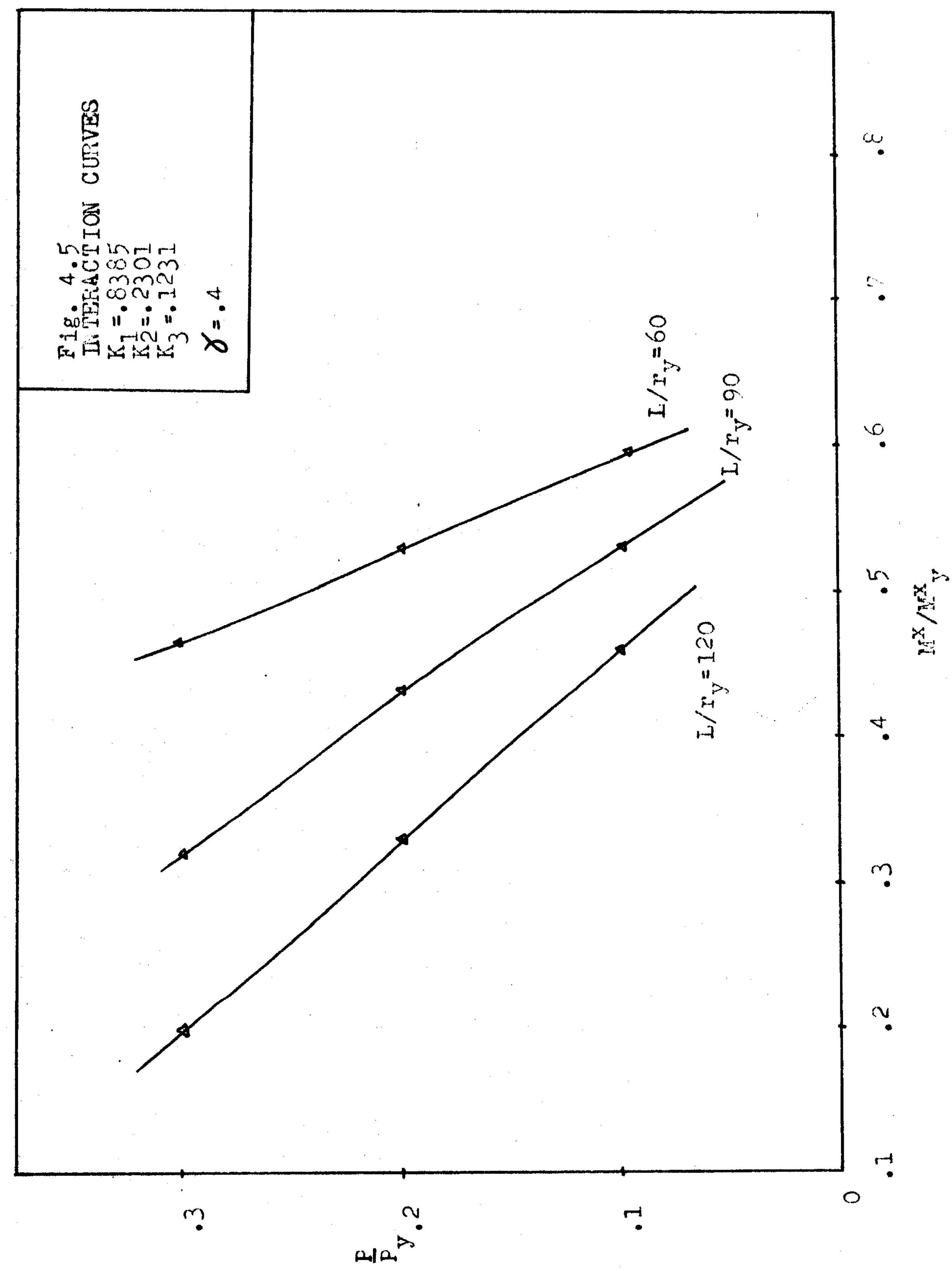

Fig. 4.5 INTERACTION CURVES

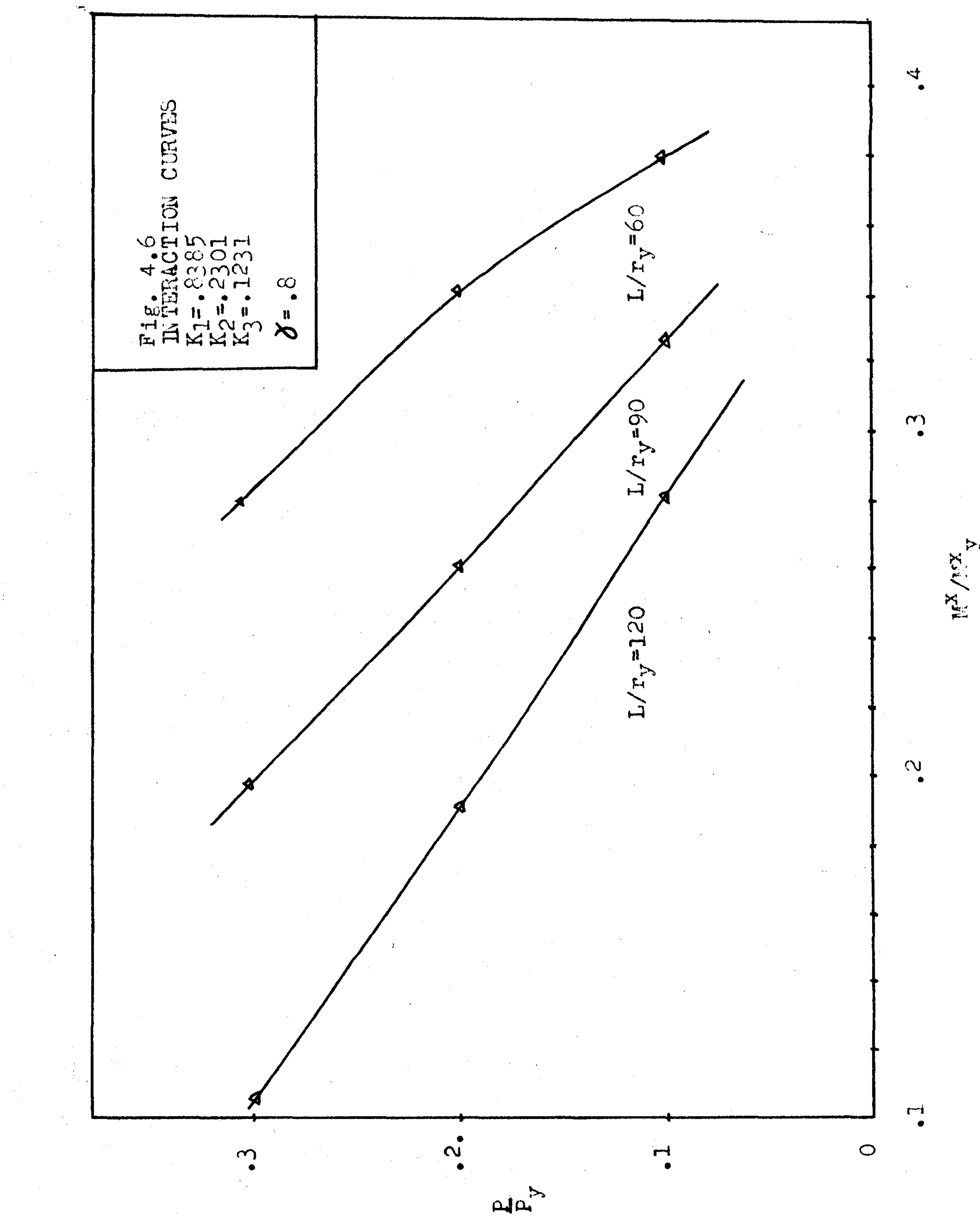
Fig. 4.6
INTERACTION CURVES
K1=.8385
K2=.2301
K3=.1231
γ=.8
L/ry=60
L/ry=90
L/ry=120
P/Py
Mx/Mxy
0
.1
.2
.3
.4

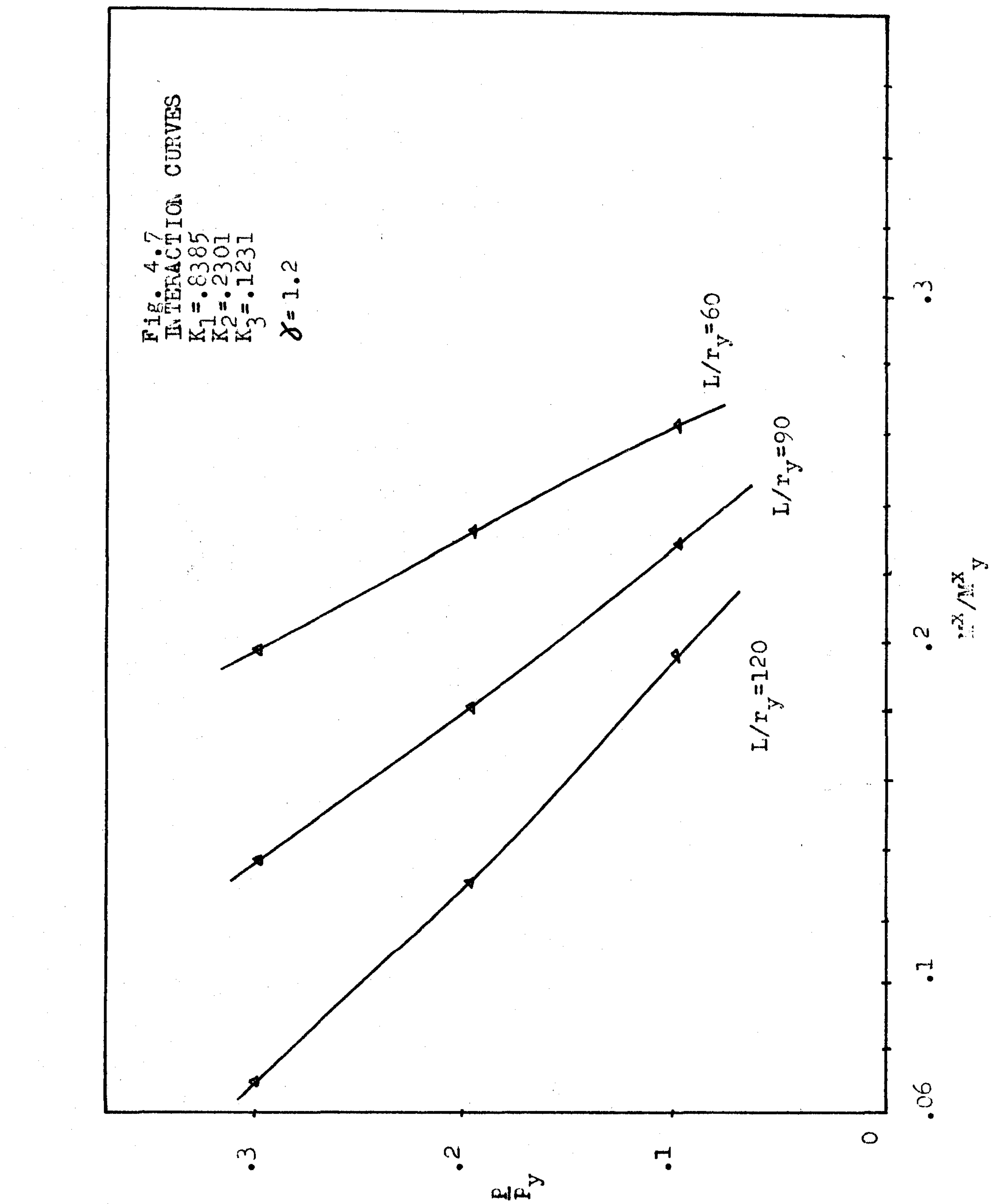
Fig. 4.7
INTERACTION CURVES
K_1 = .8385
K_2 = .2301
K_3 = .1231
γ = 1.2
L/r_y=60
L/r_y=90
L/r_y=120
.06
.1
.2
.3
M^x/M^x_y
0
.1
.2
.3
P/P_y

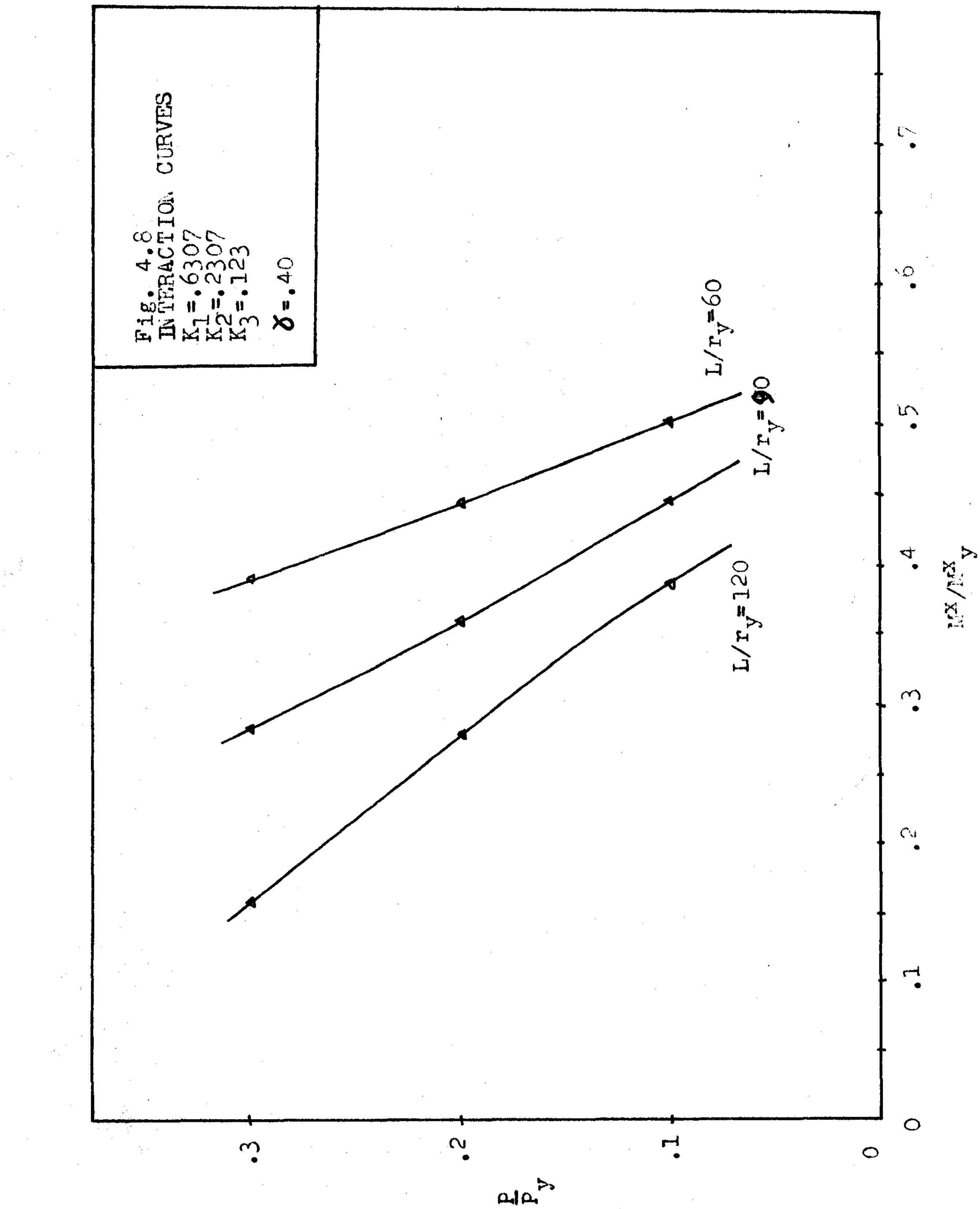
Fig. 4.8
INTERACTION CURVES
K_1=.6307
K_2=.2307
K_3=.123
δ=.40
L/r_y=60
L/r_y=90
L/r_y=120
P/P_y
M^x/M^x_y
0
.1
.2
.3
.4
.5
.6
.7

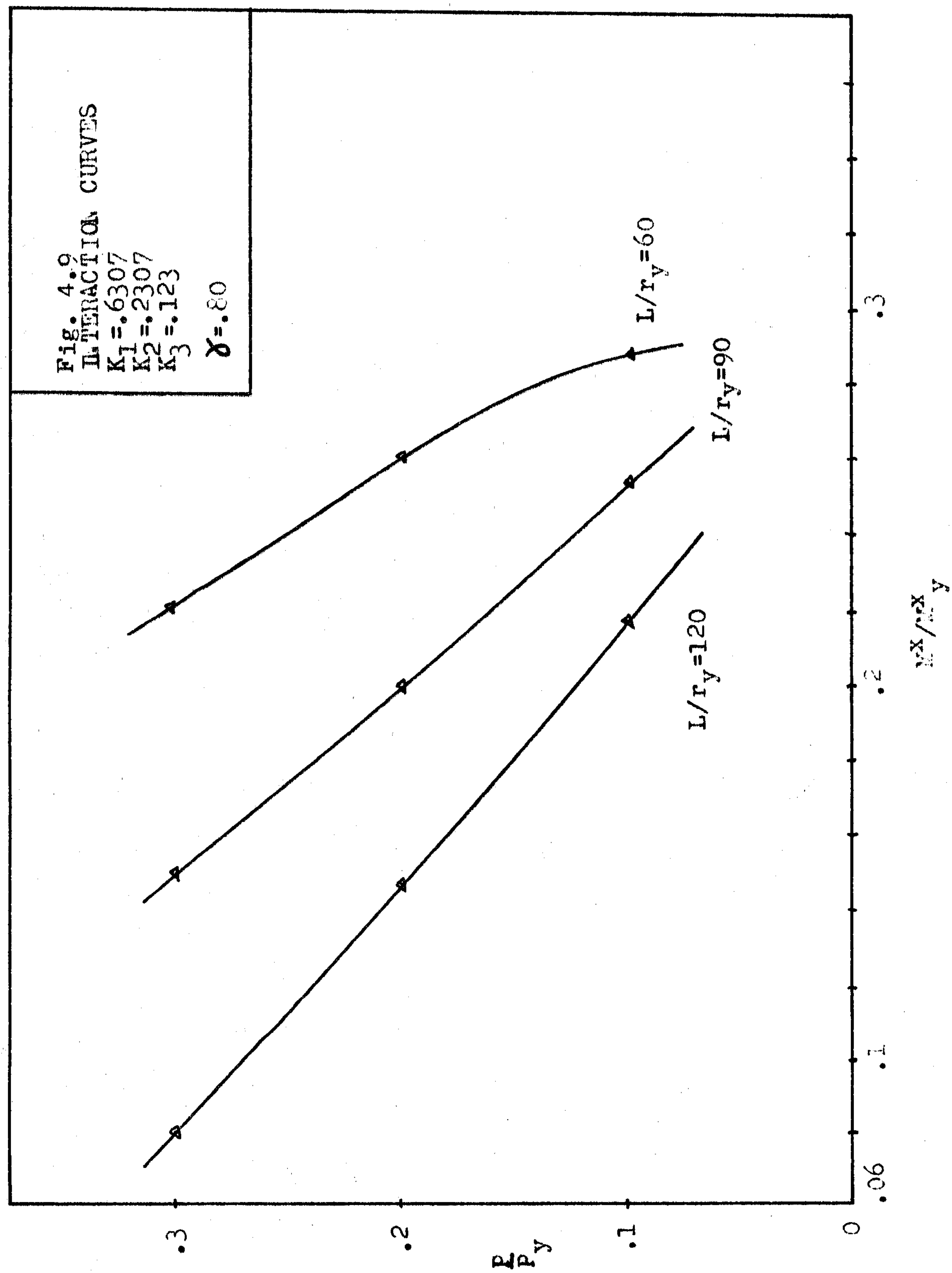
Fig. 4.9
INTERACTION CURVES
K1=.6307
K2=.2307
K3=.123
γ=.80
L/ry=60
L/ry=90
L/ry=120
P/Py
.3
.2
.1
0
Mx/Mx y
.06
.1
.2
.3

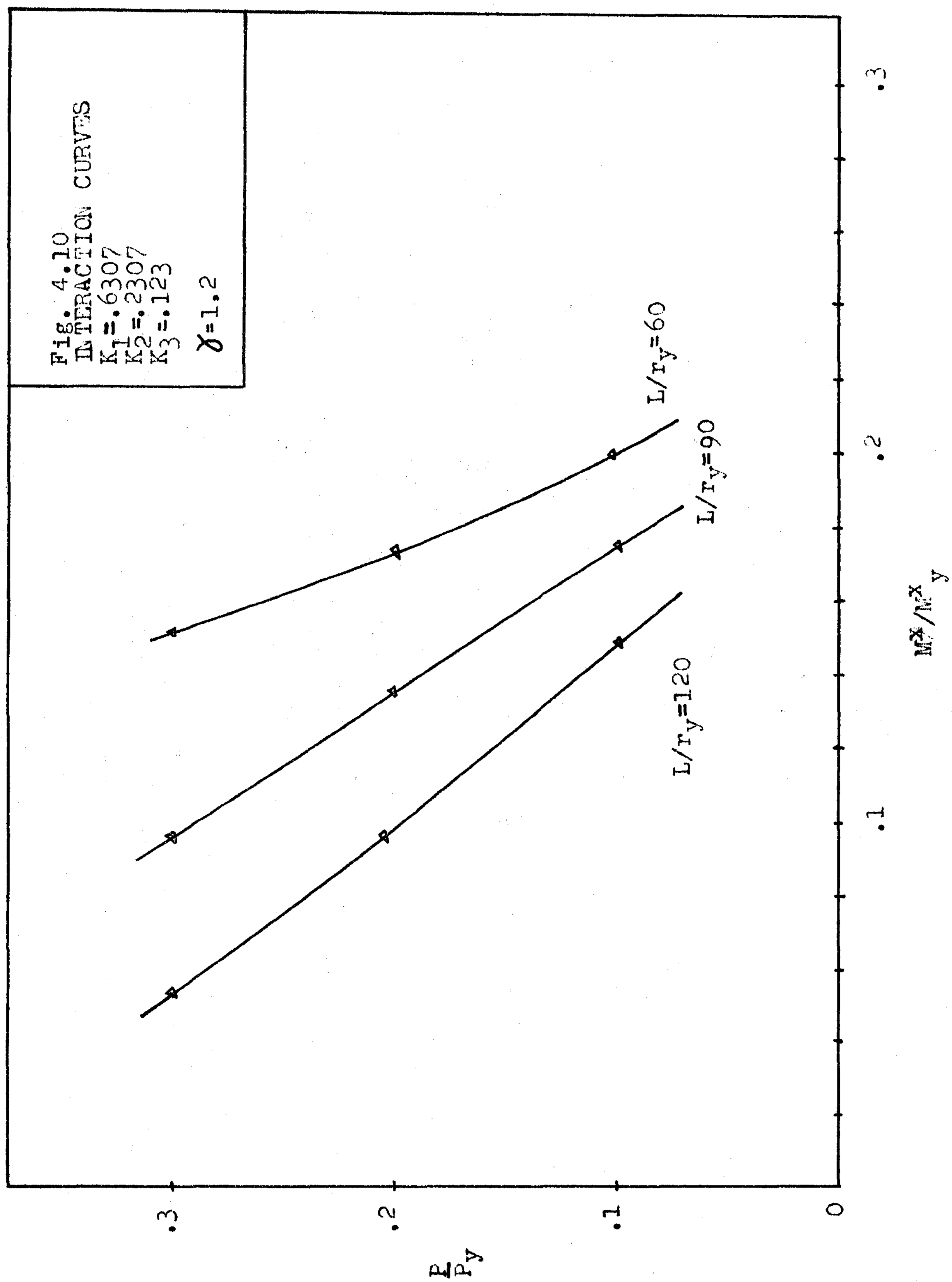
Fig. 4.10
INTERACTION CURVES
K_1=.6307
K_2=.2307
K_3=.123
γ=1.2
L/r_y=60
L/r_y=90
L/r_y=120
M^x/M^x_y
$\frac{P}{P_y}$
0
.1
.2
.3

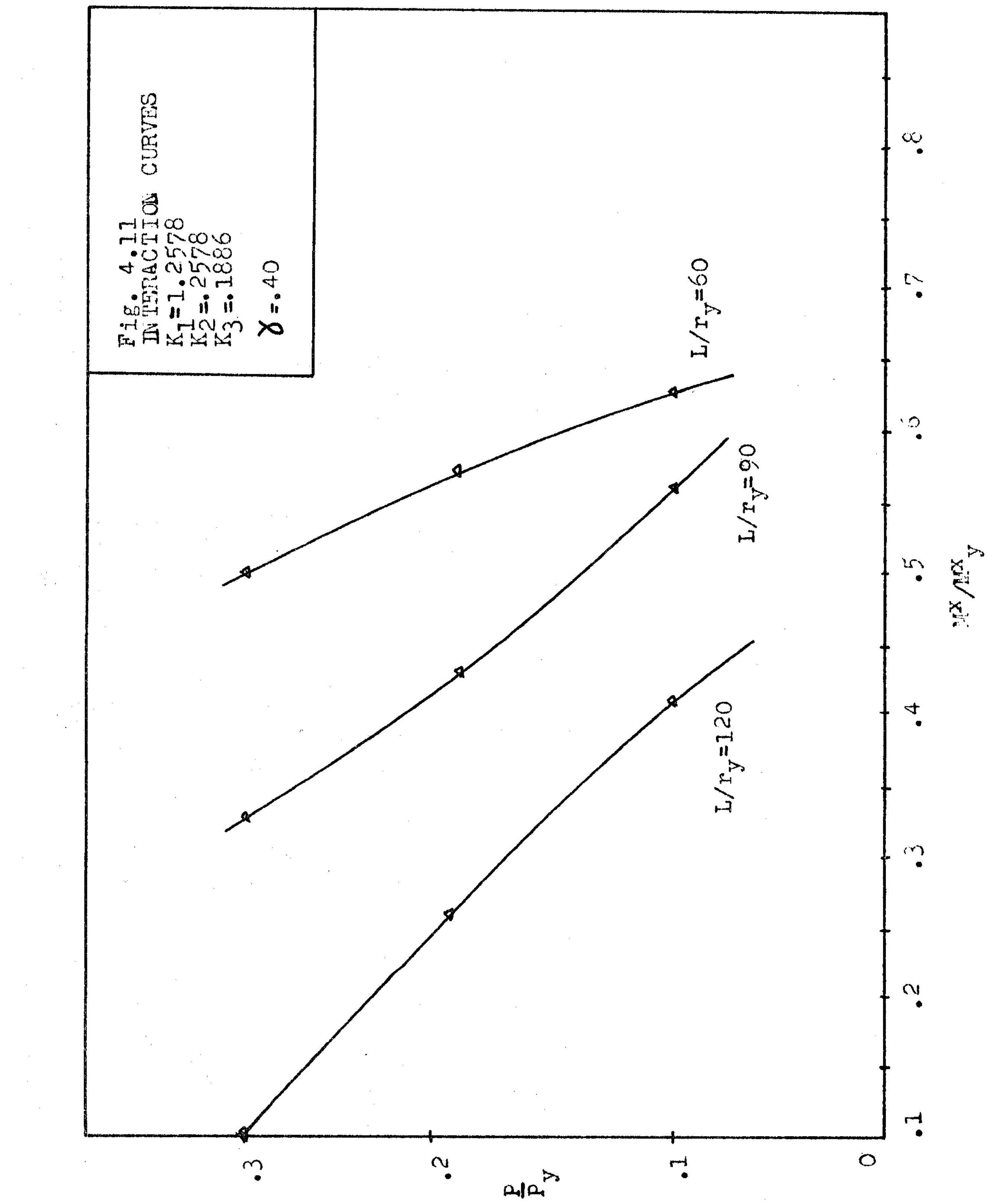

Fig. 4.11
INTERACTION CURVES
K_1=1.2578
K_2=.2578
K_3=.1886
γ=.40
L/r_y=60
L/r_y=90
L/r_y=120
M^x/M^x_y
$\frac{P}{P_y}$
.1
.2
.3
.4
.5
.6
.7
.8
0
.1
.2
.3

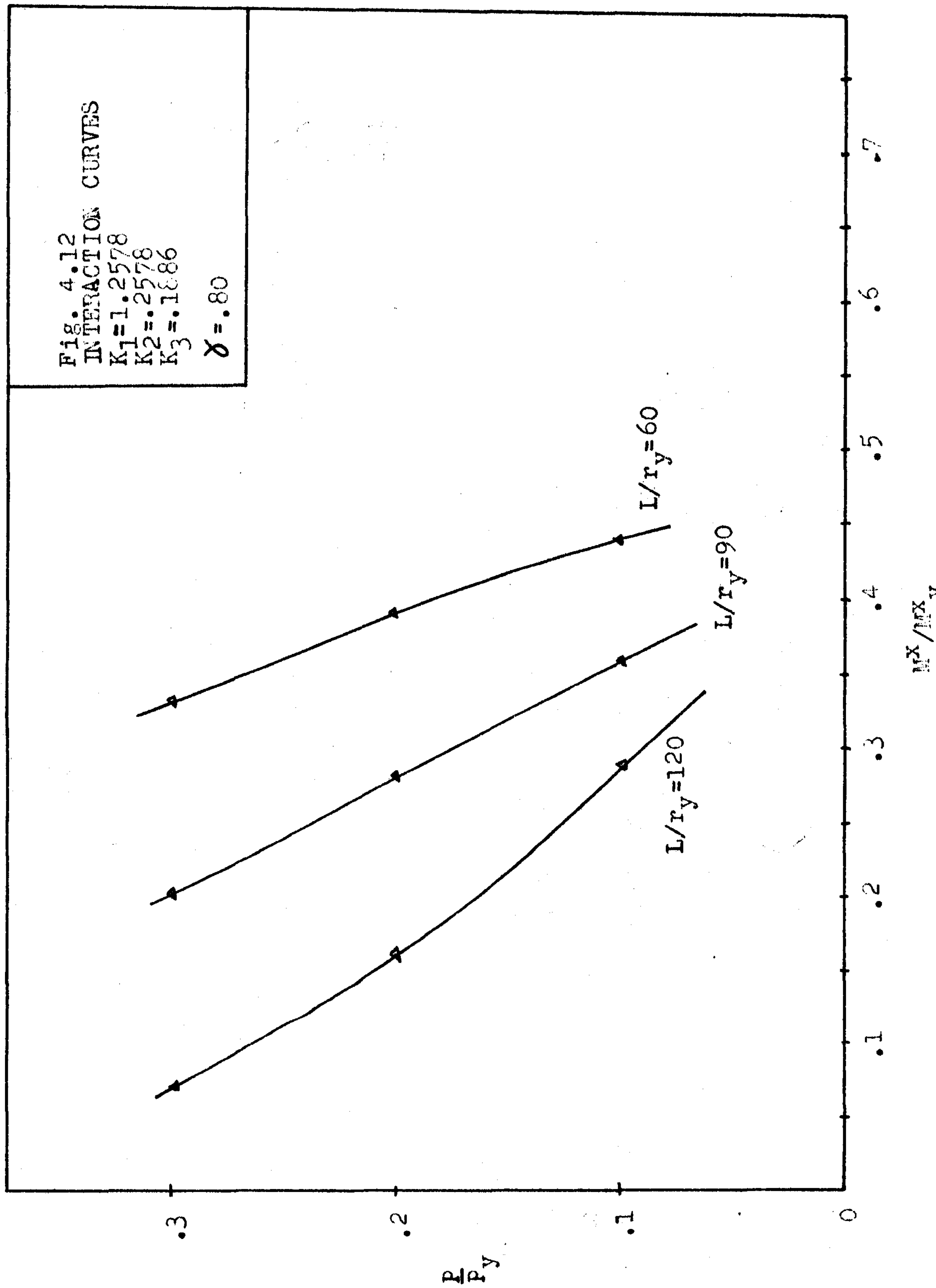

Fig. 4.12
INTERACTION CURVES
K_1=1.2578
K_2=.2578
K_3=.1886
γ=.80

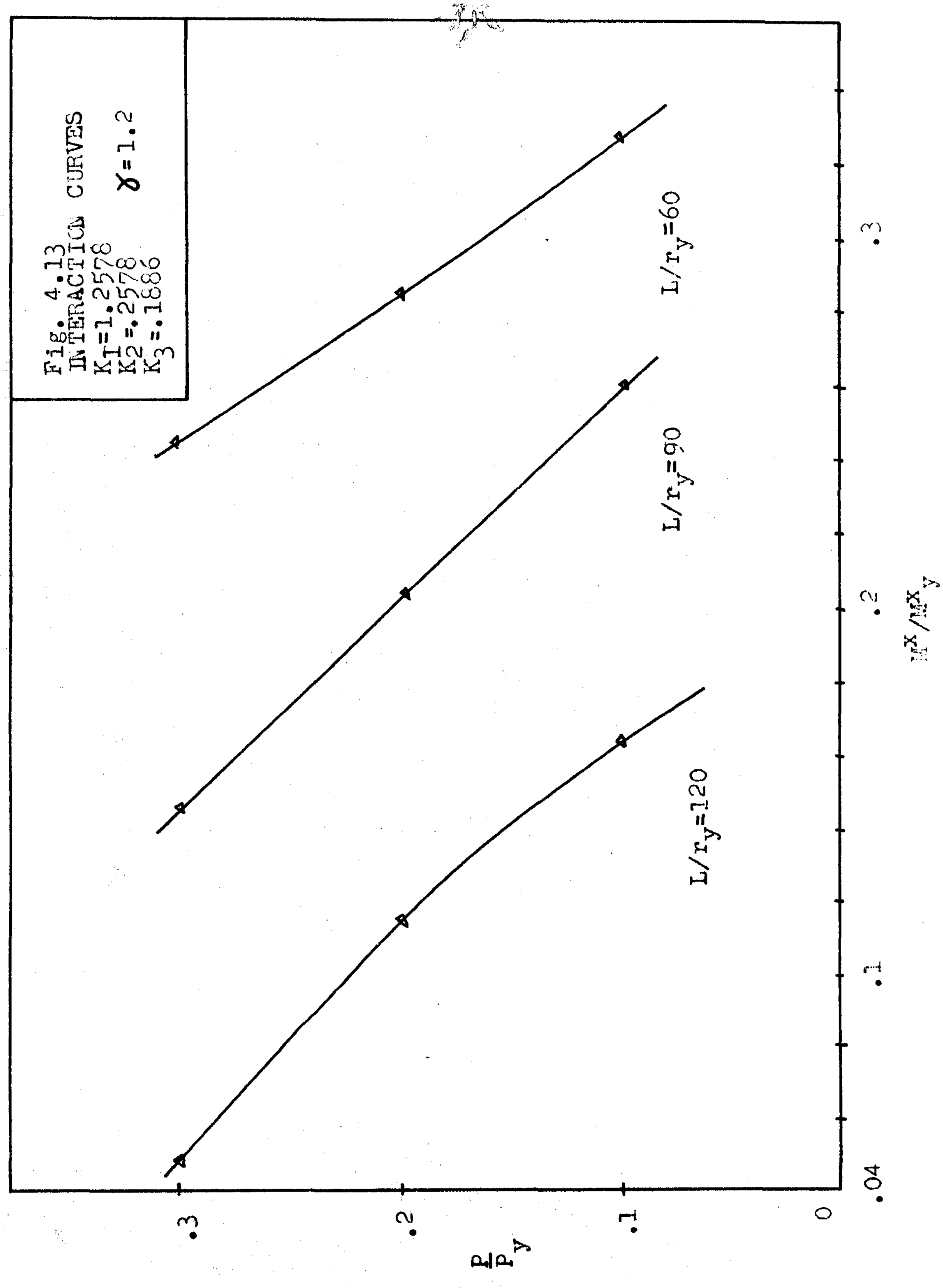
Fig. 4.13
INTERACTION CURVES
K1=1.2578
K2=.2578
K3=.1886
γ=1.2
L/ry=60
L/ry=90
L/ry=120
P/Py
Mx/Mxy
.04
.1
.2
.3
0
.1
.2
.3

BIBLIOGRAPHY

1. Bijlaard, P. P., Buckling of Columns With Equal and Unequal Eccentricities and Unequal Rotational End Restraints, Proceedings, 2nd U. S. Nat'l Congress of Applied Mech., 1954.

2. Birnstiel, C., and J. Michalos, Ultimate Load of H-Columns Under Biaxial Bending, Proceedings, ASCE, Vol. 89 ST2, 1963.

3. Bluch, F., Buckling Strength of Metal Structures, McGraw-Hill Book Co., New York, 1952.

4. Chajes, Alexander, and Winter, George, Torsional-Flexural Buckling of Thin-Walled Members, Presented at the ASCE structural Engineering Conference and Annual Meeting, October 19-23, 1964. Conference Reprint 117.

5. Chubkin, G. M., Experimental Research on the Stability of Thin Plate Steel Members With Biaxial Eccentricity, Paper N^{o} 6 in the book Analysis of Spatial Structures, Vol. 5, Moscow, 1959 (G. I. L. S.)

6. Ellis, J. S., E. J. Jury and D. W. Kirk, Ultimate Capacity of Steel Columns Loaded Biaxially, EJC, BR and STR 2, 1964.

7. Ellis J. S., and P. J. Marshall, The Ultimate Capacity of Steel Columns Loaded Biaxially, Paper presented at the annual meeting of the Column Research Council, 1967.

8. Galambos, T. V., Review of Tests on Biaxially Loaded Steel Wide-Flange Beam-Columns, Report to the Column Research Council, Task Group N^{o} 3, Ultimate Strength of Columns with Biaxially Eccentric Loading, April, 1963, Fitz Engineering Laboratory Report N^{o} 287.4.

9. Galambos, T. V., Bending and Compression, Chapter 6 of Structural Steel Design, Civil Engineering Department Staff, Lehigh University, Fritz Engineering Laboratory Report 354.3.

10. Huber, A. W., and R. L. Ketter, The Influence of Residual Stress on the Carrying Capacity of Eccentrically Loaded Columns, Publication, Int. Assoc. for Bridge and Struc. Eng., Vol. 18, Zurich, 1958.

11. Ketter, R. L., E. L. Kaminsky and L. S. Beedle, Plastic Deformation of Wide Flange Beam Columns, Trans., ASCE, Vol. 120, 1950.

12. Ketter, R. L., Lynn S. Beedle and B. G. Johnston, Column Strength Under Combined Bending and Thrust, Progress Report No 6 on Welded Continuous Frames and Their Components, December 1952.

13. Kloppel, L., E. Winkelman, Experimentelle und Theoretische Untersuchungen Uber die Traglast von Zweiachsig Aussermittig Gedruckten Stahlstaben (Experimental and Theoretical Investigations on the Ultimate Strength of Biaxially Compressed Steel Columns), Der Stahlban, February, March April, 1962, Vol. 31.

14. Lay, M. G., and T. V. Galambos, The Experimental Behavior of Restrained Columns, pulication sponsored by the Structural Steel Committee of the Welding Research Council.

15. Newmark, N. M., Numerical Procedure for Computing Deflections, Moments, and Buckling Loads, Trans., ASCE, Vol. 108, 1943.

16. McVinnie, W. W., Elastic and Inelastic Buckling of an Orthogonal Space Frame, Ph. D. Thesis, Univ. of Illinois, 1966.

17. Ojalvo, M., Restrained Columns, Proceedings, ASCE, Vol. 86, EM5, 1960.

18. Renton, J. D., A Direct Solution of the Torsional-Flexural Buckling of Axially Loaded Thin-Walled Bars, The Structural Engineer, September 1960.

19. Scott, T. L., Theoretical Analysis of Biaxially Loaded Beam-Columns, M. A. Sc. Thesis, University of Windsor, 1967.

20. Sharma, S. S., Strength of Steel Columns With Biaxially Eccentric Loads, Ph. D. Thesis, University of Illinois, 1965.

21. Timoshenko, S. P., and J. M. Gere, Theory of Elastic Stability, McGraw-Hill Book Co., New York, 1961.

Nomenclature

A_c	area of the cross section
A	constant equal to $\frac{K_1 K_2}{2(K_3 + 2K_1K_2)}$
a	length of a typical element of the column deflection curve.
Aij, Aji	factors defining the length of tension or compression yielding in the webs or flange.
B^x, B^y	bending stiffnesses about the x and y axes respectively.
B	constant equal to $\frac{K_3}{2(K_3 + 2K_1K_2)}$
b	width of half section of wide flange column.
C	St. Venants torsional constant
D, d	half depth of the cross section
E	modulus of elasticity
e^x, e^y	eccentricity for the x and y axis end moments respectively.
$I_{f_1} + I_{f_2}$	moment of intertia of the elastic portion of the cross section.
i, i + 1	adjacent points on the column deflection curve.
i	denotes left hand end of a flange or web.
j	denotes right hand end of a flange or web.
K_1	factor defining half the flange width.
K_2	factor defining the flange thickness.
K_3	factor defining the web thickness.
L,l	column length.
M^x, M^y	bending moment about the x and y axis respectively.
M^z	twisting moment about the longitudinal axis z.
m	length of the centre line of the column cross section.
P	axial load applied to the column.

Pe	Euler load
Py	yield load
Q	coefficient of the quadratic term in the equation for ϵ_o
R	coefficient of the linear term in the equation for ϵ_o
r^x, r^y	radius of gyration about the x and y axis respectively.
r	radial distance from the axis of rotation to a point on the centreline of the cross section.
S	slope of the line a d in Fig. 2.6
S	absolute value in the equation defining ϵ_o
u, v	lateral displacements of the shear centre in the x and y directions respectively.
w	warping displacement
Z	coordinate along the number
α	twisting displacemnt at Z along the column length.
α_o	twisting displacement at the column midheight.
β	ratio of the x moment at one end of column to the x moment at the other end.
γ	ratio of the y moment to the x moment at the same end of the column.
δ	deflection of i + 1 from the column deflection curve at i
DELTA	initail specified value for v
ϵ	strain
$\bar{\epsilon}$	bending strain
ϵ_o	uniform normal strain
ϵ_y	yield strain
$\epsilon_{i,j}$	strain at a flange or web tip in the column cross section.
ϵ_z	warping strain
ϵ_c	compressive residual strain at the tips of the flanges.

ϵ_R	tensile residual strain at the centre of the flanges.
ϕ^x, ϕ^y	x and y axis curvatures respectively.
ϕ^x_y	yield curvature
ϕ^ξ, ϕ^η	curvatures about the ξ and η axes
ξ, η	axes at an any α to the x and y axis respectively.
θ^x, θ^y	rotations about the x and y axis respectively
θ^x_y	yield rotation
σ	stress
ψ	change in slope between i and i + 1 on the column deflection curve.

VITA

Daniel Michael Masterson was born in Chatham, Ontario, on July 3, 1944. After graduating from highschool in Chatham in 1963, he enrolled in Engineering at the University of Windsor and obtained a Bachelor of Applied Science in Civil Engineering degree in 1967. In September, 1967, he returned to the University of Windsor for further study leading to a Master of Applied Science in Civil Engineering degree.

Mr. Masterson is a member of the Association of Professional Engineers of Ontario.